Hydrogenation Reactions Catalyzed by Manganese and Molybdenum Complexes

Towards More Sustainable Redox Reactions

Cumulative Dissertation

Niklas F. Both

University of Rostock
2024

https://doi.org/10.18453/rosdok_id00004767

Hydrogenation Reactions Catalyzed by Manganese and Molybdenum Complexes

Towards More Sustainable Redox Reactions

Cumulative Dissertation

to acquire the academic degree
doctor rerum naturalium (Dr. rer. nat.)
of the Faculty of Mathematics and Natural Sciences
at the University of Rostock

Submitted by
Niklas Felix Both
born on 7th August 1995 in Bad Soden (Taunus)

Rostock, 08th July 2024

The presented work was accomplished at the Leibniz-Institut für Katalyse e.V. in the research group of Prof. Matthias Beller during the period from September 2020 to December 2023.

Reviewer 1: Prof. Dr. Dr. h.c. mult. Matthias Beller
Leibniz-Institut für Katalyse e.V.
Angewandte Homogenkatalyse
Albert-Einstein-Straße 29a
18059 Rostock
Deutschland / Germany

Reviewer 2: Prof. Dr. Karl Kirchner
Technische Universität Wien
Getreidemarkt 9
1060 Wien / Vienna
Österreich / Austria

Date of submission: 16th January 2024
Date of defense: 16th July 2024

Statement of Authorship

I hereby affirm that I have written the present work by myself without illicit outside assistance. No resources other than stated were utilized. All verbatim extracts as well as references were quoted and all sources of information were specifically acknowledged. I have not previously submitted any of the content of this work for examination.

Hiermit versichere ich an Eides statt, dass ich die vorliegende Arbeit selbstständig und ohne unerlaubte fremde Hilfe verfasst habe. Dazu habe ich keine außer den von mir angegebenen Hilfsmitteln verwendet und alle wörtlich oder sinngemäß aus Veröffentlichungen entnommenen Stellen dieser Arbeit unter Quellenangabe einzeln kenntlich gemacht. Ich habe keine Inhalte der Arbeit zu einem früheren Zeitpunkt als Prüfungsleistung eingereicht.

Rostock, 8th July, 2024

Niklas F. Both

Acknowledgments

First, I would like to thank my supervisor **Prof. Matthias Beller** for giving me the opportunity to join his research group and to do my PhD under excellent conditions. Thank you for your kindness, your motivating attitude and your ability to see the positive and best in everything. Discussions and meetings with you were always inspiring and often opened a new perspective for me on how to approach a problem. I very much enjoyed the provided freedom to follow my own ideas and interests and I realized how much I have learned over the past years.

I am grateful to **Dr. Kathrin Junge** for welcoming me to the subgroup "Sustainable Redox Reactions". Thank you for your support with all kinds of personal and scientific challenges I was facing during my PhD, for your precise and fast proofreading of manuscripts and for your calm and analytic view that helped me many times. You created a pleasant working environment in which I felt comfortable and in which it was fun to do chemistry. Your organization of many cake breaks and multiple group activities contributed greatly to the positive atmosphere in the group.

Furthermore, I would like to thank **Prof. Haijun Jiao** for his interest in my work, many insightful scientific discussions and his friendly and supportive attitude. To no lesser extent, I am thankful to **Dr. Anke Spannenberg** for her patience and accuracy and her willingness to always support my research.

Also, I appreciate the fruitful cooperation with **Dr. Johannes Panten** and **Dr. Bernhard Rußbüldt** from Symrise AG and I am grateful for the interesting insights into the industrial R&D sector.

For the analysis of numerous samples by NMR and IR spectroscopy, HR-MS and elemental analysis as well as fulfilling many special request from my side, I would like to thank **Susann Buchholz**, **Susanne Schareina**, **Andreas Koch**, **Dr. Dilver Pena Fuentes**, **PD Dr. Wolfgang Baumann**, **Dr. Marcus Klahn**, **Astrid Lehmann** and **Sandra Leiminger**.

Moreover, I would like to thank **Andreas Hutter** for always being ready to fix anything at any time.

I am especially grateful to all the current and former members of the subgroup "Sustainable Redox Reactions" for the great and supportive working atmosphere in LIKAT and, evenly important, many activities outside of LIKAT. In this regard, I would like to thank: **Dr. Johannes Fessler** for many excellent discussions and good conversations not only about chemistry; **Dr. Thomas Leischner** for your great help at the beginning of my PhD and for bringing Mo chemistry to our group; my current and former labmates **Dr. Florian Bourriquen**, **Loris Geminiani**, **Dr. Julien Hervochon**, **Dr. Rafał Kusy**, **Dr. David Leonard**, **Dr. Peter McNeice** and **Dr. Ruiyang Qu** for good times and laughs in the lab and office; **Jannik Thaens** for your valuable work on the joint project, I could not have hoped for a better Master student; **Helen Hornke** and **Katja Andres** for your support in the lab and being patient with me learning how to supervise; **Sebastian Ahrens**, **Dr. Svenja Budweg**, **Dr. Soumyashree Jena**, **German Lopez Robledo**, **Dr. Shuxin Mao**, **Dr. Haifeng Qi** and **Dr. Dennis Verspeek** for always being supportive and making my time in LIKAT much better; our visiting researchers **Dr. Leandro Duarte de Almeida**, **Dr. Maria Gutierrez Blanco**, **Juan José Mateu Campos**, **Dr. Jorge Quesada Sanchez**, **Dr. Raquel Jimenez Rama** and **Andrea Vicenzi** for bringing your expertise and joy for chemistry to the group. Furthermore, I would like to thank **Dr. Soumyadeep Chakrabortty**, **Dr. Andrea Dell'Acqua**, **Simon Haida**, **Hendrik Kempf**, **Leonardo Scarpa**, **Claas Schünemann**, **Carolin Stein** and **Rafał Wolicki** as members from other groups in LIKAT for the good time spent together, your support in the lab and the pleasant collaboration. Thank you all for many good laughs in the lunch breaks, helpful suggestions for my research and for cheering me up many times!

Dr. Johannes Fessler, **Dr. Soumyashree Jena**, **Dr. Dennis Verspeek**, **Dr. David Leonard** and **Dr. Kathrin Junge** are thanked for thorough proofreading of this thesis and numerous valuable comments and suggestions.

I would particularly like to thank my parents **Gabriela** and **Udo** for their continuous support. Thank you for always believing in me!

Finally, I would like to thank my wife **Clara** for bringing much love and happiness into my life during the sometimes challenging times of my PhD. I am incredibly grateful for our time together and look forward to many more years to come.

Abstract

Hydrogenations represent one of the most important methods for the production of bulk and fine chemicals. Traditionally, homogeneous hydrogenation catalysts are largely based on noble metals such as rhodium, iridium or ruthenium. In light of a growing awareness for more sustainable chemical manufacturing, many scientific approaches focus on the replacement of these metals by non-noble metals due to their economic, ecological and toxicological benefits. Although numerous promising catalysts have been developed, these systems often rely on sophisticated ligands, which limits their practicality. In addition, previous works mainly focused on the transition metals manganese, iron and cobalt, whereas little attention has been paid to group 6 metals (chromium, molybdenum and tungsten), despite their equally attractive properties.

In this work, the synthesis of manganese complexes with easily accessible bidentate bis(NHC) ligands and their use as efficient precatalysts for the hydrogenation of carboxylic acid esters as well as ketones, nitriles, N-heteroarenes and alkenes is described. Furthermore, the use of molybdenum catalysts with PNP pincer ligands for the semihydrogenation of alkynes is investigated. Finally, the inexpensive bis(NHC) ligands are used to develop molybdenum-based catalyst systems for the hydrogenation of carboxylic acid esters. The reaction mechanisms of the novel bis(NHC) hydrogenation catalysts were investigated using spectroscopic methods, control experiments and DFT calculations.

Kurzzusammenfassung

Hydrierungen stellen eine der wichtigsten Methoden zur Produktion von Grund- und Feinchemikalien dar. Traditionell basieren homogene Hydrierkatalysatoren weitgehend auf Edelmetallen wie Rhodium, Iridium oder Ruthenium. Angesichts des wachsenden Bewusstseins für eine nachhaltigere chemische Produktion konzentrieren sich viele wissenschaftliche Ansätze auf den Ersatz dieser Metalle durch Nichtedelmetalle aufgrund deren ökonomischer, ökologischer und toxikologischer Vorteile. Obwohl zahlreiche vielversprechende Katalysatoren entwickelt wurden, nutzen diese Systeme oftmals aufwendig herzustellende Liganden, was ihre Praktikabilität limitiert. Zudem liegt der Fokus bisheriger Arbeiten größtenteils auf den Übergangsmetallen Mangan, Eisen und Kobalt, wohingegen Metallen der Gruppe 6 (Chrom, Molybdän und Wolfram) wenig Aufmerksamkeit geschenkt wurde, trotz deren ebenfalls attraktiver Eigenschaften.

In dieser Arbeit wird die Synthese von Mangan-Komplexen mit einfach zugänglichen bidentaten bis(NHC) Liganden sowie deren Verwendung als effiziente Präkatalysatoren für die Hydrierung von Carbonsäureestern sowie Ketonen, Nitrilen, N-Heteroaromaten und Alkenen beschrieben. Des Weiteren wird der Einsatz von Molybdän-Katalysatoren mit PNP-Pincerliganden für die Semihydrierung von Alkinen erforscht. Zuletzt werden die kostengünstigen bis(NHC) Liganden zur Entwicklung Molybdän-basierter Katalysatorsysteme zur Hydrierung von Carbonsäureestern verwendet. Untersuchungen der Reaktionsmechanismen dieser neuartigen bis(NHC) Hydrierkatalysatoren wurden mithilfe spektroskopischer Methoden, Kontrollexperimenten sowie DFT-Rechnungen vorgenommen.

Table of Contents

1 Introduction

1.1 Towards More Sustainable Chemistry by Catalysis

Our modern society is unimaginable without chemistry. The impact of chemistry on the development of humanity can not be underestimated, since it enables the supply of our most basic needs for food, energy, clothes, medicines or construction materials and immensely improved our quality of life over the last two centuries.

Despite its remarkable positive impacts on our society, chemistry has a poor public image and, unfortunately, there is a good reason for it: the dangerous and polluting way in which the chemical industry operated in the past.[1] Many chemical processes still applied today have been developed during an era of little awareness for the protection of our environment and human health,[2] leading to tragic chemical accidents and environmental catastrophes.[3–6] Besides the immediate health and environmental hazards, there are also far-reaching indirect consequences related to resource management and global warming since chemical processes are highly energy- and resource-demanding. For example, in 2020 the chemical industry in Germany accounted for approximately 15 % of the national energy consumption[7] and also 15 % of Germany's overall CO_2 emissions[1].[8]

In light of this, the demand for a change towards increased sustainability in chemistry drastically raised over the last decades. For the development of more sustainable chemical processes the term "Green Chemistry" was established and basic design principles of sustainable reactions, chemicals and processes have been formally introduced by Anastas and Warner.[9] One of these twelve principles is that "catalytic reagents (as selective as possible) are superior to stoichiometric reagents."[9] Catalysts improve the energy-efficiency of reactions, they can minimize the waste created during a process by enhancing selectivity and, furthermore, they enable new, more desirable methods of synthesizing chemical compounds. Since over 80 % of all manufactured products involve catalysts at some point of their processing,[10] a transformation towards a more sustainable chemical industry, and society overall, requires the development of more efficient catalysts.[10,11]

[1] The emissions consists of the direct emissions by the chemical production, indirect emissions by externally consumed energy and the carbon content in chemical products.

1.2 What is Catalysis?

The term catalysis comes from the Greek word κατάλυσις which means to „loosen“ or „untie“. It was first proposed in 1835 by Jöns Jacob Berzelius, who observed the common feature among several previously recorded chemical reactions that in addition to reactants and products another substance was involved, which apparently remained unchanged during the process.[12–14] Later, Wilhelm Ostwald systematically studied catalytic reactions and gave a first precise definition.[13,14] For his fundamental work he was awarded the Nobel Prize in Chemistry in 1909. Nowadays a catalyst is commonly defined as "*a substance that increases the rate of a reaction without modifying the overall standard Gibbs energy change [ΔG (Figure **1.1**)] in the reaction.*"[15]

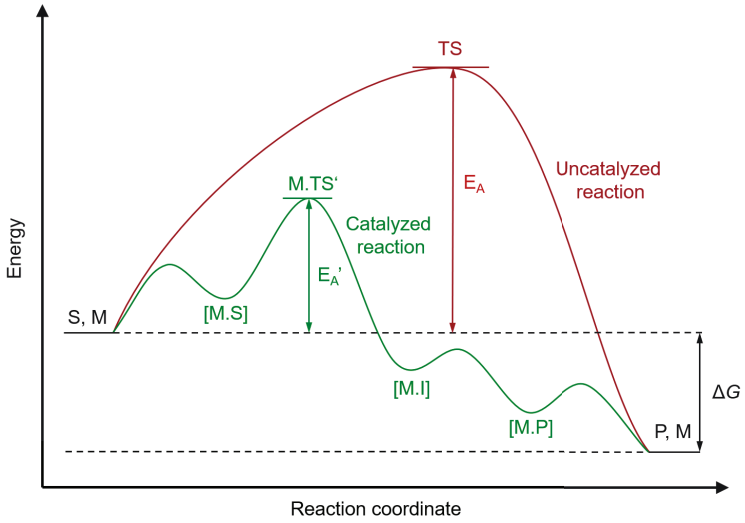

Figure 1.1: Simplified energy profile of an uncatalyzed (red) and a catalyzed (green) reaction.[Adapted from 16]

A catalyst enables an alternative reaction pathway from substrate(s) S to product(s) P with the highest energetic transition state M.TS' being lower in energy than the transition state TS of the uncatalyzed reaction pathway (Figure **1.1**). Therefore, the overall activation energy is lowered from E_A to E_A' and the reaction rate is enhanced at a given temperature according to the Transition-State-Theory.[17] Vice versa, a given reaction rate can be achieved at a lower temperature, which can save energy. A catalytic reaction is a set of sequential reactions which are called a catalytic cycle (Figure **1.2**).[16] Often, a stable precatalyst M' is initially added

to the reaction mixture and is converted under the reaction conditions to a more reactive species M, the actual catalyst. Typically, the catalytic cycle includes binding of the substrate to this catalyst under formation of a catalyst-substrate complex [M.S], its conversion via intermediates [M.I] to a catalyst-product complex [M.P] and, finally, the release of product P under regeneration of catalyst M. Theoretically, the regenerated catalyst M could reenter the catalytic cycle an infinite number of times. However, in reality side reactions can take place, leading to the reversible formation of off-cycle species [M.S'] („resting state“) or the irreversible deactivation of the catalyst [M"]. The lifetime of a catalyst is measured by the turnover number (TON), the number of catalytic cycles before catalyst deactivation, and the rate of a catalytic reaction is often given as turnover frequency (TOF), the number of catalytic cycles per unit time.[16]

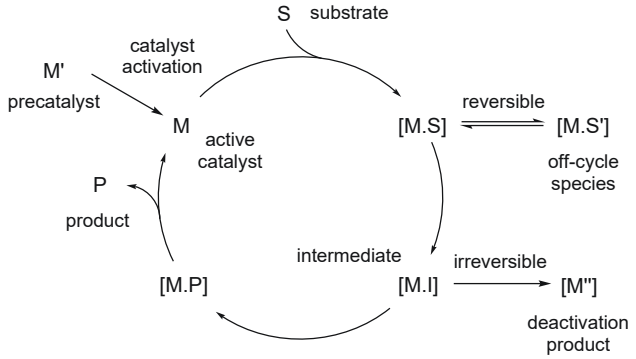

Figure 1.2: Typical catalytic cycle in schematic form.[Adapted from 16]

Besides accelerating reactions, a catalyst can also influence the selectivity of a reaction by changing the energy difference between transition states leading to different reaction products.[18] Therefore, a desired product can be obtained more favourably over an undesired sideproduct, which increases the yield of a reaction, simplifies purification of the product and, overall, reduces the generation of waste.[2] This principle applies to all kinds of selectivity such as chemoselectivity, regioselectivity and stereoselectivity.[20] Moreover, entirely different products can be obtained from the same substrates depending on the catalyst, for example, O_2 oxidation of ethylene leads to oxirane over heterogeneous Ag catalysts[21] or to acetaldehyde in the Wacker oxidation[22] using homogeneous Pd(II) catalysts (type-selectivity[23]).[16] Also, if the initial activation energy of an uncatalyzed reaction is too large (kinetically hindered)

[2] A primary principle of green chemistry: “prevention is better than cure“.[19]

to be performed under reasonable conditions, such as alkene metathesis (Section **1.6**) or hydrogenation (Section **1.3**), it can only become possible at all by applying a catalyst.

1.2.1 Homogeneous and Heterogeneous Catalysis

Commonly, catalysts are classified as heterogeneous or homogeneous referring to the state of matter (phase) of the reaction components. In heterogeneous catalysis the phases of the catalysts differ from the phases of the reactants (typically solid/liquid or solid/gas), whereas in homogeneous catalysis, catalysts and reactants exist in the same phase (typically liquid). Both types of catalysts have certain advantages and disadvantages (Table **1.1**).

Table 1.1: General comparison between homogeneous and heterogeneous catalysts.[Adapted from 24]

Criterion	Homogeneous Catalysts	Heterogeneous Catalysts
Catalyst stoichiometry	Defined	Often undefined
Catalyst structure	Defined	Often undefined
Catalyst tunability	Feasible	Challenging
Catalyst reproducibility	High	Often challenging
Mechanistic knowledge	Available	Often very limited
Reaction conditions	Usually mild	Often harsh
Diffusion problems	Barely present	Present
Catalyst poisoning	Common	Rarely
Selectivity	Usually high	Usually poor
Separation and recycling	Challenging	Facile

Heterogeneous catalysts are more widely used in industrial processes for bulk chemicals. They can be easily separated from the reaction mixture and recycled or utilized in flow reactors. Their robustness as well as their cheap and facile[3] preparation makes them efficient for the production of large quantities of platform chemicals. The synthesis of more complex molecules containing multiple functional groups often requires more selective catalysts performing under milder reaction conditions. In this regard, homogeneous catalysts are more suitable since they can be systematically finetuned to control reactivity and selectivity due to their defined structure. However, their synthesis can be more challenging and expensive and their

[3] Although the execution of the preparation procedure itself is facile, the preparation can be sensitive to various reaction parameters influencing the obtained catalyst structure and making reproducibility of catalyst batches challenging.

separation from the reaction mixture presents an ongoing problem. There are approaches to combine advantages of both catalyst classes by heterogenizing homogeneous catalysts.

Typically, homogeneous catalysts are transition metal complexes, but also catalysis by acids or bases, organic molecules (organocatalysis) or enzymes (biocatalysis) is often counted towards the area of homogeneous catalysis.

1.3 Homogeneous Hydrogenation Catalysis

Hydrogenation denotes a reaction, in which H_2 is added to an (unsaturated) substrate. It is one of the most important methods in organic synthesis and it is widely applied in industry and on laboratory scale.[25,26] Hydrogen gas is arguably the cheapest reductant and provides a much more sustainable alternative to commonly used reducing agents such as $NaBH_4$ or $LiAlH_4$ due to its superior atom economy.[27,28]

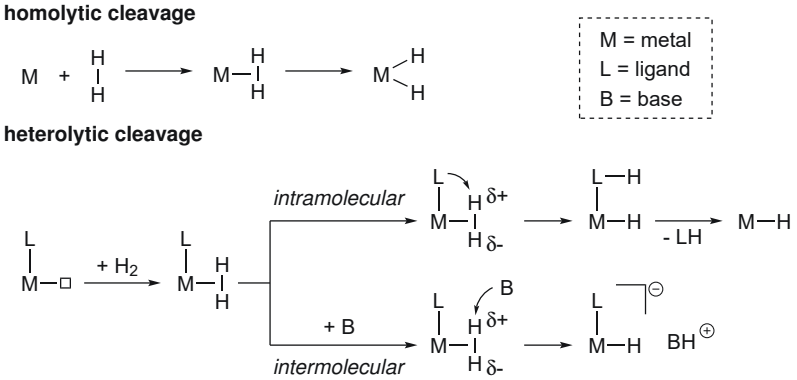

Figure 1.3: Common ways of hydrogen splitting by transition metals.[Adapted from 29,30]

Under ambient conditions, H_2 presents a rather unreactive molecule and, therefore, most of the time a catalyst is required for H_2 activation. In homogeneous hydrogenation catalysis, typically transition metal complexes are applied as catalysts. Upon activation of H_2 by these complexes, metal hydrides are obtained, which transfer the hydrogen atoms onto the substrate. Different mechanisms for the formation of metal hydrides from H_2 are known, which can be classified into homolytic or heterolytic splitting of H_2 (Figure **1.3**).[26,29–31] Initially, a dihydrogen complex is formed in both cases. Donation of electron density from the bonding H-H-σ orbital to the metal center as well as back-donation from the metal into the antibonding H-H-σ $*$ orbital leads to weakening of the H-H bond. Eventually, the bond breaks and under

oxidative addition a metal dihydride is obtained (homolytic cleavage). There can be a fine line between H_2- and dihydride-complexes, and in some cases equilibria exist in solution.[30] Furthermore, also intermolecular homolytic splitting of H_2 is known.[31,32]

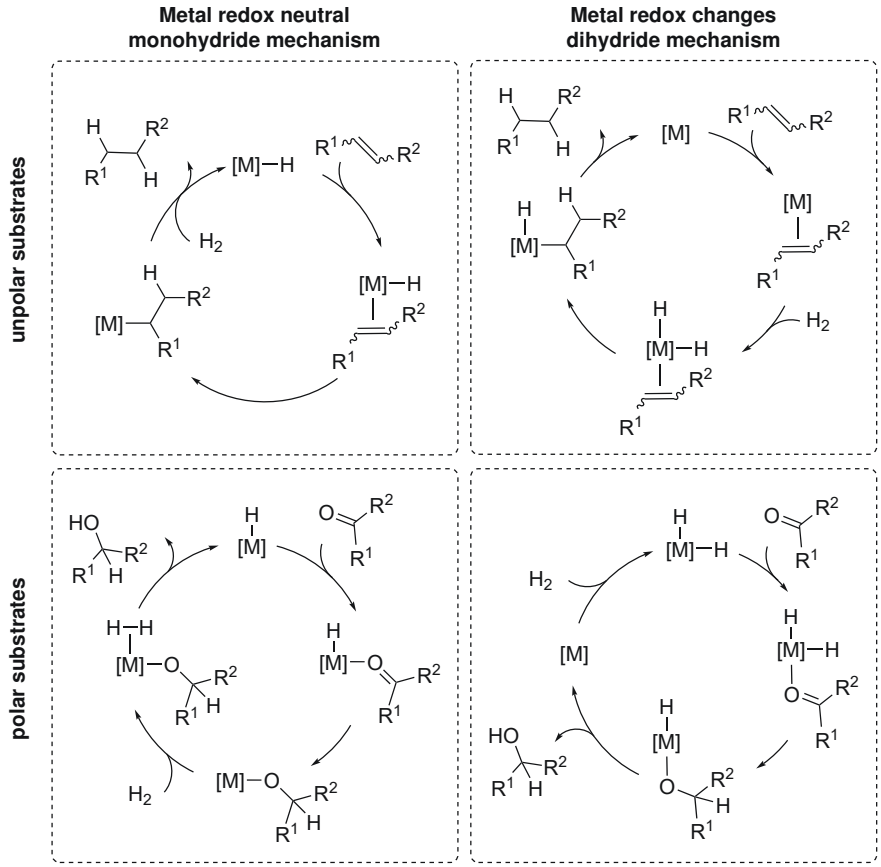

Figure 1.4: Simplified classical hydrogenation mechanisms.[Adapted from 33,34]

In case of heterolytic hydrogen splitting, the dihydrogen molecule becomes acidified upon coordination to a positively charged or electrophilic metal center and can be deprotonated by an intramolecular (a basic ligand) or intermolecular base yielding a metal hydride. If the process is intramolecular and takes place in a concerted fashion, it is called σ-bond metathesis. Dihydrogen complexes can become very acidic, i.e. more acidic than sulfuric acid, and their acidities have been intensively studied.[26,35–38] Frustrated Lewis acid-base pairs (FLPs) present another method of splitting dihydrogen, which does not involve any metal atoms.[39,40]

From a simplified viewpoint, there are two classical mechanistic scenarios for the hydrogenation of unpolar (e.g. olefins) or polar (e.g. ketones) substrates, respectively (Figure **1.4**).[33,34] In the monohydride mechanism (left) changes of the metal oxidation state are avoided. After substrate coordination and hydride transfer to the coordinated substrate, H_2 heterolysis occurs by proton transfer to alkyl (olefin hydrogenation) or alkoxy (ketone hydrogenation) ligands. In case of the dihydride mechanism (right), oxidative addition yields a dihydride complex before or after substrate coordination. This is followed by hydrogen transfer and reductive elimination. Formally, ±2 metal redox changes occur in this scenario.[33,34]

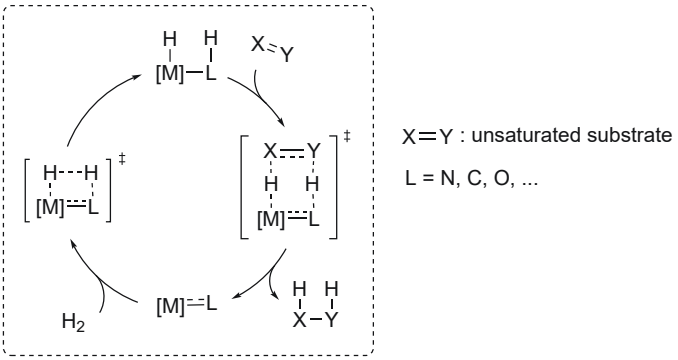

Figure 1.5: Simplified non-classical bifunctional hydrogenation mechanism.[Adapted from 33,34]

Next to the classical mechanisms, there are also several catalysts associated with a non-classical, bifunctional mechanism (Figure **1.5**).[33,34,41,42] In contrast to classical mechanisms, where ligands only act as spectators, here, both metal and ligand are directly involved in bond activation processes. Typically, the bifunctional ligand facilitates catalysis by participating in protonation/deprotonation steps and the transfer of hydrogen atoms from catalyst to substrate occurs via an outer-sphere mechanism, in which the substrate is not directly coordinated to the metal center. This concept is commonly referred to as metal-ligand cooperation (MLC).[33,41]

1.4 Homogeneous Noble Metal Hydrogenation Catalysts

The discovery of Rh complex $[Rh(PPh_3)_3Cl]$ as a catalyst for the hydrogenation of unhindered alkenes in 1965 by Wilkinson and others[43,44] marked a breakthrough and started a new era in hydrogenation catalysis (Figure **1.6**).[45] Although homogeneous hydrogenation catalysts had been described before,[46–48] it was the first time that the rates were comparable to the heterogeneous counterparts.[49] An improvement of Wilkinson's catalyst presented the cationic Rh

complexes developed in the following years by Schrock and Osborn.[50] In these complexes, one of the strongly bound phosphines is replaced by a weakly coordinating diene. Instead of dissociation of one phosphine ligand, hydrogenation of the diene yields the active catalyst more easily. Further development of the field focused on the achievement of enantio- and diastereoselective hydrogenation by the replacement of PPh_3 in the Rh complexes by chiral monodentate phosphines (Knowles,[49,51] Horner[52]) or bidentate diphosphines (Kagan,[53,54] Knowles[55,56]), which lead to the Monsanto process for the industrial production of L-DOPA, a drug for the treatment of Parkinson's disease.[57–59] The Rh-based catalysts, however, were often inefficient for trisubstituted and almost inactive for tetrasubstituted alkenes. This issue was addressed by Crabtree, who studied Ir analogues of the Schrock-Osborn catalysts.[60,61] Eventually, replacement of one phosphine for a less strongly bound pyridine ligand yielded very active catalysts, remarkably, also for highly substituted alkenes.[62] Unfortunately, its practicability was limited due to the sensitivity towards moisture and protic solvents as well as the formation of catalytically inactive iridium hydride clusters often leading to incomplete alkene conversion.[63–65] In the 1990s, the group of Pfaltz developed more stable, chiral variants[66,67] by introducing bidentate phosphine-oxazoline (PHOX) ligands.[68–70]

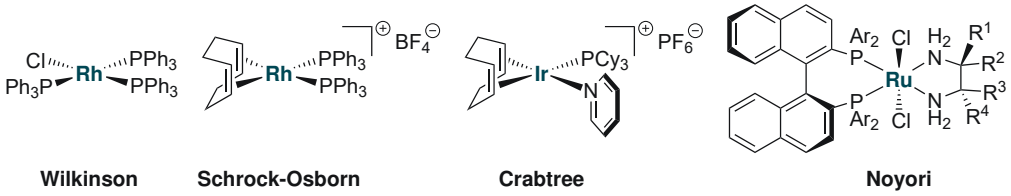

Figure 1.6: Milestones in the development of homogeneous hydrogenation catalysts.[Adapted from 45]

A major contribution was made by Noyori, who synthesized the axially chiral BINAP ligand and its Rh complexes and investigated their use in the enantioselective synthesis of amino acids from α-(acylamino)-acrylic acids or esters.[59,71–74] The hydrogenation proceeded slowly and high enantioselectivity was only obtained under certain conditions. Still, the complexes were very efficient for the asymmetric isomerization of allylamines,[75,76] leading to an industrial use in the Takasago menthol process.[77,78] Change of the metal from Rh(I) to Ru(II) successfully resulted in active catalysts for asymmetric hydrogenation of olefines and functionalized ketones.[59,79–82] The introduction of diamine ligands marked a breakthrough as it greatly improved the catalyst's activity and enabled hydrogenation of unfunctionalized ketones.[59,83–85] The increased performance by the „NH-effect" can be attributed to a change from a classical

mechanism (see Figure **1.4**) to a non-classical bifunctional mechanism, which involves the NH-function adjacent to the metal center (Figure **1.5**).[86–91] The detailed mechanism is still subject of ongoing discussions and the NH group might not be deprotonated but contribute to stabilization of transition states via hydrogen bonding.[92–95] For their groundbreaking research, Noyori and Knowles received the Nobel Prize in 2001 (together with Sharpless).

Inspired by Noyori's work, in the following years many efficient Ru-based hydrogenation catalysts bearing bifunctional ligands have been developed (Figure **1.7**).[96–102]

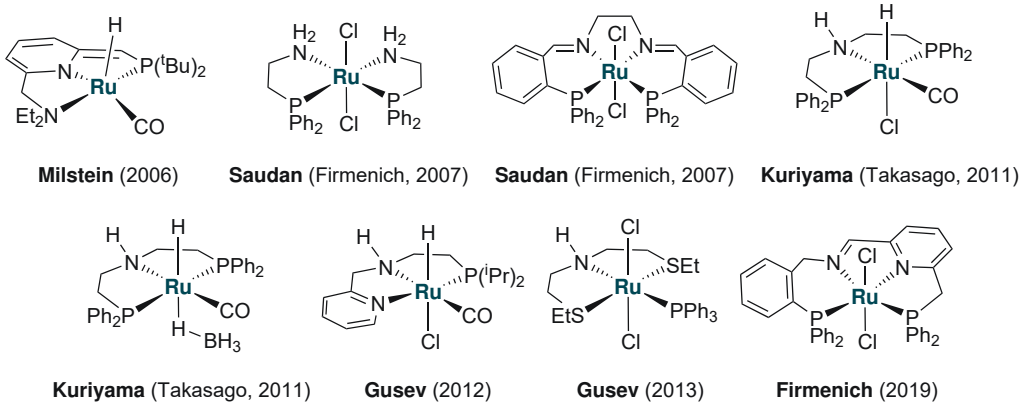

Figure 1.7: Selected highly efficient bifunctional Ru-based hydrogenation (pre)catalysts.

1.5 Homogeneous Non-Noble Metal Hydrogenation Catalysts

Due to their remarkable stability and high activity noble metal complexes have been the cornerstone of homogeneous hydrogenation catalysis as seen in the previous section. However, they have several disadvantages (Table **1.2**) and therefore, since the beginning of the millennium many efforts were made to develop non-noble metal alternatives.[34,103,104] The most obvious downside are the high costs which are linked to the low natural abundance but also the production rates of noble metals.[105] With respect to costs of a catalyst, ligands must also be considered, which can be similarly expensive (especially chiral ligands) as noble metals.[104]

Furthermore, there is a sustainability aspect in avoiding noble metals. Life-cycle assessment considering mining, purification and refining of metals estimates a significantly higher environmental footprint for noble metals.[106] Still, noble metal catalysts are usually applied at low catalyst loadings and have high end-of-life recycling rates, making their use more acceptable.[104]

A third aspect refers to toxicity. Although, toxicity can not be generalized for a certain element, since it highly depends on the corresponding (organometallic) compound and the way of exposure,[107] the oral PDE (Permitted Daily Exposure) gives an estimation of the metal's impact on human health. Especially Fe, but also Mn and Mo, have much higher PDEs than the noble metals. Because many APIs are synthesized via metal-catalyzed reactions,[108] it is beneficial to use catalysts based on metals with a high PDE to meet regulatory guidelines for residual metal contents in pharmaceutical products.[109]

Table 1.2: Comparison between selected noble and non-noble metals applied in hydrogenation catalysis.[Adapted from 110]

Metal	Conc. in Earth's Crust[111] [ppm]	Price[a] [€/kg]	Oral PDE[b] [μg day^{-1}]	Global Warming Potential[106] [kg CO_2–eq /kg]
Ru	0.0001	8224[115]	100	2110
Rh	0.00006	56353	100	35100
Pd	0.0004	31586	100	3880
Ir	0.00005	29547	100	8860
Mn	716	1.95	2500[c]	1.0
Fe	43200	0.05	13000[c]	1.5
Co	24	76.46	50	8.3
Ni	56	8.49	200	6.5
Mo	1.1	15.20	3000	5.7

[a] Average prices of 2018. Prices can vary largly and present only a rough estimate.[112]

[b] Permitted Daily Exposure (PDE) according to ICH Guideline Q3D(R1).[113]

[c] According to EMEA Guideline 2008. No longer valid since 2016.[114]

Additionally, the differing properties of non-noble metals regarding e.g., ionic radii, substrate binding constants, bond dissociation free energies, M-H hydricities, acidities of dihydrogen complexes, stability of oxidation and spin states as well as preferred coordination numbers offer the opportunity to explore new reactivity patterns which are inaccessible or challenging to achieve with noble-metals.[34,103,116] Interestingly, metalloenzymes like hydrogenases or oxidases exclusively rely on non-noble metals and exceed the efficiency of man-made catalysts by magnitudes, displaying the huge potential of non-noble metal catalysis.[116,117]

To date, many efficient catalytic systems for redox reactions but also other transformations based on non-noble metals, especially Mn, Fe, Co, Ni, Cu and Mo, have been reported[118–121]

and the field still experiences tremendous progress. In the following sections, the development of Mn- and Mo-based hydrogenation catalysts will be elaborated in more detail.

1.5.1 Homogeneous Mn-based Hydrogenation Catalysts

Inspired by the Ru-based Noyori-type catalysts (Figure **1.7**), many groups investigated non-noble metal analogs bearing bifunctional NH-group-containing ligands. A rapid development of Mn-based hydrogenation catalysts started in 2016, which has been summarized in several reviews.[34,120,122–127] Furthermore, since then many Mn catalysts for transferhydrogenation and hydrogen borrowing reactions have been developed.

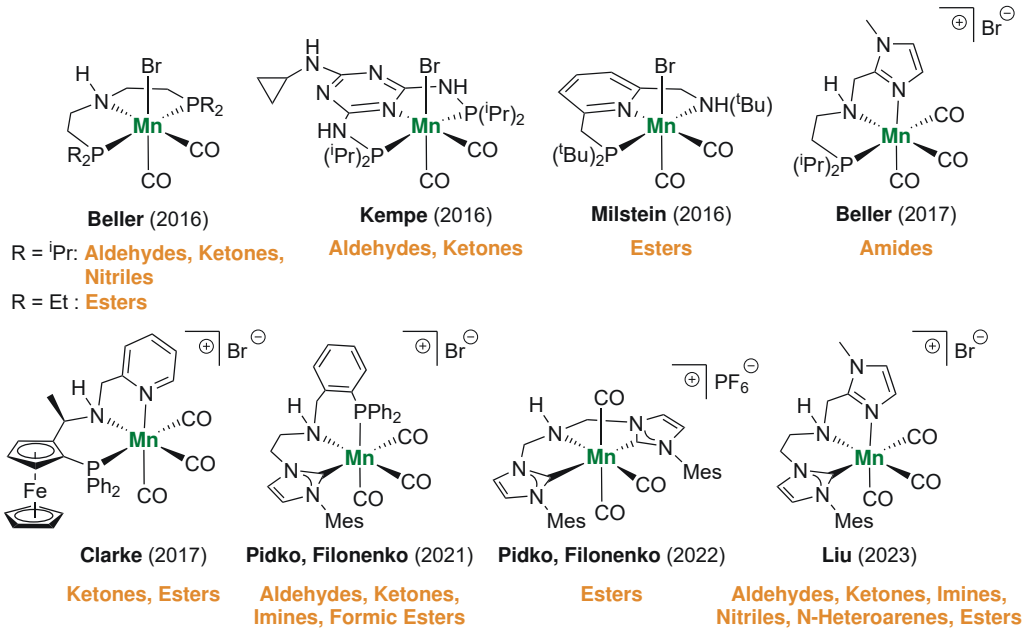

Figure 1.8: Selected Mn-based hydrogenation (pre)catalysts bearing tridentate ligands.

The starting point was Milstein's report of the first Mn-catalyzed dehydrogenative coupling,[128] closely followed by the publication of a Mn PNP pincer complex as the first Mn-based hydrogenation catalyst for aldehydes, ketones and nitriles by the Beller group (Figure **1.8**).[129] Just three months later, Kempe and coworkers described a triazine-based Mn PNP complex for the hydrogenation of aldehydes and ketones.[130] Again, some months later the Beller group reported a modified version of their initial complex, bearing Et-substituents on the phosphine donors, as catalyst for the hydrogenation of esters,[131] which was soon followed by a NNP Mn-complex of Milstein also for ester hydrogenation.[132]

Hydrogenation of amides was first achieved by an NNP Mn complex developed by Beller and coworkers.[133] The improved activity compared to the PNP congeners was investigated by the group of Liu and originated from an increased hydricity of the Mn hydrido complex paired with less steric hindrance.[134] These complexes were also applied for the hydrogenation of N-heteroarenes.[134,135]

Clarke and coworkers developed a chiral NNP Mn complex for the (asymmetric) hydrogenation of ketones, which could also hydrogenate esters at the remarkably low temperature of 75 °C.[136] More recent approaches focused on incorporation of N-heterocyclic carbenes (NHCs) as donors, which can provide certain advantages (see Section **1.6**). The groups of Pidko and Filonenko reported a mixed donor PNC Mn complex that was highly efficient for the hydrogenation of aldehydes, ketones, imines and formic esters operating at very low catalyst loadings between 0.02 mol% and 0.0005 mol%.[137] Replacement of phosphine- for NHC-donors in the classical PNP and NNP Mn complexes by the groups of Pidko and Filonenko[138] and the group of Liu[139] led to highly active and versatile catalysts for the hydrogenation of esters and various other substrate classes. However, these elaborate ligands are more tedious to synthesize and complexes were only obtained in poor yields (>30 %), limiting the practicability of these systems.

As seen so far, complexes based on tridentate pincer-type ligands experienced great success as hydrogenation catalysts. This is largely due to the fact that pincer(-type) ligands provide a well-defined, fixed coordination environment, which is highly tuneable, and that their complexes exhibit high (thermal) robustness - excellent properties for catalytic applications.[140,141] However, the synthesis of such ligands, especially unsymmetrical pincer-type ligands, can be tedious and expensive. Therefore, several hydrogenation (pre)catalysts with more simple, bidentate ligands have been developed, although there are much less examples (Figure **1.9**). These ligand structures are often easier to synthesize and therefore cheaper.[142] In 2017, the hydrogenation of esters by Mn complexes bearing bidentate P,N ligands was first reported by Pidko.[143,144] Briefly later, Sortais and coworkers also published a Mn catalyst supported by a bidentate P,N ligand for ketone hydrogenation.[145] In 2020, another contribution was made by the Khusnutdinova group with a P,N ligand-based catalyst for alkene hydrogenation.[146] A bioinspired Mn bipyridine complex was reported for the reduction of CO_2 to formate also by the groups of Khusnutdinova and Nervi.[147] In this case, the hydroxy-groups are proposed to act as proton reservoirs in a bifunctional manner, which was later confirmed when studying these systems for transferhydrogenations.[148]

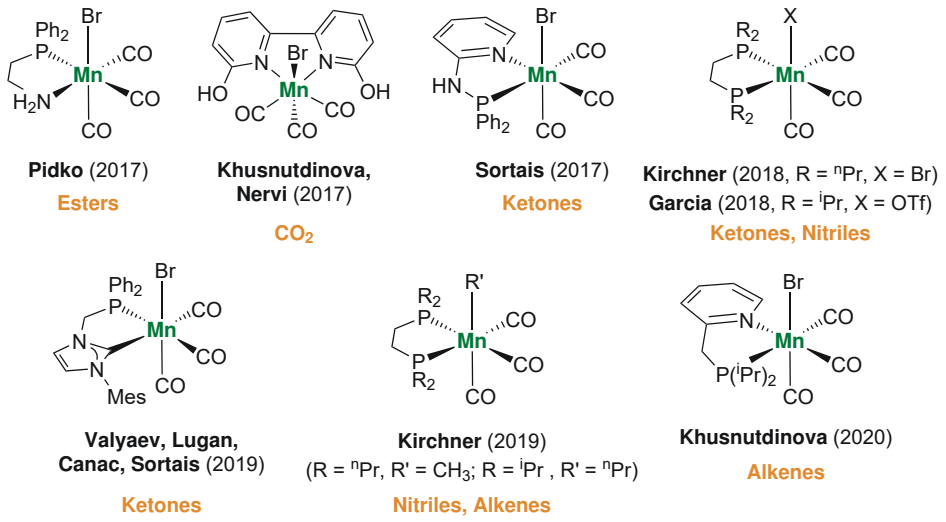

Figure 1.9: Selected Mn-based hydrogenation (pre)catalysts bearing bidentate ligands.

Independently, the groups of Kirchner and Garcia reported the use of Mn catalysts bearing simple bidentate, ethylene-bridged diphosphine ligands for ketone and nitrile hydrogenation.[149,150] Complexes with the same phosphine ligands but an alkyl instead of the bromido ligand were published later by Kirchner as precatalysts for alkene and nitrile hydrogenation.[151,152] Interestingly, with these non-bifunctional ligands an inner-sphere mechanism was proposed, in contrast to catalytic systems reported until then, which are believed to exclusively operate via outer-sphere mechanisms utilizing bifunctional ligands. The inner-sphere mechanism is enabled by the creation of a vacant coordination site after cleavage of a CO ligand through migratory insertion into the Mn-alkyl bond followed by hydrogenolysis of the resulting acyl ligand. More recently, the application of this catalytic system was extended to hydrogenation of ketones,[153] of CO_2 to formate[154] and semihydrogenation of alkynes to alkenes.[155]

Mn complexes bearing bidentate NHC-phosphine ligands developed by the groups of Valyaev, Lugan, Canac and Sortais have shown a non-classical mode of metal-ligand cooperativity.[156] Under basic conditions the methylene-linker is deprotonated resulting in a highly reactive phosphor-ylide, which readily activates dihydrogen. The complexes were applied for the hydrogenation of ketones.

1.5.2 Homogeneous Mo-based Hydrogenation Catalysts

Molybdenum is an essential trace element for nearly all organisms due to its presence in a variety of enzymes such as nitrogenase, nitrate reductases, sulphite oxidase and xanthine oxidoreductases.[157] Furthermore, a rich coordination chemistry of Mo[158,159] is known and Mo complexes are widely applied as catalysts for several organic reactions[160,161] e.g., (asymmetric) allylic substitution,[162,163] or alkene and alkyne metathesis.[164–166] Concerning hydrogenations, mainly inspired by the presence of Mo in the FeMo cofactor of nitrogenase,[167–171] many efforts were made to develope synthetic Mo-equivalents for the activation of dinitrogen.[172,173]

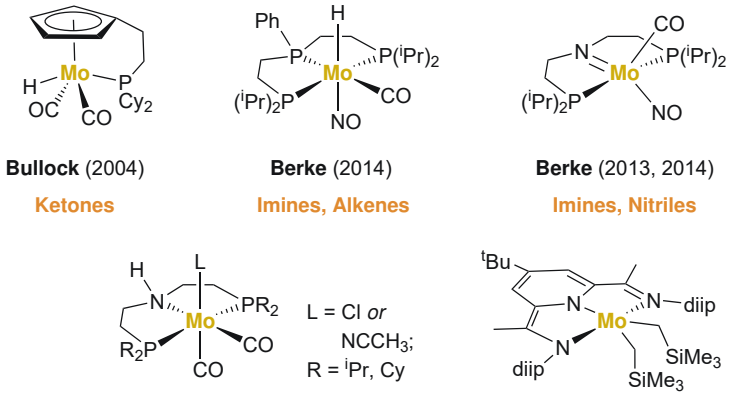

Bullock (2004)
Ketones

Berke (2014)
Imines, Alkenes

Berke (2013, 2014)
Imines, Nitriles

Beller, Nova, Junge (2018 – 2020)
Ketones, Alkenes, Formamides, Nitriles

Chirik (2018)
Alkenes, Arenes

Figure 1.10: Selected Mo-based hydrogenation (pre)catalysts.

Despite its vital role in enzyme-catalyzed redox reactions and similar properties in terms of costs, natural abundance and toxicity compared to Fe or Mn (Table **1.2**), there are far fewer reports of Mo-based hydrogenation catalysts for organic molecules (Figure **1.10**). The first report on hydrogenation by Mo complexes occurred in 1969, when Little and Frankel studied group 6 arene tricarbonyl complexes for the reduction of C=C double bonds in unsaturated fatty acid esters.[174] In the 1980s, the groups of D. and M. Darensbourg,[175–181] Markó[182,183] and Fuchikami[184] investigated the structures of anionic mono- and dinuclear group 6 carbonyl hydrides ($[HM(CO)_5]^-$ and $[(\mu\text{–}H)M_2(CO)_{10}]^-$) and their application as hydrogenation catalysts.

Bullock and coworkers developed several examples of Cp-containing Mo and W complexes as catalysts for the hydrogenation of ketones.[185–188] An ionic hydrogenation mechanism

was observed, in which acidic dihydride complexes resulting from oxidative addition of dihydrogen first undergo proton transfer followed by hydride transfer to the substrate. This is the reverse order of the classical dihydride hydrogenation mechanism (compare Figure **1.4**, bottom right).

Pursuing the ionic hydrogenation approach, the group of Berke developed NO-containing Mo complexes bearing bidentate and tridentate phosphine ligands which were successfully applied as (pre)catalysts for imine and alkene[4] hydrogenation.[189–191] Furthermore, Mo-NO complexes containing bifunctional PNP ligands were reported by the same group to catalyze the hydrogenation of imines and nitriles via a metal-ligand cooperative mechanism.[192,193] Beller and coworkers applied Mo(0) and Mo(I) complexes with the same PNP ligand framework but without a NO-ligand as (pre)catalysts for the hydrogenation of ketones, alkenes, formamides and nitriles.[194–196] The group of Chirik developed PDI-based Mo complexes as alkene and arene hydrogenation catalysts.[197] Remarkably, exchange of one imino-moiety for a chiral oxazoline-unit enabled the asymmetric hydrogenation of several fused (hetero)arenes.[198] Cyclohexadienyl hydride complexes of related Mo phosphino(oxazoline)- and phosphino(imino)-pyridine complexes were studied as catalytic intermediates.[199,200]

1.6 N-Heterocyclic Carbenes

Carbenes are defined as neutral compounds containing a divalent carbon atom with a six-electron valence shell.[201] Due to their incomplete electron octet and coordinative unsaturation, free carbenes are inherently unstable and they have been traditionally considered only as highly reactive intermediates.[201] In a seminal publication in 1988, Bertrand and coworkers achieved the first isolation and unambiguous characterization of a free carbene stabilized by adjacent phosphorus and silicon substituents.[201,202] Three years later, the group of Arduengo reported an isolable and „bottle-able“ carbene incorporated into a nitrogen heterocycle (Figure **1.11**, A).[203] This structural framework was inspired by earlier pioneering work of Wanzlick and Öfele in 1968, who described Hg and Cr complexes of such N-heterocyclic carbenes (NHCs).[204–206] The remarkable stability of NHCs mainly results from electronic stabilization provided by the nitrogen atoms. NHCs feature a singlet ground-state electronic configuration with the HOMO and LUMO best described as a formally sp^2-hybridized lone pair and an unoccupied p-orbital at the carbene carbon atom, respectively.[201] The adjacent nitro-

[4] In the case of alkenes, a classical dihydride hydrogenation mechanism is proposed.[189]

gen atoms stabilize this structure, both inductively by withdrawing electron-density from the occupied σ-orbital and mesomerically by donating electron-density into the empty p-orbital (Figure **1.11**, B). Additionally, the cyclic nature of the NHCs helps to favor this singlet ground state by forcing the carbene into a bent, more sp^2-like arrangement.[201] If the N-heterocycle is unsaturated, the resulting partial aromaticity of the 6π-electron system further stabilizes the structure.[201,206] Besides electronic effects, sterically demanding *N*-substituents (e.g. Ad) kinetically stabilize the carbene by disfavoring dimerization to the corresponding olefine (Wanzlick equilibrium).[201,207,208] NHCs containing alternative heteroatoms (e.g. S, O, P) or only one nitrogen atom have also been reported.[201,209]

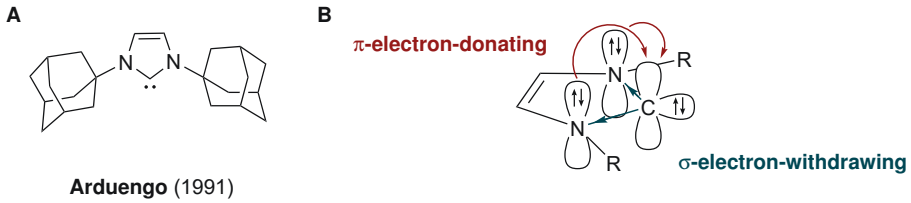

Figure 1.11: A: First isolated free NHC by Arduengo and coworkers.[203] B: Electronic effects contributing to the stabilization of NHCs.[Adapted from 201]

NHCs are mostly applied as ligands in transition metal complexes. While σ-donation is the major component of the metal-NHC bond, there are also contributions from π-backbonding into the carbene p-orbital and π-donation from the carbene p-orbital.[201,210,211] The strong σ-donor and relatively weak π-acceptor properties of NHCs make their coordination characteristics similar to those of phosphines.[212,213] However, NHCs are generally more electron-donating than phosphines as indicated by comparing, for example, Tolman electron parameters (TEP) of both ligand classes.[201,214] Therefore, typically strong NHC-metal bonds are obtained, resulting in thermally and oxidatively stable complexes. Moreover, there are differences regarding the steric properties. While sp^3-hybridization of phosphines leads to a cone-shaped spatial arrangement, NHCs are sterically more anisotropic and are often best-described as fan-shaped with the N-substituents oriented towards the metal center. The steric properties of NHCs can be conveniently quantified using the „buried volume“ descriptor ($\%V_{bur}$) developed by Nolan, Cavallo and coworkers.[215] The variation of electronic and steric parameters of NHCs can be easily realized due to the modular synthesis via various well-established routes.[201,212,216] In contrast, the structural variation of phosphines is often not trivial. Additionally, steric and electronic properties in phosphines can hardly be modified separately, since the change

of substituents affects both parameters, whereas in NHCs variation of *N*-substituents, backbone functionality and class of heterocycle offers more independent finetuning of ligand properties.[201]

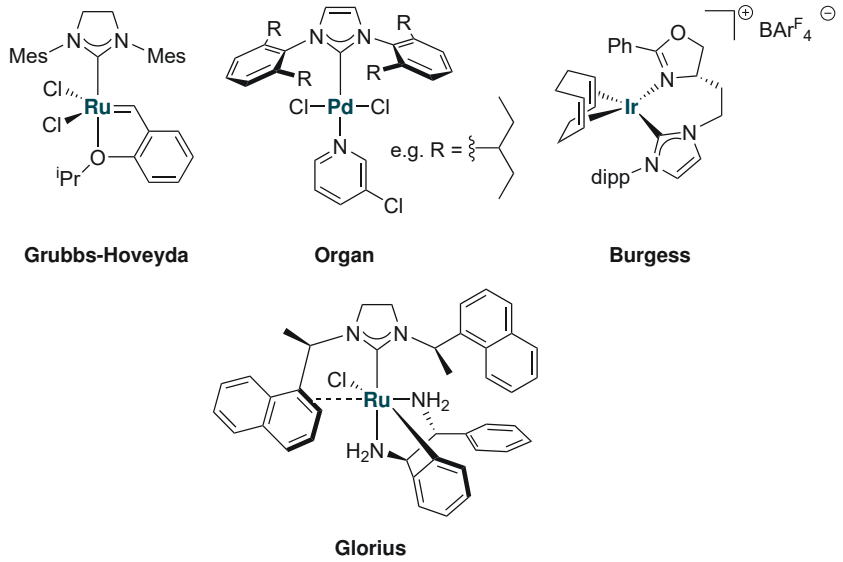

Figure 1.12: Selected NHC-containing transition metal (pre)catalysts.[217–220]

The attractive features of metal-NHC coordination led to a widespread use of NHC-transition metal complexes in homogeneous catalysis (Figure **1.12**).[201] Due to the presence of phosphine-donors in many established catalysts (see Section **1.4** and Section **1.5**), the similar properties of NHCs offered the chance of a direct replacement often resulting in improved catalysts. The probably most prominent example are Ru catalysts for alkene metathesis developed by the groups of Grubbs and later Hoveyda.[221–226] Replacement of an initially used PCy_3 ligand by an NHC moiety led to improved catalyst stability and activity in the 2nd generation catalysts.[217] Furthermore, incorporation of NHC ligands in Pd catalysts, gave very stable cross-coupling catalysts, as first established by Herrmann and coworkers in 1995.[227] Strongly electron-donating NHC ligands increase the electron-richness of the central metal atom, facilitating oxidative addition, while bulkiness of the *N*-substituents accelerates reductive elimination. Such Pd-NHC complexes, e.g. developed by Organ and coworkers, enabled the coupling of challenging substrate classes such as aryl chlorides or alkyl halides.[218,228,229] Moreover, NHCs have been incorporated into catalysts for (asymmetric) hydrogenations. For example, inspired by the successful PHOX Crabtree/Pfaltz-type catalysts for enantioselective olefine

hydrogenation (see Figure **1.6**),[230] replacement of the phosphine- by an NHC-donor was realized by the groups of Burgess[219,231] and Pfaltz,[232] among others. Also, different Ru-based catalysts bearing chiral NHC ligands have been investigated by the group of Glorius for asymmetric hydrogenations of several substrate classes including benzofuranes, indoles or benzothiophenes.[220,233–235]

Next to ligands containing a single NHC unit, many efforts were made to synthesize poly(NHC) ligands incorporating multiple NHC moieties such as bidentate bis(NHC) ligands, tripodal tris(NHC) ligands or pincer-type ligands with NHC donors.[236–241] All these ligand systems take advantage of the chelate effect[242–245] for the formation of even more stable complexes.[239] Especially, bidentate bis(NHC) ligands have attracted much attention due the high stability of corresponding metal complexes as well as their simple and modular synthesis allowing for the finetuning of steric and electronic properties.[237,241] Mainly noble metal complexes (Rh, Ir, Pd, Ru) of these ligands have found catalytic applications in e.g., cross couplings or transfer hydrogenations,[241] but also many complexes of first row transition metals are known, although their catalytic applications are more scarce.[240]

Besides the use as ligands in transition metal complexes, NHCs have been valuable for several other applications[246] e.g., as organocatalysts,[247] in surface chemistry and material science[248] or for the stabilization of reactive main group element species.[249]

2 Motivation and Objectives of this Work

Over the last decade, numerous efficient (de)hydrogenation catalysts based on non-noble metals have been developed. This trend is mainly driven by the economic and ecological benefits compared to noble metals, but also by academic interest. Despite the enormous progress, the known catalysts exhibit a low structural diversity with the vast majority of reported systems relying on phosphine-based ligands containing bifunctional sites. Often, the downside of such ligands is their tedious (and expensive) synthesis, which restricts an implementation on larger scale. Moreover, the application of structurally similar catalysts may lead to limitations for the discovery of new reactivities.

Furthermore, research mainly focused on the first-row transition metals Fe, Co, Ni and, above all, Mn. For the same economic and ecological advantages of these elements, the much less recognized group 6 metals should also be considered, as they are comparable in terms of costs, environmental impact and toxicology. In particular Mo offers great potential due to its distinctive coordination chemistry and essential role in enzymatic processes.

With this in mind, the main objectives of this work were:

- the development of non-noble metal hydrogenation catalysts with more simple and cheaper ligand structures while maintaining high catalytic activity,
- the investigation of group 6 metal complexes as hydrogenation catalysts.

Due to the omnipresence of phosphines in established hydrogenation catalysts, the similar properties of NHCs make them a promising structural moiety. The usually high (air) stability of NHC transition metal complexes paired with the possibility for precise fine-tuning of ligand properties offers huge potential for the development of improved catalysts.

In the following chapter, results from the published articles included in this thesis will be summarized. The first section deals with the development of novel Mn catalysts featuring simple, bidentate bis(NHC) ligands for the hydrogenation of various substrate classes. The second part is based on previous work on Mo PNP pincer complexes[194–196] and extends their application to the semihydrogenation of alkynes. Finally, Mo as a central atom is combined with bis(NHC) ligands, leading to novel catalysts for the hydrogenation of esters.

3 Summary of Published Articles

3.1 Bis(N-Heterocyclic Carbene) Manganese(I) Complexes: Efficient and Simple Hydrogenation Catalysts

Initially, Mn complexes with chelating bis(NHC) ligands were reported as (pre)catalysts for the electrocatalytic reduction of CO_2 by the groups of Lloret-Fillol and Royo.[250] The Royo group extended their use to hydrosilylation reactions[251–253] and, furthermore, the complexes were applied for hydrogen borrowing[254] and transfer hydrogenation reactions.[255] Due to the simplicity of the ligand framework and these promising results in reduction catalysis, the potential of bis(NHC) Mn complexes as hydrogenation catalysts should be explored.

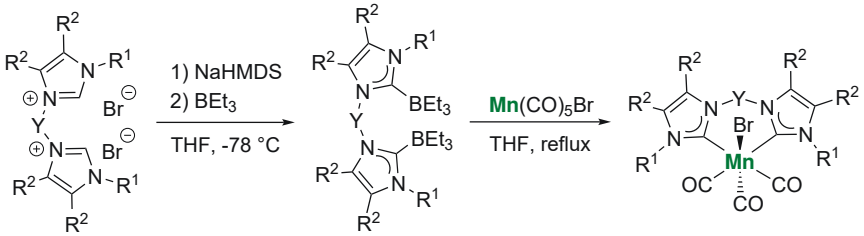

	R^1	Y	Yield [%]
3a	Me	CH_2	97
3b	^{i}Pr	CH_2	74
3d	Ph	CH_2	80
3e	Bn	CH_2	83
3i	Me	$(CH_2)_2$	80

	R^1	Y	Yield [%]
3g	Me	CH_2	91
3h	^{i}Pr	CH_2	86
3j	Me	$(CH_2)_2$	49

	R^1	Y	Yield [%]
3f	Me	CH_2	69

Scheme 3.1: Synthesis of bis(NHC)Mn complexes **3** from bis(imidazolium) salts **1** via bis(NHC)-BEt_3 adducts **2**. Combined yields over two steps.

The work started by synthesizing bis(NHC) Mn(I) complexes **3** with varying substituents to identify electronic and steric influences. Previously, complexes **3** have been prepared

directly from bis(imidazolium) salts **1**, KO^{t}Bu and $Mn(CO)_5Br$. However, this route required a tedious aqueous workup procedure to separate complexes **3** from inorganic salts.[250] Therefore, we thought of decoupling the deprotonation and complexation step by utilizing NHC-BEt_3 adducts **2** as stable NHC synthons. Since the use of $NaHBEt_3$ led to undesired products resulting from a nucleophilic attack at the bridging, electrophilic carbon atom, the less nucleophilic, sterically demanding base NaHMDS and BEt_3 were used to obtain the targeted bis(NHC)-BEt_3 adducts **2** (Scheme **3.1**). Refluxing compounds **2** with $Mn(CO)_5Br$ in THF readily yields Mn bis(NHC) complexes **3** in good to excellent yields over two steps (Scheme **3.1**).

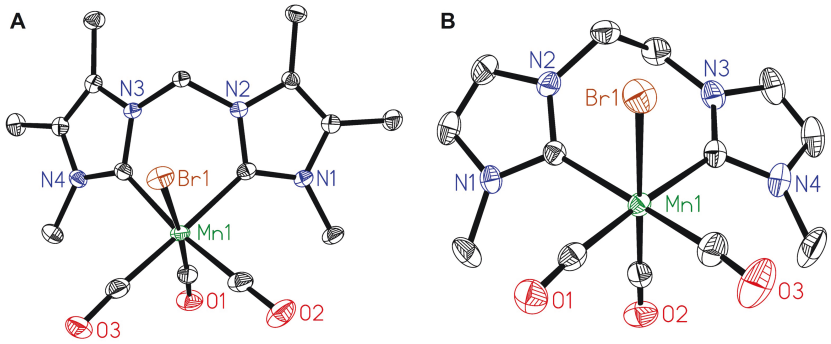

Figure 3.1: Molecular structures of complex **3g** (A) and complex **3i** (B) in the solid state. Displacement ellipsoids set at 50 % probability level. Hydrogen atoms and solvent molecules omitted for clarity. For the structure of **3i** only one of the two molecules of the asymmetric unit is shown.

The molecular structure of complex **3g** (Figure **3.1**, A) shows that for methylene-bridged complexes ($Y=CH_2$) the ligand backbone is bent, adopting a boat-shaped conformation. Therefore, two diastereomeric conformers of these complexes exist with the methylene-bridge either pointing towards (*syn*) or away (*anti*) from the bromido ligand. DFT calculations showed that for complex **3a** the *syn*-conformer is more stable by 1.69 kcal mol^{-1}, with a low ring inversion barrier between the conformers (13.52 kcal mol^{-1} for the forward and 11.83 kcal mol^{-1} for the backward inversion). This indicates an equilibrium between the conformers at room temperature which is further supported by the observation of broad signals in the ^{1}H NMR spectra of complexes **3**. For ethylene-bridged complexes ($Y=(CH_2)_2$) there are also *syn*- and *anti*-conformations, but additionally the ethylene-bridge can adopt either an eclipsed- or a staggered-conformation resulting in four possible conformers overall. The molecular structure of the *syn*-staggered-conformer of complex **3i** is shown in Figure **3.1**, B.

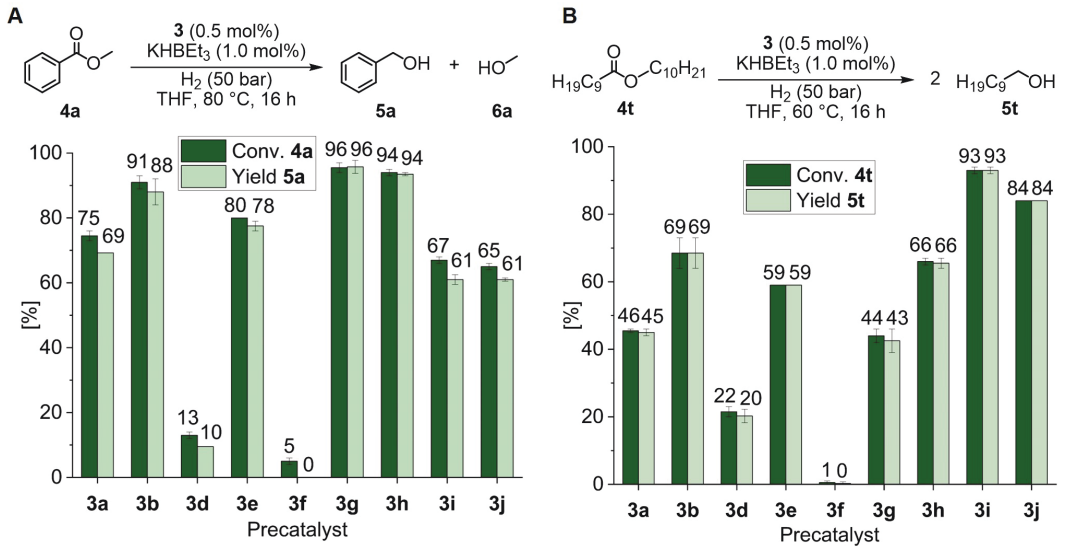

Figure 3.2: Precatalyst comparison of complexes **3** for the hydrogenation of A) methyl benzoate **4a** and B) decyl decanoate **4t**. Conditions: 1 mmol **4**, 0.5 mol% **3**, 1.0 mol% $KHBEt_3$, 4 mL THF, 50 bar H_2, 60 °C (**4t**) or 80 °C (**4a**), 16 h. Conversion of **4** and yield of **5** were determined by GC using hexadecane as internal standard. In case of **4a**, the differences of conversion and yield are mainly due to the formation of benzyl benzoate via transesterification.

The synthesized complexes **3** were tested as (pre)catalysts for the hydrogenation of esters using methyl benzoate **4a** and decyl decanoate **4t** as model substrates for aromatic and aliphatic esters, respectively (Figure **3.2**). In these experiments, 1 mol% of $KHBEt_3$ was added for precatalyst activation. Generally, more electron-donating bis(NHC) ligands led to more active catalysts.[1] This trend is observed for the ligand backbone (4,5-dimethyl-imidazole > imidazole > benzimidazole; e.g. **3g** > **3a** > **3k**) as well as for the wing-tip substituents (^{i}Pr > Bn > Me > Ph; e.g. **3b** > **3e** > **3a** > **3d**). For methyl benzoate, ethylene-bridged complexes **3j** and **3i** showed lower activity than their methylene-bridged congeners **3g** and **3a**, despite the higher inherent electron donicity of the ligands. Therefore, the worse performance is assigned to changes in the complex geometries rather than the electronic properties of these ligands.

Interestingly, for decyl decanoate, ethylene-bridged complexes **3j** and **3i** provided better results than their methylene-bridged analogs with complex **3i** giving the best yield. For wing-tip substituents, the same trend as for methyl benzoate was observed, however, dimethylation

[1] The electron donator strength of these bis(NHC) ligands has been previously studied using Pd complexes.[256] Similar trends as observed in this work have later also been reported by the groups of Royo and Tubaro.[257]

of the backbone had almost no effect and similar results for complexes **3g** and **3a** as well as **3h** and **3b** are obtained, respectively. As in the case of methyl benzoate **4a**, electron-poor complex **3k** showed almost no activity. Overall, complex **3g** yielded the best results for the hydrogenation of methyl benzoate **4a** and complex **3i** for decyl decanoate **4t**.

Since the activity of molecularly-defined ester hydrogenation catalysts often strongly depends on the applied additive, the use of various additives has been investigated. At low additive loading (1.0 mol%) $KHBEt_3$ led to the best results, while, e.g. KO^tBu, KHMDS and KH displayed significantly lower activity. KO^tBu has also been tested at higher loading (20 mol%) resulting in full conversion, but lower yield compared to $KHBEt_3$ (see original publication for details).[258]

To investigate the scope and limitations of the catalytic system, various aromatic and aliphatic esters were tested under hydrogenation conditions applying complexes **3g** (for aromatic esters) or **3i** (for aliphatic esters) as precatalysts (Scheme **3.2**). Unfunctionalized aromatic or aliphatic esters are typically smoothly converted to their corresponding alcohols in very good yields, except for some sterically hindered substrates (**4d**) or esters yielding (too) acidic alcohols such as phenol (**4e**). In this case, the formation of stable alkoxide complexes is proposed to deactivate the catalyst. Hydroxyl- (**4v**) and tertiary, secondary and, remarkably, even primary amine-groups (**4j** and **4m**) are tolerated, which was further demonstrated by the hydrogenation of the pharmaceuticals trimebutine **4av** and tetracaine **4aw**. For halogenated esters, Cl- or Br-substituents are readily tolerated (**4h** and **4i**), while F-containing substrates showed no or lower conversion depending on the fluorinated position (**4f**, **4g**), which could be overcome by increasing catalyst and/or $KHBEt_3$ loading. Presumably, the fluorinated positions are susceptible to hydrodehalogenation via nucleophilic aromatic substitution. Generally, heteroaromatic substrates proved to be challenging, still, niacin-derived ester **4p** could be converted to its corresponding alcohol with moderate yield. Interestingly, besides reduction of the ester-group, for ester **4s** reduction of the quinoline-moiety is observed. Similarly, for esters containing terminal or disubstituted C=C double bonds (**4x**, **4y**, **4z**) partial hydrogenation and/or isomerization of the double bond takes place. This reactivity is not observed for traditional bifunctional tridentate Mn-based hydrogenation catalysts (Figure **1.8**) and there are only few examples[146,151,259] for alkene hydrogenation with Mn catalysts containing bidentate ligands.[2] Due to this observed hydrogenation of other functional groups, the application

[2] The catalytic system reported by Filonenko, Pidko and coworkers contains a tridentate ligand, in which decoordination of one donor atom is observed upon precatalyst activation.[259]

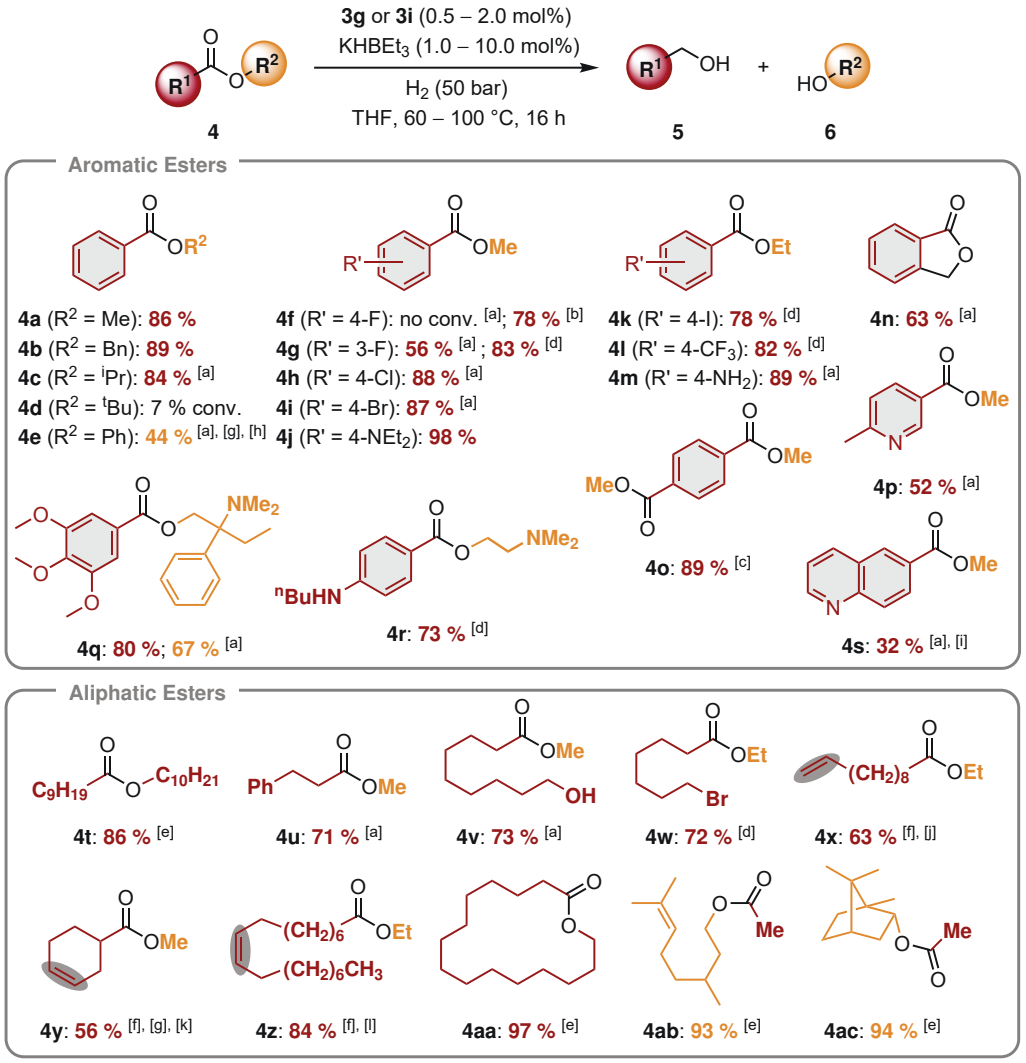

Scheme 3.2: Mn-catalyzed hydrogenation of various aromatic and aliphatic esters **4** to their corresponding alcohols **5** (red) and **6** (yellow). Isolated yields given. Precatalyst **3g** applied for aromatic esters and precatalyst **3i** for aliphatic esters. Standard conditions: 1 mmol **4**, 0.5 mol% **3**, 1 mol% $KHBEt_3$, 50 bar H_2, 4 mL THF, 80 °C, 16 h. [a] 100 °C, 1 mol% **3**, 2 mol% $KHBEt_3$; [b] 100 °C, 1 mol% **3**, 10 mol% $KHBEt_3$; [c] 80 °C, 2 mol% **3**, 4 mol% $KHBEt_3$; [d] 100 °C, 2 mol% **3**, 4 mol% $KHBEt_3$; [e] 60 °C, 0.5 mol% **3**, 1 mol% $KHBEt_3$; [f] 80 °C, 1 mol% **3**, 2 mol% $KHBEt_3$; [g] Yield determined by GC analysis; [h] 22 % benzyl benzoate observed by GC analysis. [i] 20 % methyl 1,2,3,4-tetrahydroquinoline-6-carboxylate isolated; [j] 1-undecanol was isolated; [k] 13 % cyclohexylmethanol, 5 % cyclohex-2-enylmethanol, 3 % cyclohex-1-enylmethanol and 5 % methyl cyclohexanecarboxylate observed by GC analysis; [l] Mixture of regioisomers and diastereomers with an overall (*Z*) : (*E*) ratio of 55 : 45.

of the developed catalyst system towards other substrate classes such as ketones, nitriles, N-heteroarenes as well as alkenes has been realized (Scheme **3.3**).

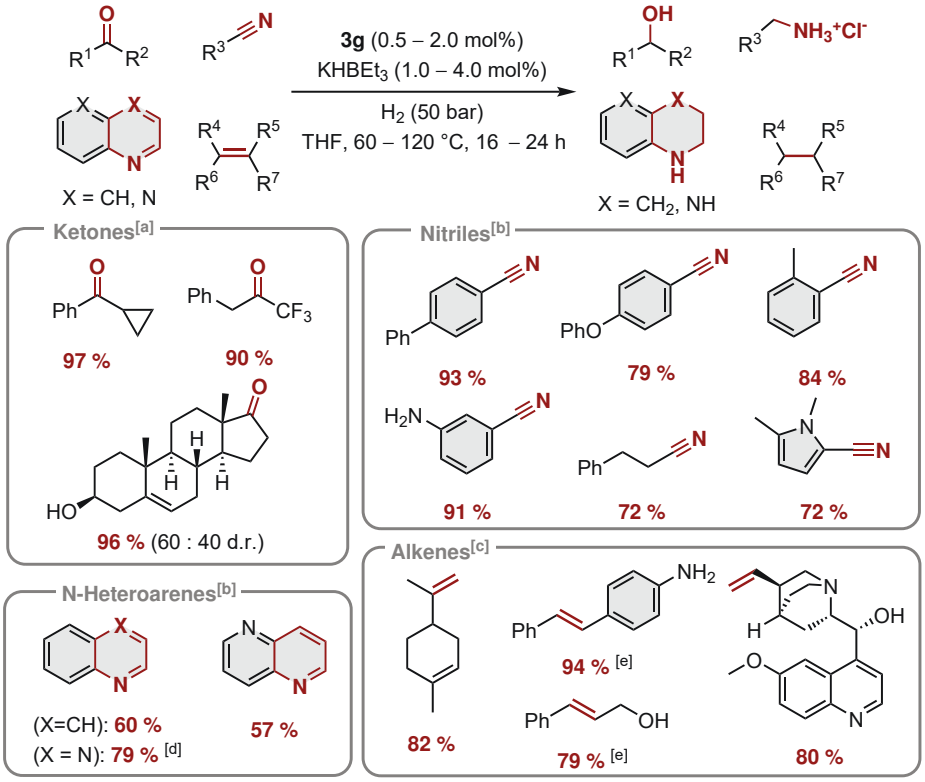

Scheme 3.3: Mn-catalyzed hydrogenation of ketones, nitriles, N-heteroarenes and alkenes. [a] 1 mmol of ketone, 1 mol% **3g**, 2 mol% $KHBEt_3$, 50 bar H_2, 4 mL THF, 80 °C, 16 h; [b] 0.5 mmol of nitrile or N-heteroarene, 2 mol% **3g**, 4 mol% $KHBEt_3$, 50 bar H_2, 2 mL THF, 120 °C, 24 h. Amines from nitriles isolated as hydrochloride salts; [c] 1 mmol of alkene, 0.5 mol% **3g**, 1 mol% $KHBEt_3$, 50 bar H_2, 4 mL THF, 80 °C, 16 h; [d] 1 mol% **3g**, 2 mol% $KHBEt_3$; [e] 100 °C, 1 mol% **3g**, 2 mol% $KHBEt_3$.

Since the catalytic system presents a scarce example of a Mn-based hydrogenation catalyst bearing a ligand expected to be non-bifunctional, an understanding of the mechanism is of high interest and mechanistic investigations by control experiments and DFT calculations were performed. Reaction of bromido complex **3a** with equimolar amount of $KHBEt_3$ at room temperature for 24 h quantitatively yielded hydrido complex **7a**. Interestingly, hydrido complex **7a** without any additive is not active in the hydrogenation of methyl benzoate (Table **3.1**, entry 2). Catalytic activity is restored, if $KHBEt_3$ or BEt_3 are added (entries 3 and 4). Therefore, $KHBEt_3$ is assumed to not only be responsible for formation of hydrido complex **7a**,

but also produce BEt_3 which is needed for catalytic activity. Besides BEt_3, other boron-based additives were tested with **7a** and, e.g. 9-BBN or $B(O^iPr)_3$ also resulted in conversion of methyl benzoate (see original publication for detail). Furthermore, the presence of strongly coordinating ligands such as CO or PMe_3 results in a complete shutdown of reactivity (entries 6 and 7).

Table 3.1: Control experiments and mechanistic investigations.[a]

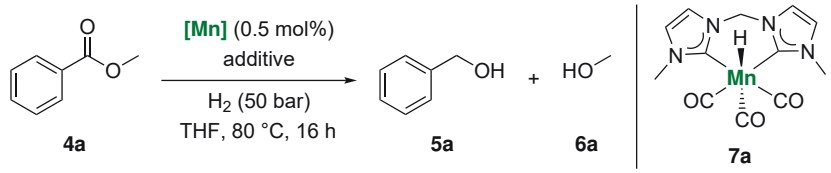

Entry	[Mn]	additive	add. load. [mol%]	Conv. **4a**[b] [%]	Yield **5a**[b] [%]
1	**3a**	$KHBEt_3$	1.0	75(2)[c]	69[c]
2	**7a**	-	-	2[c]	1(1)[c]
3	**7a**	$KHBEt_3$	0.5	73	64
4	**7a**	BEt_3	1.0	61(1)[c]	59(1)[c]
5	**3a**	BEt_3	1.0	0	0
6[d]	**3a**	$KHBEt_3$	1.0	0	0
7[e]	**3g**	$KHBEt_3$	1.0	0	0

[a] Reaction conditions: 1 mmol **4a**, 0.5 mol% [Mn], 4 mL THF, 50 bar H_2, 80 °C, 16 h.
[b] Determined by GC analysis using hexadecane as internal standard.
[c] Average of two experiments given. Standard deviation in parentheses.
[d] The autoclave was charged with 10 bar of CO and 50 bar H_2.
[e] Reaction was performed in the presence of 5 mol% PMe_3.

Also, the reaction of hydrido complex **7a**, BEt_3 and methyl benzoate **4a** in a 1:1:2 ratio was investigated by NMR spectroscopy. While no reaction was observed after heating at 80 °C for 16 h, analyzing a sample from an autoclave reaction at 50 bar H_2 pressure for 3 h confirmed quantitative conversion to benzyl alcohol and methanol. Besides **7a**, another unidentified Mn complex as well as decomposition of BEt_3 was observed. Moreover, a blue, insoluble solid was formed. IR analysis of the solid revealed two CO absorption bands at low wavenumbers (1854, 1781 cm^{-1}) indicative for an electron-rich Mn complex bearing two CO ligands. The unidentified species was catalytically inactive in the presence and absence of $KHBEt_3$.

The catalytic inactivity of hydrido complex **7a**, the observed inhibition by strongly coordinating molecules as well as the only two observed carbonyl stretches in the reaction residue, all pointed towards an inner-sphere mechanism with creation of a vacant coordination site by

loss of a CO ligand. DFT calculations were performed to gain further mechanistic insights. However, no energetically favorable pathway for the loss of a CO ligand was found. Therefore, it remains unclear how exactly a vacant coordination site is created. Due to the necessity of $KHBEt_3/BEt_3$ for catalytic activity, it is assumed that CO cleavage might be facilitated by these species, although their detailed role in the catalytic system is not clear until now.

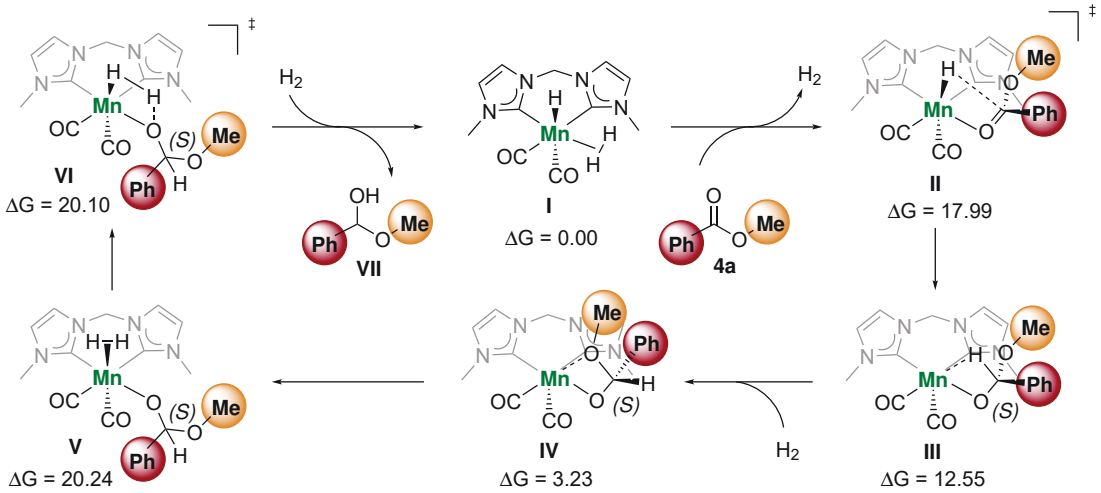

Scheme 3.4: Mechanistic proposal for the Mn-catalyzed hydrogenation of methyl benzoate. Gibbs free energies (M06L-SCRF) are given in kcal mol^{-1} and referred to **I**.

Still, a DFT-based proposal for an inner-sphere hydrogenation mechanism of methyl benzoate **4a** is presented in Scheme **3.4**. Starting from **I**, Mn-H transfer to coordinated methyl benzoate via transition state **II** occurs, followed by reorganization of the resulting methoxy-(phenyl)methanolate ligand. Hydrogenolysis of **IV** represents the rate-determining step with an apparent Gibbs free energy barrier of 20.24 kcal mol^{-1}. The liberated hemiacetale **VII** is in equilibrium with methanol and benzaldehyde, which is further hydrogenated to benzylalcohol in an analogous manner (not shown here). As expected, a much lower apparent Gibbs free energy barrier (6.88 kcal mol^{-1}) was computed for benzaldehyde hydrogenation.

Simultaneously to this work, the groups of Bastin and Sortais reported a similar Mn-based catalytic system with a methylene-bridged bis(NHC) ligand containing N-mesityl-substituents (Y=CH_2, R^1=Mes).[260] Many results are in line with observations from this work: $KHBEt_3$ was found to be the most efficient additive in 2-MeTHF. In accordance with the electronic trends observed in this work (Figure **3.2**), their precatalyst required slightly higher temperatures (100–140 °C) than the more electron-rich precatalysts **3g** and **3i** used here. Furthermore, a

comparable functional group tolerance has been observed and the corresponding hydrido complex to their precatalyst was catalytically also inactive in the absence of $KHBEt_3$.

3.2 Low-Valent Molybdenum PNP Pincer Complexes as Catalysts for the Semihydrogenation of Alkynes

As described in Section **1.5.1**, Mn PNP pincer complexes are efficient catalysts for the hydrogenation of ketones, aldehydes, nitriles and esters. Due to the success of the PNP pincer ligand motif, related complexes based on Mo have been developed and applied in hydrogenation reactions of various substrate classes (Section **1.5.2**).[194–196] Since recently the application of Mn complexes has been extended to the (*Z*)-selective semihydrogenation of alkynes,[261] the potential of the analogous Mo complexes in this transformation was explored.

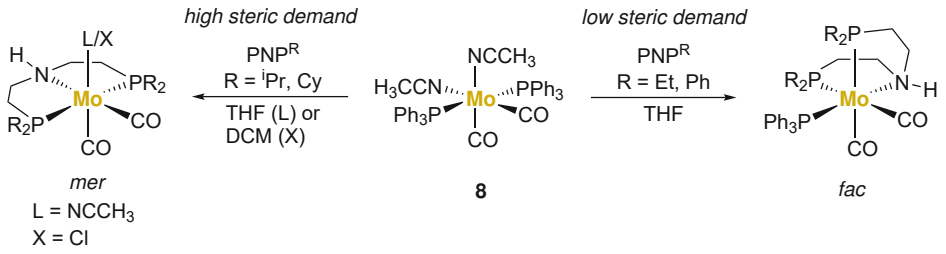

Scheme 3.5: General synthesis of low-valent Mo PNP complexes from precursor **8**.

Low-valent Mo PNP complexes have been prepared from $Mo(CH_3CN)_2(CO)_2(PPh_3)_2$ **8** and the corresponding PNP ligands according to previously published protocols (Scheme **3.5**).[194,196] In general, sterically low demanding substituents on the phosphines yield facial complexes with two CO ligands and one PPh_3 ligand remaining in the coordination sphere. With sterically more demanding substituents (e.g. ^{i}Pr, Cy) a meridional coordination of the PNP ligand is observed, in which the phosphines are further apart and therefore steric repulsion is minimized. Due to the structure of precursor **8**, in this case, a labile CH_3CN ligand remains coordinated. These meridional complexes are readily chlorinated by DCM, yielding Mo(I) complexes containing a formally anionic Cl ligand.

According to this general procedure, the syntheses of Mo complexes with a ^{t}Bu-substituted PNP ligand (PNP^{tBu}) was investigated (Scheme **3.6**). Reaction of precursor **8** with PNP^{tBu} yielded complex **13a**, for which the absence of the usually observed CH_3CN-ligand is proposed based on elemental analysis and IR spectroscopy. This can be rationalized by the high steric

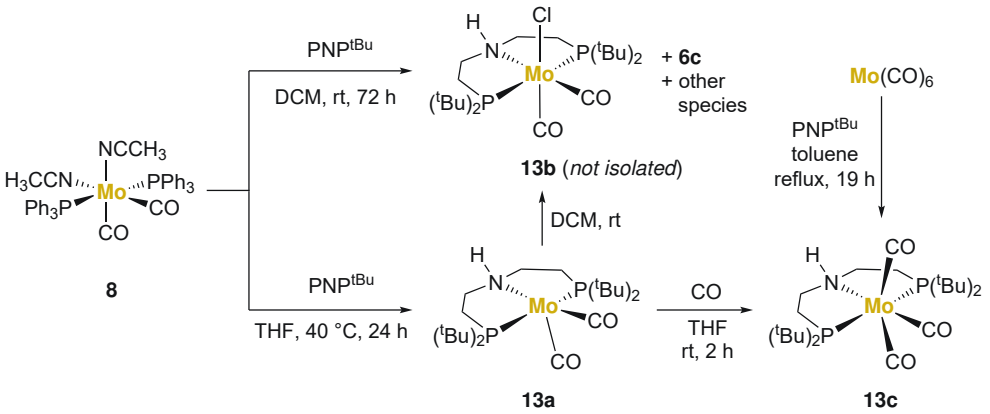

Scheme 3.6: Synthesis of ^{t}Bu-substituted Mo PNP complexes **13a**, **13b**, **13c**.

demand of the ^{t}Bu-groups. As expected, in DCM chlorination to form **13b** occurs. Exposure of complex **13a** to a CO atmosphere, yielded the tricarbonyl-complex **13c**, which could also be synthesized separately from $Mo(CO)_6$ and the respective PNP ligand. Due to the high steric demand of the ^{t}Bu-groups, the PNP ligand coordinates meridionally[3] forcing two CO ligands in *trans*-positions to each other. A strongly distorted geometry results with a C21-Mo-C23 angle of 153.79(8)°, far from linearity (Figure **3.3**, A).

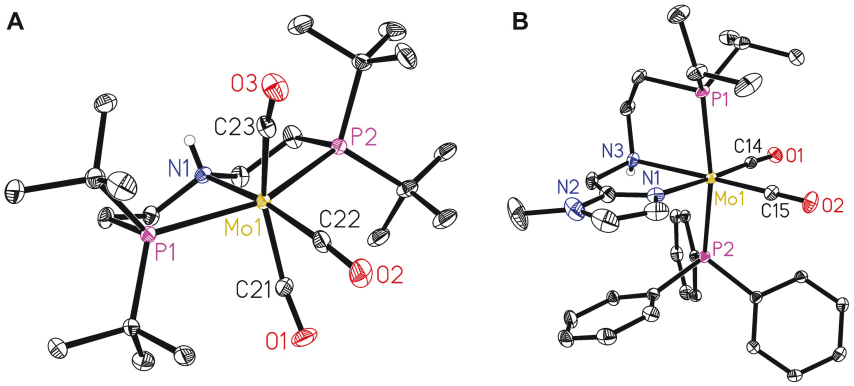

Figure 3.3: Molecular structures of Mo complexes **13c** (A) and **14** (B). Displacements ellipsoids correspond to 30 % probability. Carbon-bound hydrogen atoms and, in case of **13c**, the lower occupied atoms of the disordered ^{t}Bu-groups are omitted for clarity.

Since Mn NNP complexes showed high activity in hydrogenation reactions, a Mo complex with this ligand framework bearing ^{i}Pr-substituents at the phosphine-donor (**14**) was synthe-

[3] For related ^{i}Pr-substituted ligands a facial coordination of the PNP ligand is observed in the solid state.[194]

sized by stirring precursor **8** with the corresponding NNP ligand in THF at room temperature. In the solid state the NNP ligand coordinates facially with the phosphine-donor being located *trans* to a PPh_3 ligand remaining from the precursor (Figure **3.3**, B). Complex **14** exhibits helical chirality, resulting in the diastereotopicity of protons bound to the same carbon atom in the methylene and ethylene linker in the ligand backbone as well as the two ^{i}Pr-groups, respectively.

Various Mo precatalysts were tested for the semihydrogenation of alkynes using diphenylacetylene **15a** as model substrate (Table **3.2**). With higher steric demand of the phosphine-substituents, the activity of Mo(0) PNP complexes and also the diastereoselectivity for (*Z*)-stilbene increased (**9**<**10**<**11a**<**12a**). However, ^{t}Bu-substituents appeared to be too bulky and showed almost no activity (entries 7 and 8). The chlorinated Mo(I) complexes **11b** and **12b** performed worse than their Mo(0) counterparts **11a** and **12a** (entries 3 and 5). The novel Mo NNP complex **14** showed only poor activity despite a promising diastereoselectivity (entry 9). Interestingly, the simple Mo precursor **8** also displayed moderate activity with preferential formation of (*E*)-stilbene (entry 10). This is in accordance with the increasing (*E*)-selectivity for less sterically demanding PNP ligands (*vide supra*). In all cases, only minor overhydrogenation to diphenylethane **17a** is observed. Overall, the best results were obtained with Cy-substituted Mo(0) complex **12a** giving 89 % yield of **16a** with a 85 : 15 diastereoselectivity for (*Z*)-stilbene.

Using precatalyst **12a**, reactions parameters such as solvent, base, precatalyst loading, temperature and H_2 pressure were investigated. Non-polar, aprotic solvents and $NaHBEt_3$ were found to be necessary for obtaining high activity, although NaHMDS also showed good results. The reaction rate decreased with lower precatalyst loading, temperature and/or H_2 pressure, whereas the precatalyst loading had the strongest influence. The diastereomeric ratio was found to be independent of these parameters, except for a complete loss of selectivity at (too) low precatalyst loading. Details can be found in the original publication.[262]

To investigate scope and limitations of the catalytic system, various substituted diphenylacetylenes were reacted under the optimized reaction conditions (Scheme **3.7**). While para- and meta-methylated diphenylacetylene (**15b**, **15c**) show comparable results to unsubstituted diphenylacetylene **15p**, an ortho-Me-substituent (**15d**) gives much lower conversion, likely due to steric hindrance. For halogenated substrates varying results are obtained: While F-containing alkyne **15e** is smoothly hydrogenated, more reactive Cl- or Br-substituents lead to decreased activity and traces of hydrodehalogenated products are observed. Electron-donating

Table 3.2: Screening of various Mo precatalysts for the semihydrogenation of diphenylacetylene **15a**.[a]

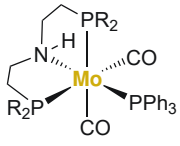

R = Et: **9**
R = Ph: **10**

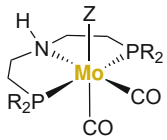

R = ^{i}Pr: **11a** (Z = $NCCH_3$); **11b** (Z = Cl)
R = Cy: **12a** (Z = $NCCH_3$); **12b** (Z = Cl)
R = ^{t}Bu; Y = none: **13a**

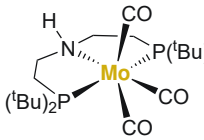

13c

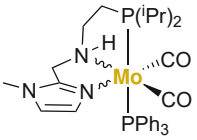

14

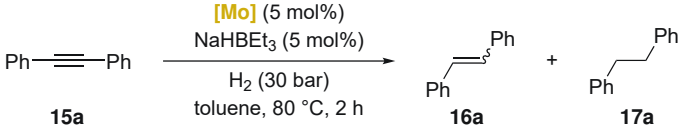

15a **16a** **17a**

Entry	[Mo]	Conv. **15a**[b] [%]	Yield **16a**[b] [%]	(*Z*)/(*E*) **16a**[b]	Yield **17a**[b] [%]
1	**9**	17	15	36 : 64	2
2	**10**	54	51	57 : 43	3
3	**11a**	68	65	75 : 25	3
4	**11b**	14	7	76 : 24	7
5	**12a**	93	89	85 : 15	4
6	**12b**	7	2	n.d.	5
7	**13a**	1	1	n.d.	0
8	**13c**	3	2	n.d.	1
9	**14**	19	15	77 : 23	4
10	**8**	21	13	33 : 67	8

[a] Reaction Conditions: 0.5 mmol **15a**, 5 mol% [Mo], 5 mol% $NaHBEt_3$ (0.5 M in toluene), 2 mL toluene, 30 bar H_2, 80 °C, 2 h. n.d. = not determined.
[b] Determined by GC analysis using hexadecane as internal standard.

substituents such as TMS (**15h**), OMe (**15i**, **15l**) or SMe (**15j**) are well tolerated and applying a longer reaction time at lower temperature (16 h at 60 °C) resulted in excellent diastereoselectivities up to 91 : 9. If an electron-withdrawing group such as CF_3 is present (**15k**, **15m**), only poor conversions and diastereoselectivities are observed, probably due to inhibition of the catalyst by formation of stable alkyne-complexes. Alkynes bearing heteroaromatic-moieties proved to be challenging, still, 27 % conversion were observed for thiophene-containing substrate **15n**. The dialkyne **15o** is smoothly converted to the corresponding dialkene. A very good diastereoselectivity for the (*Z*,*Z*)-diastereomer of 86 : 14 is obtained, and this diastereomer could be isolated in a fair yield of 47 %.

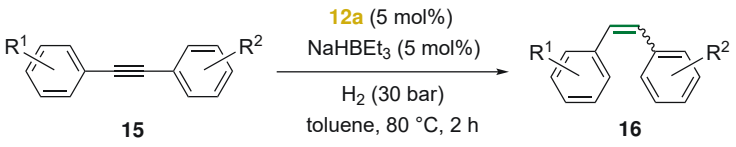

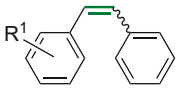

15a (R^1 = H): **98 / 96 / 87 %; 85:15**
15b (R^1 = 4-Me): **95 / 90 / 65 %; 83:17**
15c (R^1 = 3-Me): **>99 / 95 / 85 %; 85:15**
15d (R^1 = 2-Me): **9 / 5 / - %; 85:15**
15e (R^1 = 4-F): **>99 / 97 / 91 %; 81:19**
15f (R^1 = 4-Cl): **67 / 57 / - %; 81:19**
15g (R^1 = 4-Br): **8 / 5 / - %; 75:25**
15h (R^1 = 4-TMS): **>99 / 96 / 91 %; 91:9**[a]
15i (R^1 = 4-OMe): **>99 / 90 / 86 %; 84:16**[a]
15j (R^1 = 4-SMe): **98 / 96 / 91 %; 91:9**[a]
15k (R^1 = 4-CF_3): **7 / 6 / - %; 61:39**

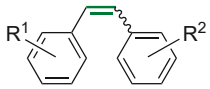

15l (R^1 = Et, R^2 = OMe): **98 / 97 / 90 %; 79:21**[a]
15m (R^1 = CF_3, R^2 = OMe): **8 / 5 / - %; 51:49**

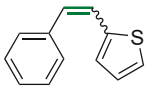

15n: **27 / 27 / - %; 55:45**[a]

15o: **>99 / 91 / 47 (*Z*,*Z*) %; 86:14**[b]

Scheme 3.7: Mo-catalyzed semihydrogenation of various alkynes. Reaction conditions: 0.5 mmol **15**, 5 mol% [Mo], 5 mol% $NaHBEt_3$ (0.5 M in toluene), 1 mL toluene, 30 bar H_2, 80 °C, 2 h. Values correspond to GC-conv./GC-yield/isolated yield. [a] 60 °C, 16 h. [b] GC-yield for all diastereomers, isolated yield for (*Z*,*Z*) diastereomer, diastereomeric ratio of (*Z*,*Z*) to other diastereomers.

Mechanistic experiments, using (*Z*)- or (*E*)-stilbene as substrates, revealed that no isomerization between these diastereomers takes place under reaction conditions. Furthermore, the inactivity of the N-methylated congener of complex **11a** confirmed the importance of the "NH" function and indicated hydrogenation via a bifunctional outer-sphere mechanism (see original publication for details).[262]

3.3 Hydrogenation of Esters Catalyzed by Bis(N-Heterocyclic Carbene) Molybdenum Complexes

Due to the high activity of Mn complexes bearing chelating bis(NHC) ligands as hydrogenation catalysts (Section **3.1**), the potential of this simple and cheap ligand class should be explored for other central metal atoms. Promising results in reduction catalysis have been obtained previously by Ke and coworkers, who successfully applied bis(NHC) Mo and Cr complexes in hydrogen borrowing reactions.[263–265] However, these complexes have not yet been described for hydrogen activation or catalytic hydrogenation and should therefore be investigated in this respect. Carboxylic acid esters were targeted as substrates, due to the efficiency of related Mn complexes in this transformation. Furthermore, no homogeneous Mo-based catalysts has been reported to catalyze the hydrogenation of esters, although Topf and coworkers previously reported a Cp-ligated W complex for this reaction.[266]

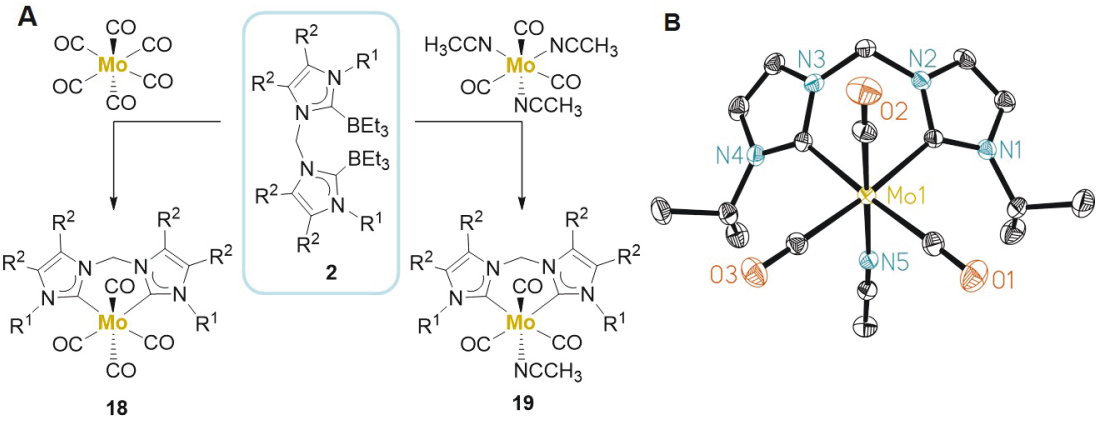

Scheme 3.8: A) Synthesis of bis(NHC) Mo complexes **18** and **19**. Reaction conditions: For **18**: toluene (56 mM), 90 °C, 16 h; for **19**: CH_3CN (75 mM), 65 °C, 16 h. B) Molecular structure of complex **19b** in the solid state. Displacement ellipsoids set at 50 % probability. Hydrogen atoms and solvent molecule are omitted for clarity. Only one of the two molecules of the asymmetric unit is shown.

The synthesis of complexes **18** and **19** followed a similar approach as for their Mn congeners using bis(NHC)-BEt_3 adducts **2** (Scheme **3.8**, A). The coordinated bis(NHC) ligands exhibit boat-shaped conformations as can be seen from Scheme **3.8**, B.

Complexes **18** and **19** have been tested as precatalysts for the hydrogenation of esters using ethyl oleate **4z** as model substrate, due to the high industrial relevance of fatty acid ester reduction (Table **3.3**).[267] Under given conditions, catalytic activity is observed for all selected

Table 3.3: Screening of various Mo precatalysts for the hydrogenation of ethyl oleate **4z**.[a]

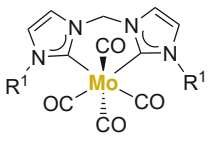

18a: R^1 = Me
18b: R^1 = ^{i}Pr

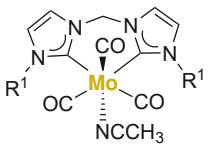

19a: R^1 = Me
19b: R^1 = ^{i}Pr
19c: R^1 = Bn

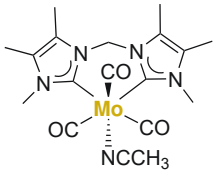

19d

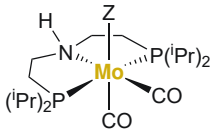

11a: Z = $NCCH_3$
11b: Z = Cl

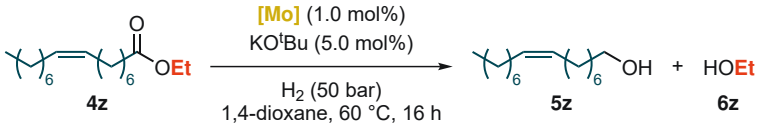

4z **5z** **6z**

Entry	[Mo]	Conv. **4z**[b] [%]	Yield **5z**[b] [%]
1	**18a**	52	17
2	**18b**	60	23
3	**19a**	48	14
4	**19b**	90	73
5	**19c**	91	76
6	**19d**	53	18
7[c]	**11a**	9	1
8[c]	**11b**	8	7

[a] Reaction conditions: 0.5 mmol **4z**, 1 mol% **[Mo]**, 5 mol% KO^{t}Bu, 4 mL 1,4-dioxane, 50 bar H_2, 60 °C, 16 h.
[b] Determined by GC analysis using hexadecane as internal standard. Difference between conversion and yield is mainly due to the formation of oleyl oleate by transesterification.
[c] 5 mol% **[Mo]**, 5 mol% $NaHBEt_3$, 2 mL toluene, 120 °C, 24 h.

precatalysts. Complexes **19b** and **19c** display the best results with similarly high conversions of 90–91 % and yields of 73–76 % (entries 4 and 5). Methyl-substituted complexes **19a** and **19d** are less active (entries 3 and 6), which might be caused by their lower solubility in 1,4-dioxane compared to **19b** and **19c**. The tetracarbonyl complexes **18a** and **18b** display moderate activity. Notably, in contrast to bis(NHC) Mn complexes (Section **3.1**), no hydrogenation of the olefin is observed for any of these precatalysts. Additionally, Mo PNP pincer complexes **11a** and **11b** were tested under suitable hydrogenation conditions (see Section **3.2**), however, only poor activity is observed (entries 7 and 8). Due to its lower molecular weight and less steric bulk around the metal center, complex **19b** was selected over complex **19c** for further investigations. Different additives have been tested with precatalyst **19b** showing that alkoxide

bases or KHMDS are best suited. Additionally, the influence of precatalyst and KO^{t}Bu loading, temperature, H_2 pressure and solvents was investigated (see original publication for details).

The catalytic system consisting of precatalyst **19b** and KO^{t}Bu displays a broad scope of aliphatic, aromatic and, remarkably, also heteroaromatic esters as well as lactones and diesters (Scheme **3.9**). A high tolerance of functional groups such as olefins (**4z**, **4x**, **4y**), hydroxyl-groups (**4v**), amines (**4ah**, **4ai**, **4ak**), halides (**4ak**, **4al**, **4f**, **4h**, **4i**, **4an**), nitriles (**4ao**) or acetals (**4aq**) is observed. Furthermore, the catalyst enables excellent chemoselectivty towards other reducible moieties like C=C double bonds (**4z**, **4x**, **4y**), nitriles (**4ao**) or quinolines (**4s**). The potential of the developed procedure is further demonstrated by the hydrogenation of late-stage molecules such as cholesteryl octanoate **4aj**, clofibrate **4al** and, remarkably, even highly-functionalized clopidogrel **4ak**.

Since the use of bis(NHC)Mo complexes **18** and **19** as hydrogenation catalysts has been unknown so far, investigation of the reaction mechanism is of particular importance and NMR spectroscopic studies, control experiments and DFT computations have been performed for that purpose. First, following the reaction of complex **19b** with KO^{t}Bu by NMR spectroscopy, leads to the observation of two new species (Scheme **3.10**). These were assigned to the anionic complexes **20b** and **21b**, resulting from substitution of the labile CH_3CN ligand by O^tBu^- or CH_2CN^-, respectively. Exposure of a mixture of **20b** and **21b** to an H_2 atmosphere at room temperature leads to the formation of a hydrido complex. Since for this species a 1:2 ratio of the hydridic resonance to the resonances of the ligand backbone is found and only one set of signals is observed for the ligand backbone, the species is assumed to be the binuclear complex **22b** with a bridging μ-hydride ligand, which is a common coordination motif for group 6 carbonyl complexes.[268,269] The same species **22b** is obtained almost exclusively by the reaction of **19b** with KO^{t}Bu under 50 bar H_2 pressure at 80 °C after 1 h. The decomposition of **22b** to complexes **20b** and **21b** upon release of H_2 pressure indicates an H_2-dependent equilibrium between these species. If D_2 is used instead of H_2, H/D-exchange for the acidic protons of **H**O^{t}Bu and C**H**$_3$CN and the bridging hydridic proton in **22b** takes place. Additionally, formation of HD and H_2 as well as very slow incorporation of D in one aromatic position of the ligand backbone of **22b** is observed. These findings, indicate a reversible heterolytic splitting of H_2/D_2. Importantly, no deuteration of the methylene-bridge of complexes **20b**, **21b** and **22b** is found, excluding the involvement of these protons in a bifunctional manner in the hydrogenation process.

Based on these experiments, DFT calculations were performed to complement the mechanistic picture (Scheme **3.11**). As observed experimentally, reaction of **19b** with an alkoxide

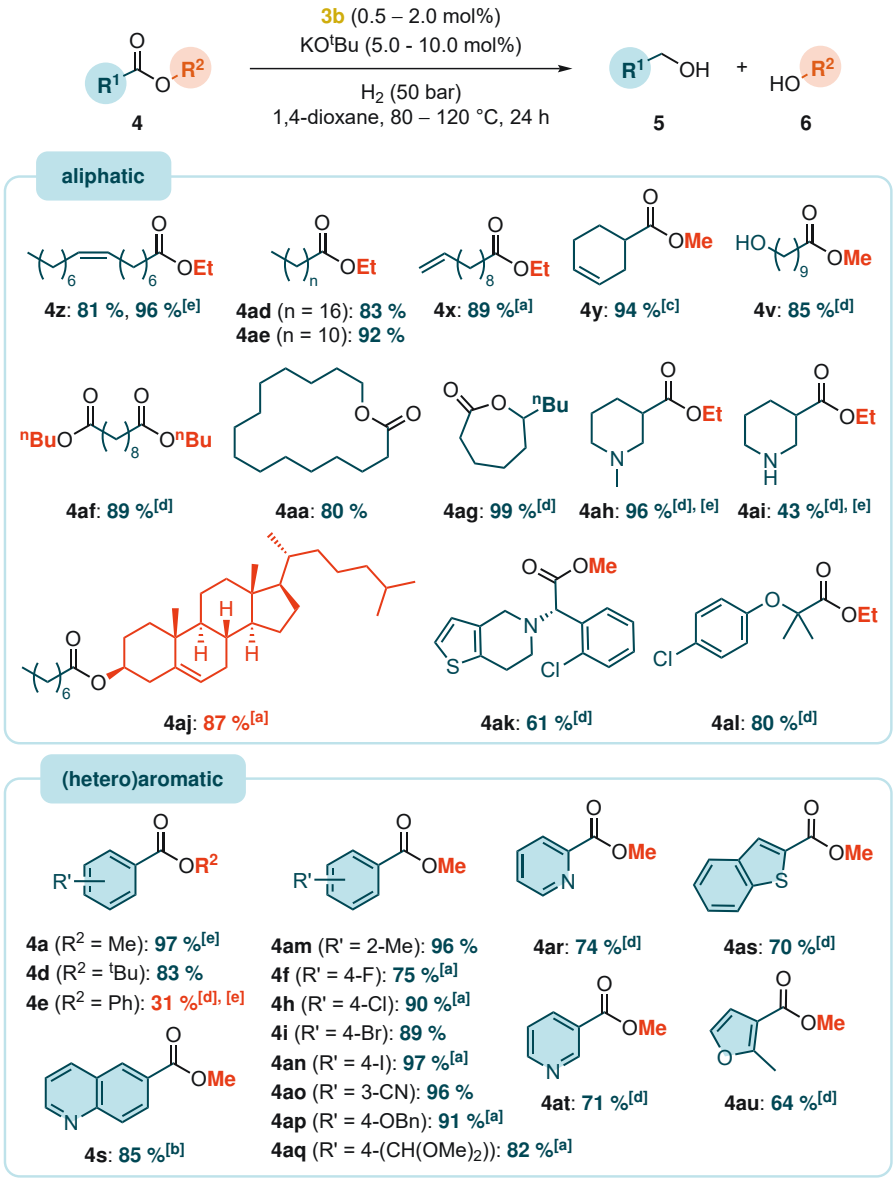

Scheme 3.9: Mo-catalyzed hydrogenation of various aliphatic and (hetero)aromatic esters. Values below the Lewis structures represent the isolated yield(s) of the corresponding alcohol(s) **5** (blue) and/or **6** (orange). Conditions: 1.0 mmol **4**, 0.5 mol% **19b**, 5 mol% KO^{t}Bu, 4 mL 1,4-dioxane, 50 bar H_2, 80 °C, 24 h. [a] 0.5 mmol **4**, 1.0 mol% **19b**, 10 mol% KO^{t}Bu, 2 mL 1,4-dioxane; [b] 0.5 mmol **4**, 1.0 mol% **19b**, 5 mol% KO^{t}Bu, 2 mL 1,4-dioxane, 100 °C. [c] 1.0 mmol **4**, 1.0 mol% **19b**, 5 mol% KO^{t}Bu, 4 mL 1,4-dioxane, 100 °C; [d] 0.5 mmol **4**, 2.0 mol% **19b**, 10 mol% KO^{t}Bu, 2 mL 1,4-dioxane, 120 °C; [e] Yield determined by GC analysis using hexadecane as internal standard.

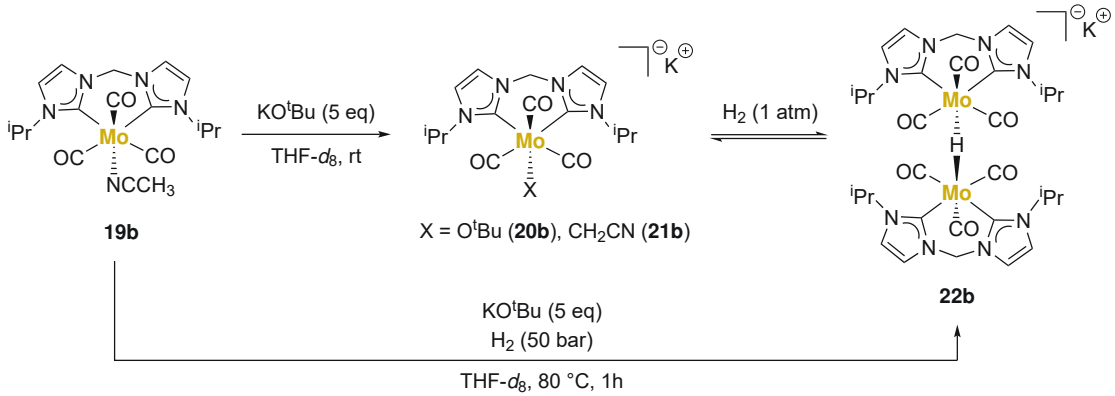

Scheme 3.10: NMR spectroscopic investigations for activation of precatalyst **19b** with KO^{t}Bu.

leads to the exergonic formation of alkoxide complexes (**20b**, **25b**, **26b**, **27b**). Highly acidic alcohols like phenol were computed to form stable alkoxide complexes (e.g. −19.71 kcal mol^{-1} for **27b**), a dead-end for catalysis. The alkoxide complexes are assumed to undergo endergonic hydrogenolysis forming the mononuclear hydrido complex **23b**. In case of L=CH_3CN, hydrogenolysis of **21b** presents an alternative pathway. Interestingly, the mononuclear hydrido complex **23b** is not observed spectroscopically and formation of complex **22b** from **23b** is found to be slightly endergonic (ΔG = 1.32 kcal mol^{-1}). However, from the stoichiometry it is clear, that higher H_2 pressures shift the equilibria from **20b** and from **22b** to mononuclear hydride **23b**, respectively. Therefore, we assume that **23b** is formed in sufficient quantities under reaction conditions (elevated temperatures and high H_2 pressures) and actually presents the catalytically competent species. Starting from complex **23b**, direct hydrogen transfer to methyl benzoate presents the rate determining step with an apparent barrier of 14.22 kcal mol^{-1} (**23b-TS1**). The resulting hemiacetalate complex **24b** eliminates acetaldehyde to form methoxide complex **25b** which regenerates hydrido complex **23b** upon hydrogenolysis. As expected, the barrier for benzaldehyde hydrogenation was calculated to be lower (8.74 kcal mol^{-1}). Due to the formation of benzoxide complex **26b** after benzaldehyde hydrogenation, an overall apparent barrier of 23.01 kcal mol^{-1} results.

In contrast, for related bis(NHC) Mn complexes an inner sphere hydrogenation mechanism after initial loss of a CO ligand was proposed, although the way of CO dissociation could not be clarified satisfyingly (Scheme **3.4**). In the related Mo complexes, a much stronger coordination of the CO ligands due to increased π-backbonding is expected as confirmed by lower wavenumbers of the CO absorption bands in the IR spectra (e.g. **19b**: 1883, 1741 cm^{-1},

7a: 1962, 1866, 1823 cm^{-1}). This is further supported by DFT calculations indicating a very high overall energetic barrier for an inner-sphere mechanism (54.5 kcal mol^{-1}), mainly resulting from the highly endergonic cleavage of CO from O^{t}Bu-complex **20b**. Therefore, the loss of a CO ligand appears energetically unfavorable, rendering hydrogenation via an inner-sphere mechanism in case of the studied bis(NHC) Mo complexes unlikely.

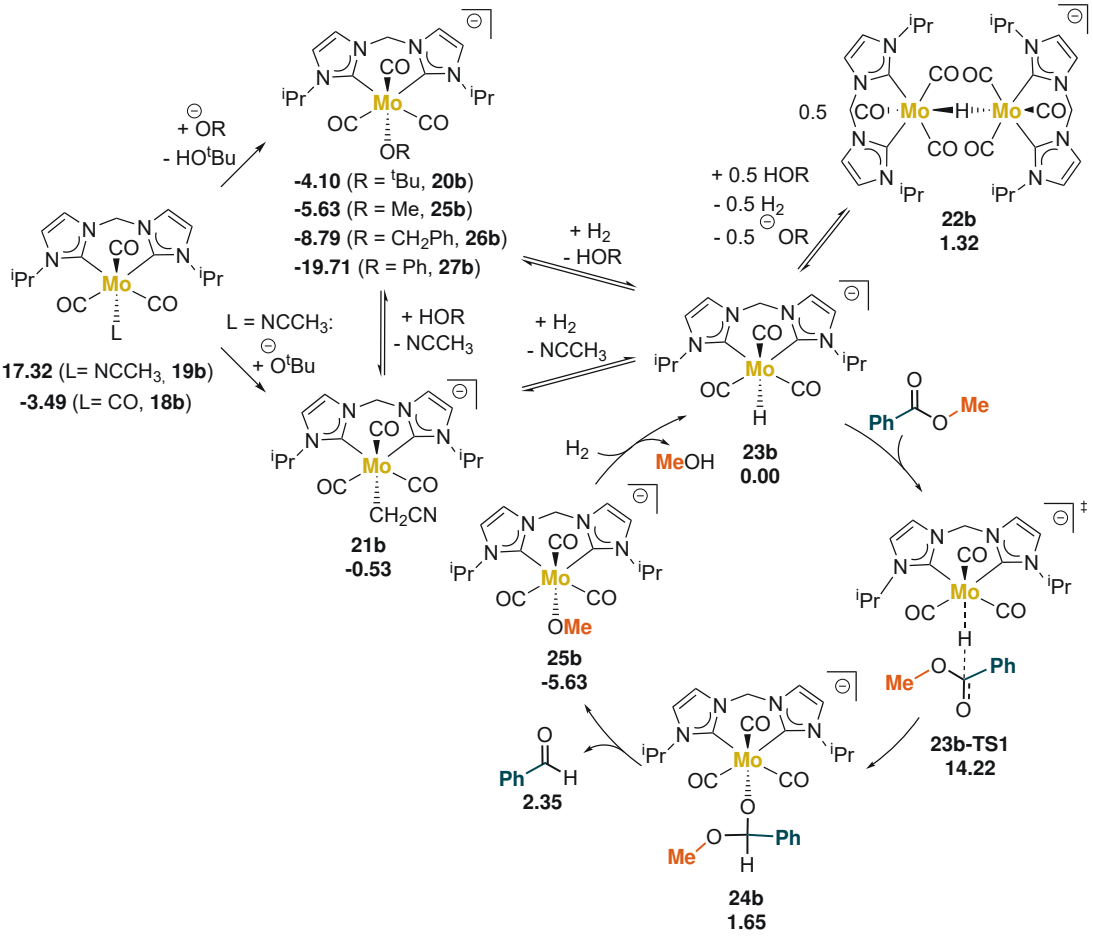

Scheme 3.11: DFT-supported mechanistic rationale for the Mo-catalyzed hydrogenation of methyl benzoate **4a**. Values below Lewis-structures represent Gibbs Free Energies in kcal mol^{-1} calculated on a M06L-SCRF/TZVP level of theory.

4 Conclusions and Outlook

Bis(NHC) Mn complexes have been prepared in high yields via an improved, straightforward protocol utilizing bis(NHC)-BEt_3 adducts as stable NHC synthons. After activation by $KHBEt_3$, the phosphine-free complexes efficiently hydrogenate various esters at low temperatures and catalyst loadings. This high activity, however, reduces their chemoselectivity, instead, the highly versatile catalysts enable hydrogenation of several other substrate classes. Based on control experiments and DFT calculations an inner-sphere mechanism is proposed. BEt_3 is necessary for catalytic activity, however, its detailed role is not fully understood yet.

Next, ^{t}Bu-substituted Mo PNP complexes, a Mo NNP complex as well as previously reported Mo PNP complexes have been investigated as precatalyst for the semihydrogenation of alkynes. By applying a Cy-substituted Mo PNP pincer complex high (*Z*)-diastereoselectivity without significant overhydrogenation is achieved. Downsides of this catalytic system remain the necessity of high catalyst loadings and a narrow substrate scope.

Building on the success of related Mn complexes, Mo catalysts bearing simple and inexpensive bis(NHC) ligands have been synthesized. In the presence of KO^tBu, these complexes hydrogenate a variety of esters at low catalyst loadings, clearly outperforming established Mo PNP pincer complexes. The lower activity compared to bis(NHC) Mn catalysts leads to improved functional group tolerance and chemoselectivity, enabling a broad substrate scope. NMR spectroscopic studies complemented by DFT computations indicate a non-bifunctional outer-sphere mechanism.

The catalytic systems presented show that efficient non-noble metal hydrogenation catalysts can be based on simple, non-bifunctional ligands and that bifunctionality is therefore not a prerequisite for high catalytic activity. Due to the proposed unusual mechanisms, future work should focus on more detailed mechanistic studies to provide an improved understanding of hydrogenation processes catalyzed by non-bifunctional systems. Furthermore, the potential of these catalysts should be explored in the hydrogenation of other, even more challenging substrate classes such as amides or CO_2. This work will inspire researchers to develop simpler yet efficient non-noble metal catalysts for wider application and the implementation of more sustainable redox reactions.

5 List of Abbreviations

ΔG difference of Gibbs free energy

%V_{bur} buried volume

^{i}Pr *iso*-propyl

^{n}Bu *n*-butyl

^{n}Pr *n*-propyl

^{t}Bu *tert*-butyl

2-MeTHF 2-methyltetrahydrofuran

9-BBN 9-borabicyclo[3.3.1]nonane

Ad adamantyl

API active pharmaceutical ingredient

Ar aryl

BAr^{F}_{4} tetrakis[3,5-bis(trifluoromethyl)phenyl]borate

BINAP ([1,1'-binaphthalene]-2,2'-diyl)bis(diphenylphosphane)

Bn benzyl

Cp cyclopentadienyl

Cy cyclohexyl

DCM dichloromethane

DFT density-functional theory

dipp 2,6-diisopropylphenyl

DOPA 3,4-dihydroxyphenylalanine

EMEA European Medicines Evaluation Agency

Et ethyl

FLP frustrated Lewis acid-base pair

GC gas chromatography

HMDS hexamethyldisilazide

HOMO highest occupied molecular orbital

ICH International Council for Harmonisation of Technical Requirements for Pharmaceuticals for Human Use

IR infrared

LUMO lowest unoccupied molecular orbital

Me methyl

Mes mesityl

MLC metal-ligand cooperation/cooperativity

n.d. not determined

NHC N-heterocyclic carbene

NMR nuclear magnetic resonance

OTf triflate, trifluoromethanesulfonate

PDE permitted daily exposure

PDI pyridine(diimine)

Ph phenyl

PHOX phosphine-oxazoline

R (organic) rest

rt room temperature

SC single crystal

SCRF self-consistent reaction field

TEP Tolman electronic paramter

THF tetrahydrofuran

TMS trimethylsilyl

TOF turnover frequency

TON turnover number

TS transition state

TZVP valence triple-zeta polarization

XRD X-ray diffraction

6 References

[1] G. Rothenberg, *Catalysis: Concepts and Green Applications*, 2nd Edition, John Wiley & Sons, **2017**.

[2] R. A. Sheldon, *J. R. Soc. Interface* **2016**, *13*, 20160087.

[3] E. R. Koch, F. Vahrenholt, *Seveso ist überall: die tödlichen Risiken der Chemie*, Kiepenheuer & Witsch, **1978**.

[4] W. Bogard, *The Bhopal Tragedy: Language, Logic, and Politics in the Production of a Hazard*, Westview Press, **1989**.

[5] W. Giger, *UWSF* **2007**, *19*, 11–23.

[6] E. Mihailidou, K. Antoniadis, M. Assael, *IRECHE* **2012**, *4*, 1–12.

[7] Umweltbundesamt, Branchenabhängiger Energieverbrauch des verarbeitenden Gewerbes, Bundesministerium für Wirtschaft und Klimaschutz, **2023**, https://www.umweltbundesamt.de/daten/umwelt-wirtschaft/industrie/branchenabhaengiger-energieverbrauch-des#der-energiebedarf-deutschlands (visited on 10/02/2023).

[8] R. Geres, A. Kohn, S. Lenz, F. Ausfelder, A. M. Bazzanella, A. Möller, Roadmap Chemie 2050, (Eds.: F. C. GmbH, D. G. für Chemische Technik und Biotechnologie e.V.), **2019**.

[9] P. Anastas, J. Warner, *Green Chemistry: Theory and Practice*, Oxford University Press, **1998**.

[10] C. R. Catlow, M. Davidson, C. Hardacre, G. J. Hutchings, *Philos. Trans. R. Soc. A* **2016**, *374*, 20150089.

[11] J. M. White, J. Bercaw, Opportunities for Catalysis in The 21st Century. A Report from the Basic Energy Sciences Advisory Committee, Basic Energy Sciences Advisory Committee, **2002**.

[12] B. Lindström, L. J. Pettersson, *CATTECH* **2003**, *7*, 130–138.

[13] J. Wisniak, *Educ. Quim.* **2010**, *21*, 60–69.

[14] C. Datta, T. V. Kondra, M. Miller, A. Streltsov, *Rep. Prog. Phys.* **2023**, *86*, 116002.

[15] A. McNaught, A. Wilkinson, *IUPAC. Compendium of Chemical Terminology (the "Gold Book")*, 2nd Edition, Blackwell Science, **1997**.

[16] R. H. Crabtree, *The Organometallic Chemistry of the Transition Metals*, 7th ed., John Wiley & Sons, **2019**.

[17] K. J. Laidler, M. C. King, *J. Phys. Chem* **1983**, *87*, 2657–2664.

[18] J. Mahatthananchai, A. M. Dumas, J. W. Bode, *Angew. Chem. Int. Ed.* **2012**, *51*, 10954–10990.

[19] B. W. Cue, M. Cann, D. J. C. Constable, N. D. Anastas, C. C. Jiménez-González, R. Wool, P. J. Dunn, R. A. Sheldon, R. Williams, D. Raynie, S. Bradley, D. C. Finster, T. Goodwin, 12 Principles of Green Chemistry, https://www.acs.org/greenchemistry/principles/12-principles-of-green-chemistry.html (visited on 09/22/2023).

[20] B. M. Trost, *Science* **1983**, *219*, 245–250.

[21] S. Rebsdat, D. Mayer in *Ullmann's Encyclopedia of Industrial Chemistry*, John Wiley & Sons, **2001**.

[22] R. Jira, *Angew. Chem.* **2009**, *121*, 9196–9199.

[23] D. Seebach, *Angew. Chem.* **1979**, *91*, 259–278.

[24] A. Behr, P. Neubert, *Applied Homogeneous Catalysis*, John Wiley & Sons, **2012**.

[25] P. A. Chaloner, M. A. Esteruelas, F. Joó, L. A. Oro in *Homogeneous Hydrogenation*, Springer Netherlands, Dordrecht, **1994**, pp. 119–181.

[26] G. J. Kubas, *Science* **2006**, *314*, 1096–1097.

[27] B. M. Trost, *Science* **1991**, *254*, 1471–1477.

[28] B. M. Trost, *Angew. Chem. Int. Ed.* **1995**, *34*, 259–281.

[29] G. Kubas, *Metal Dihydrogen and σ-Bond Complexes: Structure, Theory, and Reactivity*, Springer US, **2001**.

[30] G. J. Kubas, *J. Organomet. Chem.* **2009**, *694*, 2648–2653.

[31] P. G. Jessop, R. H. Morris, *Coord. Chem. Rev.* **1992**, *121*, 155–284.

[32] C. Rettenmeier, H. Wadepohl, L. H. Gade, *Chem. Eur. J.* **2014**, *20*, 9657–9665.

[33] M. Trincado, H. Grützmacher in *Cooperative Catalysis*, John Wiley & Sons, **2015**, Chapter 3, pp. 67–110.

[34] L. Alig, M. Fritz, S. Schneider, *Chem. Rev.* **2018**, *119*, 2681–2751.

[35] R. H. Morris, *Can. J. Chem.* **1996**, *74*, 1907–1915.

[36] K. Abdur-Rashid, T. P. Fong, B. Greaves, D. G. Gusev, J. G. Hinman, S. E. Landau, A. J. Lough, R. H. Morris, *J. Am. Chem. Soc.* **2000**, *122*, 9155–9171.

[37] R. H. Morris, *J. Am. Chem. Soc.* **2014**, *136*, 1948–1959.

[38] R. H. Morris, *Chem. Rev.* **2016**, *116*, 8588–8654.

[39] D. W. Stephan, *Science* **2016**, *354*, aaf7229.

[40] D. W. Stephan, *J. Am. Chem. Soc.* **2021**, *143*, 20002–20014.

[41] J. R. Khusnutdinova, D. Milstein, *Angew. Chem. Int. Ed.* **2015**, *54*, 12236–12273.

[42] F. Agbossou-Niedercorn, C. Michon, *Coord. Chem. Rev.* **2020**, *425*, 213523.

[43] J. F. Young, J. A. Osborn, F. H. Jardine, G. Wilkinson, *Chem. Commun. (London)* **1965**, 131–132.

[44] D. Evans, J. Osborn, F. Jardine, G. Wilkinson, *Nature* **1965**, *208*, 1203–1204.

[45] G. Helmchen, *Chem. Eur. J.* **2023**, e202301488.
[46] M. Calvin, M. Polanyi, *Trans. Faraday Soc.* **1938**, *34*, 1181–1191.
[47] M. Calvin, *J. Am. Chem. Soc.* **1939**, *61*, 2230–2234.
[48] J. Halpern, J. Harrod, B. James, *J. Am. Chem. Soc.* **1961**, *83*, 753–754.
[49] W. S. Knowles, *Acc. Chem. Res.* **1983**, *16*, 106–112.
[50] J. Shapley, R. Schrock, J. Osborn, *J. Am. Chem. Soc.* **1969**, *91*, 2816–2817.
[51] W. S. Knowles, M. J. Sabacky, *Chem. Commun. (London)* **1968**, 1445–1446.
[52] L. Horner, H. Siegel, H. Büthe, *Angew. Chem. Int. Ed.* **1968**, *7*, 942–942.
[53] T. Dang, H. Kagan, *J. Chem. Soc. Chem. Commun.* **1971**, 481–481.
[54] H. B. Kagan, T.-P. Dang, *J. Am. Chem. Soc.* **1972**, *94*, 6429–6433.
[55] W. Knowles, M. Sabacky, B. Vineyard, D. Weinkauff, *J. Am. Chem. Soc.* **1975**, *97*, 2567–2568.
[56] B. D. Vineyard, W. S. Knowles, M. J. Sabacky, G. L. Bachman, D. J. Weinkauff, *J. Am. Chem. Soc.* **1977**, *99*, 5946–5952.
[57] W. S. Knowles, *J. Chem. Educ.* **1986**, *63*, 222.
[58] W. S. Knowles, *Angew. Chem. Int. Ed.* **2002**, *41*, 1998–2007.
[59] R. Noyori, *Angew. Chem. Int. Ed.* **2002**, *41*, 2008–2022.
[60] R. H. Crabtree, H. Felkin, G. E. Morris, *J. Chem. Soc. Chem. Commun.* **1976**, 716–717.
[61] R. H. Crabtree, G. E. Morris, *J. Organomet. Chem.* **1977**, *135*, 395–403.
[62] R. H. Crabtree, H. Felkin, G. E. Morris, *J. Organomet. Chem.* **1977**, *141*, 205–215.
[63] R. H. Crabtree, M. Lavin, *J. Chem. Soc. Chem. Commun.* **1985**, 1661–1662.
[64] Y. Xu, D. M. P. Mingos, J. M. Brown, *Chem. Commun.* **2008**, 199–201.
[65] Y. Xu, M. A. Celik, A. L. Thompson, H. Cai, M. Yurtsever, B. Odell, J. C. Green, D. M. P. Mingos, J. M. Brown, *Angew. Chem. Int. Ed.* **2009**, *48*, 582–585.
[66] P. Schnider, G. Koch, R. Prétôt, G. Wang, F. M. Bohnen, C. Krüger, A. Pfaltz, *Chem. Eur. J.* **1997**, *3*, 887–892.
[67] A. Lightfoot, P. Schnider, A. Pfaltz, *Angew. Chem. Int. Ed.* **1998**, *37*, 2897–2899.
[68] J. Sprinz, G. Helmchen, *Tetrahedron Lett.* **1993**, *34*, 1769–1772.
[69] P. Von Matt, A. Pfaltz, *Angew. Chem. Int. Ed.* **1993**, *32*, 566–568.
[70] G. J. Dawson, C. G. Frost, J. M. Williams, S. J. Coote, *Tetrahedron Lett.* **1993**, *34*, 3149–3150.
[71] a. Miyashita, A. Yasuda, H. Takaya, K. Toriumi, T. Ito, T. Souchi, R. Noyori, *J. Am. Chem. Soc.* **1980**, *102*, 7932–7934.
[72] A. Miyashita, H. Takaya, T. Souchi, R. Noyori, *Tetrahedron* **1984**, *40*, 1245–1253.

[73] K. J. Brown, M. S. Berry, K. C. Waterman, D. Lingenfelter, J. R. Murdoch, *J. Am. Chem. Soc.* **1984**, *106*, 4717–4723.

[74] H. Takaya, K. Mashima, K. Koyano, M. Yagi, H. Kumobayashi, T. Taketomi, S. Akutagawa, R. Noyori, *J. Org. Chem.* **1986**, *51*, 629–635.

[75] K. Tani, T. Yamagata, S. Akutagawa, H. Kumobayashi, T. Taketomi, H. Takaya, *J. Am. Chem. Soc.* **1984**, *106*, 5208–5217.

[76] S. Inoue, H. Takaya, K. Tani, S. Otsuka, T. Sato, R. Noyori, *J. Am. Chem. Soc.* **1990**, *112*, 4897–4905.

[77] M. Emura, H. Matsuda, *Chem. Biodivers.* **2014**, *11*, 1688–1699.

[78] D. Dylong, P. J. Hausoul, R. Palkovits, M. Eisenacher, *Flavour Fragr. J.* **2022**, *37*, 195–209.

[79] H. Takaya, T. Ohta, N. Sayo, H. Kumobayashi, S. Akutagawa, S. Inoue, I. Kasahara, R. Noyori, *J. Am. Chem. Soc.* **1987**, *109*, 1596–1597.

[80] T. Ohta, H. Takaya, M. Kitamura, K. Nagai, R. Noyori, *J. Org. Chem.* **1987**, *52*, 3174–3176.

[81] R. Noyori, T. Ohkuma, M. Kitamura, H. Takaya, N. Sayo, H. Kumobayashi, S. Akutagawa, *J. Am. Chem. Soc.* **1987**, *109*, 5856–5858.

[82] M. Kitamura, T. Ohkuma, S. Inoue, N. Sayo, H. Kumobayashi, S. Akutagawa, T. Ohta, H. Takaya, R. Noyori, *J. Am. Chem. Soc.* **1988**, *110*, 629–631.

[83] T. Ohkuma, H. Ooka, S. Hashiguchi, T. Ikariya, R. Noyori, *J. Am. Chem. Soc.* **1995**, *117*, 2675–2676.

[84] H. Doucet, T. Ohkuma, K. Murata, T. Yokozawa, M. Kozawa, E. Katayama, A. F. England, T. Ikariya, R. Noyori, *Angew. Chem. Int. Ed.* **1998**, *37*, 1703–1707.

[85] T. Ohkuma, M. Koizumi, H. Doucet, T. Pham, M. Kozawa, K. Murata, E. Katayama, T. Yokozawa, T. Ikariya, R. Noyori, *J. Am. Chem. Soc.* **1998**, *120*, 13529–13530.

[86] K. Abdur-Rashid, M. Faatz, A. J. Lough, R. H. Morris, *J. Am. Chem. Soc.* **2001**, *123*, 7473–7474.

[87] K. Abdur-Rashid, S. E. Clapham, A. Hadzovic, J. N. Harvey, A. J. Lough, R. H. Morris, *J. Am. Chem. Soc.* **2002**, *124*, 15104–15118.

[88] C. A. Sandoval, T. Ohkuma, K. Muñiz, R. Noyori, *J. Am. Chem. Soc.* **2003**, *125*, 13490–13503.

[89] R. Abbel, K. Abdur-Rashid, M. Faatz, A. Hadzovic, A. J. Lough, R. H. Morris, *J. Am. Chem. Soc.* **2005**, *127*, 1870–1882.

[90] S. Takebayashi, N. Dabral, M. Miskolzie, S. H. Bergens, *J. Am. Chem. Soc.* **2011**, *133*, 9666–9669.

[91] J. M. John, S. Takebayashi, N. Dabral, M. Miskolzie, S. H. Bergens, *J. Am. Chem. Soc.* **2013**, *135*, 8578–8584.

[92] P. A. Dub, N. J. Henson, R. L. Martin, J. C. Gordon, *J. Am. Chem. Soc.* **2014**, *136*, 3505–3521.

[93] P. A. Dub, B. L. Scott, J. C. Gordon, *J. Am. Chem. Soc.* **2017**, *139*, 1245–1260.

[94] P. A. Dub, J. C. Gordon, *ACS Catal.* **2017**, *7*, 6635–6655.

[95] P. A. Dub, J. C. Gordon, *Nat. Rev. Chem.* **2018**, *2*, 396–408.

[96] J. Zhang, G. Leitus, Y. Ben-David, D. Milstein, *Angew. Chem. Int. Ed.* **2006**, *45*, 1113–1115.

[97] L. A. Saudan, C. M. Saudan, C. Debieux, P. Wyss, *Angew. Chem. Int. Ed.* **2007**, *46*, 7473–7476.

[98] W. Kuriyama, T. Matsumoto, O. Ogata, Y. Ino, K. Aoki, S. Tanaka, K. Ishida, T. Kobayashi, N. Sayo, T. Saito, *Org. Process Res. Dev.* **2012**, *16*, 166–171.

[99] D. Spasyuk, S. Smith, D. G. Gusev, *Angew. Chem. Int. Ed.* **2013**, *52*, 2538–2542.

[100] J. Schörgenhumer, A. Zimmermann, M. Waser, *Org. Process Res. Dev.* **2018**, *22*, 862–870.

[101] P. Dupau, L. Bonomo, L. Kermovan, M. Haldiman Sanchez (F. SA), WO2019/175158, **2019**.

[102] L. Saudan, J. Quintaine, *ChemCatChem* **2023**, *15*, e202300508.

[103] T. Zell, R. Langer, *ChemCatChem* **2018**, *10*, 1930–1940.

[104] J. F. Teichert, *Homogeneous Hydrogenation With Non-Precious Catalysts*, John Wiley & Sons, **2019**.

[105] P. C. Vesborg, T. F. Jaramillo, *RSC Adv.* **2012**, *2*, 7933–7947.

[106] P. Nuss, M. J. Eckelman, *PloS one* **2014**, *9*, e101298.

[107] K. S. Egorova, V. P. Ananikov, *Organometallics* **2017**, *36*, 4071–4090.

[108] J. D. Hayler, D. K. Leahy, E. M. Simmons, *Organometallics* **2018**, *38*, 36–46.

[109] L. C. Forfar, P. M. Murray in *Organometallics in Process Chemistry*, (Eds.: T. J. Colacot, V. Sivakumar), Springer International Publishing, Cham, **2019**, pp. 217–252.

[110] J. Fessler, PhD thesis, University of Rostock, **2023**.

[111] K. H. Wedepohl, *Geochim. Cosmochim. Acta* **1995**, *59*, 1217–1232.

[112] Metalary - Metal Prices, **2023**, https://www.metalary.com/ (visited on 10/27/2023).

[113] ICH, Guideline For Elemental Impurities Q3D(R1), European Medicines Agency, **2019**, https://www.ema.europa.eu/en/documents/scientific-guideline/international-conference-harmonisation-technical-requirements-registration-pharmaceuticals-human-use_en-32.pdf (visited on 11/30/2023).

[114] CHMP, Guideline on the Specification Limits for Residues of Metal Catalysts or Metal Reagents, European Medicines Agency, **2008**, https://www.ema.europa.eu/en/documents/scientific-guideline/guideline-specification-limits-residues-metal-catalysts-metal-reagents_en.pdf (visited on 11/30/2023).

[115] Daily Metal Prices, **2023**, http://www.dailymetalprice.com/metaltables.php?d=2018-12-28 (visited on 10/27/2023).

[116] R. M. Bullock, J. G. Chen, L. Gagliardi, P. J. Chirik, O. K. Farha, C. H. Hendon, C. W. Jones, J. A. Keith, J. Klosin, S. D. Minteer, et al., *Science* **2020**, *369*, eabc3183.

[117] M. D. Wodrich, X. Hu, *Nat. Rev. Chem.* **2017**, *2*, 0099.

[118] R. M. Bullock, *Catalysis Without Precious Metals*, *Vol. 15*, Wiley-VCH Verlag GmbH & Co. KGaA, **2010**.

[119] B. Su, Z.-C. Cao, Z.-J. Shi, *Acc. Chem. Res.* **2015**, *48*, 886–896.

[120] G. A. Filonenko, R. Van Putten, E. J. Hensen, E. A. Pidko, *Chem. Soc. Rev.* **2018**, *47*, 1459–1483.

[121] B. M. Hockin, C. Li, N. Robertson, E. Zysman-Colman, *Catal. Sci. Technol.* **2019**, *9*, 889–915.

[122] M. Garbe, K. Junge, M. Beller, *Eur. J. Org. Chem.* **2017**, *2017*, 4344–4362.

[123] B. Maji, M. K. Barman, *Synthesis* **2017**, *49*, 3377–3393.

[124] F. Kallmeier, R. Kempe, *Angew. Chem. Int. Ed.* **2018**, *57*, 46–60.

[125] Y. Wang, M. Wang, Y. Li, Q. Liu, *Chem* **2021**, *7*, 1180–1223.

[126] K. Das, S. Waiba, A. Jana, B. Maji, *Chem. Soc. Rev.* **2022**, *51*, 4386–4464.

[127] P. Schlichter, C. Werlé, *Synthesis* **2022**, *54*, 517–534.

[128] A. Mukherjee, A. Nerush, G. Leitus, L. J. Shimon, Y. Ben David, N. A. Espinosa Jalapa, D. Milstein, *J. Am. Chem. Soc.* **2016**, *138*, 4298–4301.

[129] S. Elangovan, C. Topf, S. Fischer, H. Jiao, A. Spannenberg, W. Baumann, R. Ludwig, K. Junge, M. Beller, *J. Am. Chem. Soc.* **2016**, *138*, 8809–8814.

[130] F. Kallmeier, T. Irrgang, T. Dietel, R. Kempe, *Angew. Chem. Int. Ed.* **2016**, *55*, 11806–11809.

[131] S. Elangovan, M. Garbe, H. Jiao, A. Spannenberg, K. Junge, M. Beller, *Angew. Chem. Int. Ed.* **2016**, *55*, 15364–15368.

[132] N. A. Espinosa-Jalapa, A. Nerush, L. J. Shimon, G. Leitus, L. Avram, Y. Ben-David, D. Milstein, *Chem. Eur. J.* **2017**, *23*, 5934–5938.

[133] V. Papa, J. R. Cabrero-Antonino, E. Alberico, A. Spanneberg, K. Junge, H. Junge, M. Beller, *Chem. Sci.* **2017**, *8*, 3576–3585.

[134] Y. Wang, L. Zhu, Z. Shao, G. Li, Y. Lan, Q. Liu, *J. Am. Chem. Soc.* **2019**, *141*, 17337–17349.

[135] V. Papa, J. Fessler, F. Zaccaria, J. Hervochon, P. Dam, C. Kubis, A. Spannenberg, Z. Wei, H. Jiao, C. Zuccaccia, et al., *Chem. Eur. J.* **2023**, *29*, e202202774.

[136] M. B. Widegren, G. J. Harkness, A. M. Slawin, D. B. Cordes, M. L. Clarke, *Angew. Chem. Int. Ed.* **2017**, *56*, 5825–5828.

[137] W. Yang, I. Y. Chernyshov, R. K. van Schendel, M. Weber, C. Müller, G. A. Filonenko, E. A. Pidko, *Nat. Commun.* **2021**, *12*, 12.

[138] W. Yang, T. Y. Kalavalapalli, A. M. Krieger, T. A. Khvorost, I. Y. Chernyshov, M. Weber, E. A. Uslamin, E. A. Pidko, G. A. Filonenko, *J. Am. Chem. Soc.* **2022**, *144*, 8129–8137.

[139] Z. Wei, H. Li, Y. Wang, Q. Liu, *Angew. Chem. Int. Ed.* **2023**, *62*, e202301042.

[140] G. Van Koten, D. Milstein, *Organometallic Pincer Chemistry*, *Vol. 40*, Springer, **2013**.

[141] E. Peris, R. H. Crabtree, *Chem. Soc. Rev.* **2018**, *47*, 1959–1968.

[142] E. S. Gulyaeva, E. S. Osipova, R. Buhaibeh, Y. Canac, J.-B. Sortais, D. A. Valyaev, *Coord. Chem. Rev.* **2022**, *458*, 214421.

[143] R. Van Putten, E. A. Uslamin, M. Garbe, C. Liu, A. Gonzalez-de-Castro, M. Lutz, K. Junge, E. J. Hensen, M. Beller, L. Lefort, et al., *Angew. Chem. Int. Ed.* **2017**, *56*, 7531–7534.

[144] C. Liu, R. van Putten, P. O. Kulyaev, G. A. Filonenko, E. A. Pidko, *J. Catal.* **2018**, *363*, 136–143.

[145] D. Wei, A. Bruneau-Voisine, T. Chauvin, V. Dorcet, T. Roisnel, D. A. Valyaev, N. Lugan, J.-B. Sortais, *Adv. Synth. Catal.* **2018**, *360*, 676–681.

[146] S. W. Rahaman, D. K. Pandey, O. Rivada-Wheelaghan, A. Dubey, R. R. Fayzullin, J. R. Khusnutdinova, *ChemCatChem* **2020**, *12*, 5912–5918.

[147] A. Dubey, L. Nencini, R. R. Fayzullin, C. Nervi, J. R. Khusnutdinova, *ACS Catal.* **2017**, *7*, 3864–3868.

[148] A. Dubey, S. W. Rahaman, R. R. Fayzullin, J. R. Khusnutdinova, *ChemCatChem* **2019**, *11*, 3844–3852.

[149] S. Weber, B. Stöger, K. Kirchner, *Org. Lett.* **2018**, *20*, 7212–7215.

[150] J. A. Garduno, J. J. García, *ACS Catal.* **2018**, *9*, 392–401.

[151] S. Weber, B. Stöger, L. F. Veiros, K. Kirchner, *ACS Catal.* **2019**, *9*, 9715–9720.

[152] S. Weber, L. F. Veiros, K. Kirchner, *Adv. Synth. Catal.* **2019**, *361*, 5412–5420.

[153] S. Weber, J. Brünig, L. F. Veiros, K. Kirchner, *Organometallics* **2021**, *40*, 1388–1394.

[154] S. Kostera, S. Weber, M. Peruzzini, L. F. Veiros, K. Kirchner, L. Gonsalvi, *Organometallics* **2021**, *40*, 1213–1220.

[155] R. A. Farrar-Tobar, S. Weber, Z. Csendes, A. Ammaturo, S. Fleissner, H. Hoffmann, L. F. Veiros, K. Kirchner, *ACS Catal.* **2022**, *12*, 2253–2260.

[156] R. Buhaibeh, O. A. Filippov, A. Bruneau-Voisine, J. Willot, C. Duhayon, D. A. Valyaev, N. Lugan, Y. Canac, J.-B. Sortais, *Angew. Chem. Int. Ed.* **2019**, *58*, 6727–6731.

[157] G. Schwarz, R. R. Mendel, M. W. Ribbe, *Nature* **2009**, *460*, 839–847.

[158] P. Mitchell, *Coord. Chem. Rev.* **1966**, *1*, 315–350.

[159] C. Garner, *Coord. Chem. Rev.* **1981**, *37*, 117–156.

[160] J. M. Khurana, S. Chauhan, A. Agrawal, *Org. Prep. Proced. Int.* **2004**, *36*, 201–276.

[161] R. I. Khusnutdinov, T. M. Oshnyakova, U. M. Dzhemilev, *Russ. Chem. Rev.* **2017**, *86*, 128.

[162] A. V. Malkov, I. R. Baxendale, D. Dvořák, D. J. Mansfield, P. Kocovskỳ, *J. Org. Chem.* **1999**, *64*, 2737–2750.

[163] O. Belda, C. Moberg, *Acc. Chem. Res.* **2004**, *37*, 159–167.

[164] R. R. Schrock, A. H. Hoveyda, *Angew. Chem. Int. Ed.* **2003**, *42*, 4592–4633.

[165] R. R. Schrock, *Chem. Rev.* **2009**, *109*, 3211–3226.

[166] A. Fürstner, *Angew. Chem. Int. Ed.* **2013**, *52*, 2794–2819.

[167] O. Einsle, F. A. Tezcan, S. L. Andrade, B. Schmid, M. Yoshida, J. B. Howard, D. C. Rees, *Science* **2002**, *297*, 1696–1700.

[168] L. C. Seefeldt, B. M. Hoffman, D. R. Dean, *Annu. Rev. Biochem.* **2009**, *78*, 701–722.

[169] K. M. Lancaster, M. Roemelt, P. Ettenhuber, Y. Hu, M. W. Ribbe, F. Neese, U. Bergmann, S. DeBeer, *Science* **2011**, *334*, 974–977.

[170] B. M. Hoffman, D. Lukoyanov, D. R. Dean, L. C. Seefeldt, *Acc. Chem. Res.* **2013**, *46*, 587–595.

[171] T. Spatzal, K. A. Perez, O. Einsle, J. B. Howard, D. C. Rees, *Science* **2014**, *345*, 1620–1623.

[172] K. C. MacLeod, P. L. Holland, *Nat. Chem.* **2013**, *5*, 559–565.

[173] Y. Tanabe, Y. Nishibayashi, *Coord. Chem. Rev.* **2022**, *472*, 214783.

[174] E. Frankel, F. Little, *J. Am. Oil Chem. Soc.* **1969**, *46*, 256–261.

[175] D. J. Darensbourg, A. Rokicki, M. Y. Darensbourg, *J. Am. Chem. Soc.* **1981**, *103*, 3223–3224.

[176] M. Y. Darensbourg, J. C. Deaton, *Inorg. Chem.* **1981**, *20*, 1644–1646.

[177] J. Hanckel, M. Darensbourg, *J. Am. Chem. Soc.* **1983**, *105*, 6979–6980.

[178] D. J. Darensbourg, C. Ovalles, *J. Am. Chem. Soc.* **1984**, *106*, 3750–3754.

[179] P. L. Gaus, S. Kao, K. Youngdahl, M. Y. Darensbourg, *J. Am. Chem. Soc.* **1985**, *107*, 2428–2434.

[180] P. A. Tooley, C. Ovalles, S. Kao, D. J. Darensbourg, M. Y. Darensbourg, *J. Am. Chem. Soc.* **1986**, *108*, 5465–5470.

[181] M. Y. Darensbourg, M. M. Ludvig, *Inorg. Chem.* **1986**, *25*, 2894–2898.

[182] J. Palágyi, Z. Nagy-Magos, L. Markó, *Transit. Met. Chem.* **1985**, *10*, 336–338.

[183] L. Markó, Z. Nagy-Magos, *J. Organomet. Chem.* **1985**, *285*, 193–203.

[184] T. Fuchikami, Y. Ubukata, Y. Tanaka, *Tetrahedron Lett.* **1991**, *32*, 1199–1202.

[185] R. M. Bullock, M. H. Voges, *J. Am. Chem. Soc.* **2000**, *122*, 12594–12595.

[186] M. H. Voges, R. M. Bullock, *J. Chem. Soc. Dalton Trans.* **2002**, 759–770.

[187] B. F. Kimmich, P. J. Fagan, E. Hauptman, R. M. Bullock, *Chem. Commun.* **2004**, 1014–1015.

[188] B. F. Kimmich, P. J. Fagan, E. Hauptman, W. J. Marshall, R. M. Bullock, *Organometallics* **2005**, *24*, 6220–6229.

[189] S. Chakraborty, O. Blacque, T. Fox, H. Berke, *Chem. Eur. J.* **2014**, *20*, 12641–12654.

[190] A. Dybov, O. Blacque, H. Berke, *Eur. J. Inorg. Chem.* **2011**, *2011*, 652–659.

[191] S. Chakraborty, O. Blacque, T. Fox, H. Berke, *Chem. Asian J.* **2014**, *9*, 2896–2907.

[192] S. Chakraborty, H. Berke, *ACS Catal.* **2014**, *4*, 2191–2194.

[193] S. Chakraborty, O. Blacque, T. Fox, H. Berke, *Chem. Asian J.* **2014**, *9*, 328–337.

[194] T. Leischner, A. Spannenberg, K. Junge, M. Beller, *Organometallics* **2018**, *37*, 4402–4408.

[195] T. Leischner, L. A. Suarez, A. Spannenberg, K. Junge, A. Nova, M. Beller, *Chem. Sci.* **2019**, *10*, 10566–10576.

[196] T. Leischner, A. Spannenberg, K. Junge, M. Beller, *ChemCatChem* **2020**, *12*, 4543–4549.

[197] M. V. Joannou, M. J. Bezdek, P. J. Chirik, *ACS Catal.* **2018**, *8*, 5276–5285.

[198] P. Viereck, G. Hierlmeier, P. Tosatti, T. P. Pabst, K. Puentener, P. J. Chirik, *J. Am. Chem. Soc.* **2022**, *144*, 11203–11214.

[199] G. Hierlmeier, P. Tosatti, K. Puentener, P. J. Chirik, *Angew. Chem. Int. Ed.* **2023**, *62*, e202216026.

[200] G. Hierlmeier, P. Tosatti, K. Puentener, P. J. Chirik, *J. Am. Chem. Soc.* **2023**, *145*, 21027–21039.

[201] M. N. Hopkinson, C. Richter, M. Schedler, F. Glorius, *Nature* **2014**, *510*, 485–496.

[202] A. Igau, H. Grutzmacher, A. Baceiredo, G. Bertrand, *J. Am. Chem. Soc.* **1988**, *110*, 6463–6466.

[203] A. J. Arduengo III, R. L. Harlow, M. Kline, *J. Am. Chem. Soc.* **1991**, *113*, 361–363.

[204] H.-W. Wanzlick, H.-J. Schönherr, *Angew. Chem. Int. Ed. Engl.* **1968**, *7*, 141–142.

[205] K. Öfele, *J. Organomet. Chem.* **1968**, *12*, P42–P43.

[206] W. A. Herrmann, C. Köcher, *Angew. Chem. Int. Ed. Engl.* **1997**, *36*, 2162–2187.

[207] H.-W. Wanzlick, E. Schikora, *Angew. Chem.* **1960**, *72*, 494–494.

[208] H.-W. Wanzlick, E. Schikora, *Chem. Ber.* **1961**, *94*, 2389–2393.

[209] M. Melaimi, M. Soleilhavoup, G. Bertrand, *Angew. Chem. Int. Ed.* **2010**, *49*, 8810–8849.

[210] S. Díez-González, S. P. Nolan, *Coord. Chem. Rev.* **2007**, *251*, 874–883.

[211] H. Jacobsen, A. Correa, A. Poater, C. Costabile, L. Cavallo, *Coord. Chem. Rev.* **2009**, *253*, 687–703.

[212] W. A. Herrmann, *Angew. Chem. Int. Ed.* **2002**, *41*, 1290–1309.

[213] R. H. Crabtree, *J. Organomet. Chem.* **2005**, *690*, Carbene Chemistry, 5451–5457.

[214] H. V. Huynh, *Chem. Rev.* **2018**, *118*, 9457–9492.

[215] A. C. Hillier, W. J. Sommer, B. S. Yong, J. L. Petersen, L. Cavallo, S. P. Nolan, *Organometallics* **2003**, *22*, 4322–4326.

[216] L. Benhamou, E. Chardon, G. Lavigne, S. Bellemin-Laponnaz, V. César, *Chem. Rev.* **2011**, *111*, 2705–2733.

[217] S. B. Garber, J. S. Kingsbury, B. L. Gray, A. H. Hoveyda, *J. Am. Chem. Soc.* **2000**, *122*, 8168–8179.

[218] M. G. Organ, S. Çalimsiz, M. Sayah, K. H. Hoi, A. J. Lough, *Angew. Chem. Int. Ed.* **2009**, *48*, 2383–2387.

[219] M. T. Powell, D.-R. Hou, M. C. Perry, X. Cui, K. Burgess, *J. Am. Chem. Soc.* **2001**, *123*, 8878–8879.

[220] W. Li, T. Wagener, L. Hellmann, C. G. Daniliuc, C. Mück-Lichtenfeld, J. Neugebauer, F. Glorius, *J. Am. Chem. Soc.* **2020**, *142*, 7100–7107.

[221] S. T. Nguyen, L. K. Johnson, R. H. Grubbs, J. W. Ziller, *J. Am. Chem. Soc.* **1992**, *114*, 3974–3975.

[222] P. Schwab, M. B. France, J. W. Ziller, R. H. Grubbs, *Angew. Chem. Int. Ed. Engl.* **1995**, *34*, 2039–2041.

[223] P. Schwab, R. H. Grubbs, J. W. Ziller, *J. Am. Chem. Soc.* **1996**, *118*, 100–110.

[224] M. Scholl, S. Ding, C. W. Lee, R. H. Grubbs, *Org. Lett.* **1999**, *1*, 953–956.

[225] J. S. Kingsbury, J. P. A. Harrity, P. J. Bonitatebus, A. H. Hoveyda, *J. Am. Chem. Soc.* **1999**, *121*, 791–799.

[226] G. C. Vougioukalakis, R. H. Grubbs, *Chem. Rev.* **2010**, *110*, 1746–1787.

[227] W. A. Herrmann, M. Elison, J. Fischer, C. Köcher, G. R. J. Artus, *Angew. Chem. Int. Ed. Engl.* **1995**, *34*, 2371–2374.

[228] C. J. O'Brien, E. A. B. Kantchev, C. Valente, N. Hadei, G. A. Chass, A. Lough, A. C. Hopkinson, M. G. Organ, *Chem. Eur. J.* **2006**, *12*, 4743–4748.

[229] N. Kambe, T. Iwasaki, J. Terao, *Chem. Soc. Rev.* **2011**, *40*, 4937–4947.

[230] J. J. Verendel, O. Pàmies, M. Diéguez, P. G. Andersson, *Chem. Rev.* **2014**, *114*, 2130–2169.

[231] M. C. Perry, X. Cui, M. T. Powell, D.-R. Hou, J. H. Reibenspies, K. Burgess, *J. Am. Chem. Soc.* **2003**, *125*, 113–123.

[232] S. Nanchen, A. Pfaltz, *Chem. Eur. J.* **2006**, *12*, 4550–4558.

[233] S. Urban, N. Ortega, F. Glorius, *Angew. Chem. Int. Ed.* **2011**, *50*, 3803–3806.

[234] N. Ortega, S. Urban, B. Beiring, F. Glorius, *Angew. Chem. Int. Ed.* **2012**, *51*, 1710–1713.

[235] F. Zhang, H. S. Sasmal, C. G. Daniliuc, F. Glorius, *J. Am. Chem. Soc.* **2023**, *145*, 15695–15701.

[236] E. Peris, R. H. Crabtree, *Coord. Chem. Rev.* **2004**, *248*, 2239–2246.

[237] J. A. Mata, M. Poyatos, E. Peris, *Coord. Chem. Rev.* **2007**, *251*, 841–859.
[238] D. Pugh, A. A. Danopoulos, *Coord. Chem. Rev.* **2007**, *251*, 610–641.
[239] M. Poyatos, J. A. Mata, E. Peris, *Chem. Rev.* **2009**, *109*, 3677–3707.
[240] V. Charra, P. de Frémont, P. Braunstein, *Coord. Chem. Rev.* **2017**, *341*, 53–176.
[241] M. G. Gardiner, C. C. Ho, *Coord. Chem. Rev.* **2018**, *375*, 373–388.
[242] A. E. Martell in *Werner Centennial*, **1967**, Chapter 19, pp. 272–294.
[243] J. J. R. Frausto da Silva, *J. Chem. Educ.* **1983**, *60*, 390.
[244] D. C. Bowman, *J. Chem. Educ.* **2006**, *83*, 1158.
[245] E. G. Moschetta, K. M. Gans, R. M. Rioux, *J. Catal.* **2014**, *309*, 11–20.
[246] P. Bellotti, M. Koy, M. N. Hopkinson, F. Glorius, *Nat. Rev. Chem.* **2021**, *5*, 711–725.
[247] D. Enders, O. Niemeier, A. Henseler, *Chem. Rev.* **2007**, *107*, 5606–5655.
[248] A. V. Zhukhovitskiy, M. J. MacLeod, J. A. Johnson, *Chem. Rev.* **2015**, *115*, 11503–11532.
[249] V. Nesterov, D. Reiter, P. Bag, P. Frisch, R. Holzner, A. Porzelt, S. Inoue, *Chem. Rev.* **2018**, *118*, 9678–9842.
[250] F. Franco, M. F. Pinto, B. Royo, J. Lloret-Fillol, *Angew. Chem. Int. Ed.* **2018**, *57*, 4603–4606.
[251] M. Pinto, S. Friães, F. Franco, J. Lloret-Fillol, B. Royo, *ChemCatChem* **2018**, *10*, 2734–2740.
[252] S. C. A. Sousa, C. J. Carrasco, M. F. Pinto, B. Royo, *ChemCatChem* **2019**, *11*, 3839–3843.
[253] S. C. A. Sousa, S. Realista, B. Royo, *Adv. Synth. Catal.* **2020**, *362*, 2437–2443.
[254] M. Huang, Y. Li, Y. Li, J. Liu, S. Shu, Y. Liu, Z. Ke, *Chem. Commun.* **2019**, *55*, 6213–6216.
[255] K. Ganguli, A. Mandal, S. Kundu, *ACS Catal.* **2022**, *12*, 12444–12457.
[256] Q. Teng, H. V. Huynh, *Inorg. Chem.* **2014**, *53*, 10964–10973.
[257] C. Masaro, G. Meloni, M. Baron, C. Graiff, C. Tubaro, B. Royo, *Chem. Eur. J.* **2023**, *n/a*, e202302273.
[258] N. F. Both, A. Spannenberg, H. Jiao, K. Junge, M. Beller, *Angew. Chem. Int. Ed.* **2023**, *62*, e202307987.
[259] W. Yang, I. Y. Chernyshov, M. Weber, E. A. Pidko, G. A. Filonenko, *ACS Catal.* **2022**, *12*, 10818–10825.
[260] K. Azouzi, L. Pedussaut, R. Pointis, A. Bonfiglio, R. Kumari Riddhi, C. Duhayon, S. Bastin, J.-B. Sortais, *Organometallics* **2023**, *42*, 1832–1838.
[261] M. Garbe, S. Budweg, V. Papa, Z. Wei, H. Hornke, S. Bachmann, M. Scalone, A. Spannenberg, H. Jiao, K. Junge, M. Beller, *Catal. Sci. Technol.* **2020**, *10*, 3994–4001.
[262] N. F. Both, A. Spannenberg, K. Junge, M. Beller, *Organometallics* **2022**, *41*, 1797–1805.
[263] W. Li, M. Huang, J. Liu, Y.-L. Huang, X.-B. Lan, Z. Ye, C. Zhao, Y. Liu, Z. Ke, *ACS Catal.* **2021**, *11*, 10377–10382.

[264] J. Liu, W. Li, Y. Li, Y. Liu, Z. Ke, *Chem. Asian J.* **2021**, *16*, 3124–3128.

[265] P. Su, Z. Chen, J. Ni, Z. Yang, Y. Li, Z. Ke, *ACS Catal.* **2023**, *13*, 12481–12493.

[266] T. Vielhaber, K. Faust, T. Bögl, W. Schöfberger, C. Topf, *J. Catal.* **2022**, *416*, 352–363.

[267] M. A. Sánchez, G. C. Torres, V. A. Mazzieri, C. L. Pieck, *J. Chem. Technol. Biotechnol.* **2017**, *92*, 27–42.

[268] M. Y. Darensbourg, R. El Mehdawi, T. J. Delord, F. R. Fronczek, S. F. Watkins, *J. Am. Chem. Soc.* **1984**, *106*, 2583–2591.

[269] M. Y. Darensbourg, J. L. Atwood, R. R. Burch Jr, W. E. Hunter, N. Walker, *J. Am. Chem. Soc.* **1979**, *101*, 2631–2637.

[270] N. F. Both, J. Thaens, A. Spannenberg, H. Jiao, K. Junge, M. Beller, *ACS Catalysis* **2024**, *14*, 4082–4092.

7 Published Articles

This chapter contains the original publications of the research presented in this thesis. The author's contribution to each publication is outlined.

7.1 Bis(N-Heterocyclic Carbene) Manganese(I) Complexes: Efficient and Simple Hydrogenation Catalysts

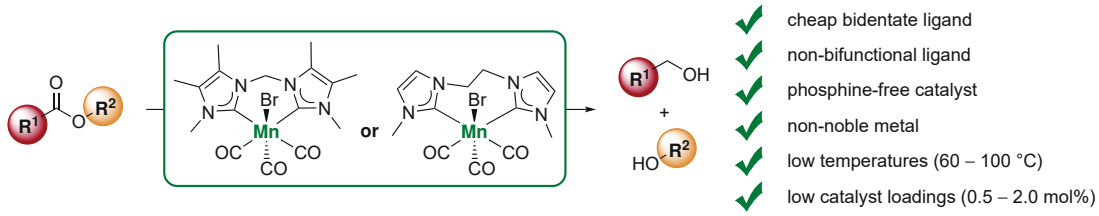

N. F. Both, A. Spannenberg, H. Jiao, K. Junge, M. Beller, *Angew. Chem. Int. Ed.* **2023**, *62*, e202307987.

DOI: 10.1002/anie.202307987. Electronic supporting information is available online.

Author's Contribution

The author initiated and conceptualized the project. The author performed the experimental work including synthesis and characterization of Mn complexes, optimization of the reaction conditions, investigation of the substrate scope and catalytic experiments for mechanistic studies. Furthermore, the author evaluated all analytical data, except for the data from single crystal X-ray diffraction, wrote the initial draft of the manuscript and the supporting information. The author's contribution approximately accounts 70 %.

Niklas F. Both	Prof. Matthias Beller
(PhD student)	(supervisor)

GDCh Research Articles Angewandte International Edition Chemie www.angewandte.org

Check for updates

How to cite: *Angew. Chem. Int. Ed.* **2023**, *62*, e202307987
doi.org/10.1002/anie.202307987

Manganese Chemistry

Bis(N-Heterocyclic Carbene) Manganese(I) Complexes: Efficient and Simple Hydrogenation Catalysts

Niklas F. Both, Anke Spannenberg, Haijun Jiao, Kathrin Junge,* and Matthias Beller**

Abstract: The use of bis(NHC) manganese(I) complexes **3** as catalysts for the hydrogenation of esters was investigated. For that purpose, a series of complexes has been synthesized via an improved two step procedure utilizing bis(NHC)-BEt_3 adducts. By applying complexes **3** with $KHBEt_3$ as additive, various aromatic and aliphatic esters were hydrogenated successfully at mild temperatures and low catalyst loadings, highlighting the efficiency of the novel catalytic system. The versatility of the developed catalytic system was further demonstrated by the hydrogenation of other substrate classes like ketones, nitriles, N-heteroarenes and alkenes. Mechanistic experiments and DFT calculations indicate an inner sphere mechanism with the loss of one CO ligand and reveal the role of BEt_3 as cocatalyst.

Introduction

The reduction of esters to alcohols is an important reaction in academic and industrial chemistry. Traditionally, this transformation has been performed in the presence of stochiometric amounts of metal-hydrides (e.g. $LiAlH_4$, DIBAL-H, $NaBH_4$), which obviously comes along with the formation of stochiometric amounts of waste, often tedious workup procedures and limited functional group tolerance. In this regard, the catalytic hydrogenation using H_2 gas represents an environmentally and economically more attractive approach. Indeed, fatty acid esters are hydrogenated since many decades to the corresponding fatty alcohols using heterogeneous copper chromite catalysts;[1] however, harsh reaction conditions (>200 C, 40–300 bar) are necessary, which omit the use of more sensitive substrates.[2] Therefore, the development of alternative systems working under milder conditions has attracted much attention over the last two decades and several active homogeneous catalysts working at lower temperature and/or pressure mainly based on Ru[3] but also on Os[3d] and Ir[4] have been reported.

More recently, many efforts focused on the replacement of noble-metals in such molecularly-defined catalysts by more abundant and cheaper 3d metals such as Mn,[5] Fe,[6] Co,[7] and Cu.[8] Especially Mn[9] attracted much scientific attention due to the limited knowledge of such complexes as hydrogenation catalysts. As shown in Figure 1, most of the reported systems rely on phosphine-based pincer ligands and include N–H or C–H acidic sites in the ligand-backbone according to the concept of bifunctional metal-ligand cooperativity.[10] From this low structural diversity, one might get the impression that a bifunctional ligand is essential for an efficient Mn-based hydrogenation catalyst. Yet, there are scarce examples of Mn complexes bearing non-bifunctional, bidentate phosphine ligands for catalytic hydrogenation reactions.[11]

However, phosphine-based ligands come along with certain disadvantages, e.g. the sensitivity towards oxygen and their often tedious preparation procedures. In this

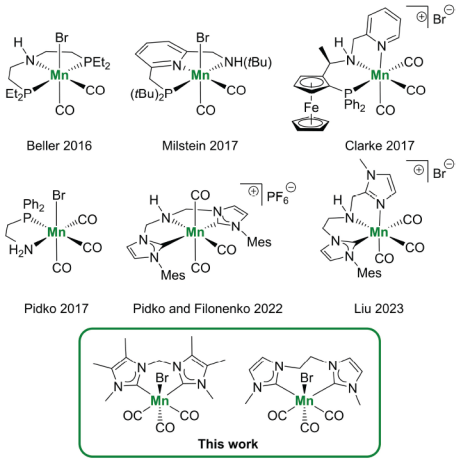

Figure 1. Selected examples of Mn-based catalysts for the hydrogenation of carboxylic acid esters.

[*] N. F. Both, Dr. A. Spannenberg, Prof. Dr. H. Jiao, Dr. K. Junge, Prof. Dr. M. Beller
Leibniz-Institut für Katalyse e.V.
Albert-Einstein-Straße 29a, 18059 Rostock (Germany)
E-mail: haijun.jiao@catalysis.de
kathrin.junge@catalysis.de
matthias.beller@catalysis.de

regard, N-heterocyclic carbenes (NHCs) offer a promising alternative to phosphine ligands and several efforts were made very recently, to replace phosphines in the classical PNP and NNP ligands by NHCs (e.g. Figure1, Pidko and Filonenko 2022, Liu 2023).[5f,h,12] Notably, due to their strong σ-donor and relatively weak π-acceptor properties, these carbene-based ligands allow for the formation of stable Mn complexes[13] and the strong electron donation paired with less steric demand at the active coordination sites compared to phosphines often leads to an enhanced reactivity of the corresponding Mn hydrido complexes.[5h] Hence, bidentate bis(NHC) ligands represent an attractive ligand class for hydrogenation catalysts due to their strong electron-donating properties as well as their easy and modular synthesis allowing for the convenient finetuning of electronic and steric properties of the corresponding Mn complexes. In 2018, Mn complexes bearing these bidentate bis(NHC) ligands were described for the electrocatalytic reduction of CO_2 to CO[14] and, recently, their application has been extended to hydrosilylation,[15] dehydrogenative coupling[16] and transfer hydrogenation[17] reactions. However, so far these systems have not been explored as catalysts for direct hydrogenation reactions. Some time ago, our group reported a Ru-based catalyst for the hydrogenation of esters containing the same bis(NHC) ligand motif,[18] therefore, we were curious about the performance and the potential advantages of bis(NHC) Mn complexes in catalytic hydrogenation reactions. Here, we report the synthesis of a series of Mn complexes bearing bidentate bis(NHC) ligands and their successful use as efficient catalysts for the hydrogenation of carboxylic acid esters. This work represents scarce examples of Mn-based hydrogenation catalysts with non-bifunctional ligands. During the preparation of this manuscript a related catalytic system has been reported by the groups of Bastin and Sortais.[19]

Results and Discussion

Synthesis and Characterisation of bis(NHC)-BEt_3 Adducts 2·2 BEt_3 and bis(NHC) Mn Complexes 3

Initially, we prepared bis(imidazolium) salts **2·2 HBr** from the corresponding alkyl dibromides and imidazoles **1** at 130 C in almost quantitative yields.[15b,20] Notably, in the preparation of the ethylene-bridged bis(imidazolium) salt **2j·2 HBr** with highly basic 1,4,5-trimethylimidazoles partial elimination occurred even at lower temperature (70 C) (see SI, section 4). However, the resulting monoionic side products could be easily removed by washing with DCM due to their better solubility in that solvent. The direct preparation of bis(NHC) manganese complexes **3** from bis(imidazolium) salts, KOtBu and $MnBr(CO)_5$ required more tedious aqueous workup/purification procedures leading to the corresponding complexes in moderate yields.[14] Therefore, an improved protocol for their synthesis via NHC-BEt_3 adducts as intermediates was developed. Using $LiHBEt_3$ for deprotonation and as BEt_3 source,[21] we observed a nucleophilic attack at the bridging, electrophilic carbon atom leading selectively to a mono(NHC)-BEt_3 adduct and 3-(triethylborane)-1-methylimidazole (see SI, section 5). Fortunately, the use of the less nucleophilic, sterically demanding base NaHMDS and the separate addition of BEt_3 resulted in the clean formation of desired **2·2 BEt_3**. A small number of BEt_3-adducts **2·2 BEt_3** was obtained as white to yellow solids in most cases in very good to quantitative yields and all compounds have been analyzed by ^1H, ^{13}C and ^{11}B NMR spectroscopy as well as elemental analysis (Scheme 1).

By refluxing bis(NHC)-BEt_3 adducts **2·2 BEt_3** with $Mn(CO)_5Br$ in THF complexation of the bis(NHC) ligands under loss of two CO ligands occurred (Scheme 1). After washing with Et_2O and *n*-pentane, complexes **3** were obtained as yellow to orange powders in good to very good yields (>80 %). Further purification could be achieved by recrystallisation of these powders from DCM/*n*-pentane mixtures to remove bis(imidazolium) salt impurities. In general, complexes **3** were characterized by NMR and IR spectroscopy, HR-MS, elemental analysis and in some cases single crystal X-ray diffraction (Figure 2). The obtained data is consistent with related manganese complexes.[14,16b]

In most cases, ^1H NMR spectra of complexes **3** show broad signals at room temperature, which can be assigned to a fluxional behavior of the ligand conformation in solution. From the obtained molecular structure of complex **3g** (Figure 2a) as well as the literature-known structure of **3a**,[14] it is well visible that for methylene-bridged complexes (Y=CH_2) the ligand backbone is bent, adopting a boat-shape conformation similar to complexes of other transition metals, e.g. Pd,[23] Rh,[24] Ir,[25] Cr,[26] Mo[26] or W[26]. The methylene-bridge between the NHC units either points towards (*syn*) or away (*anti*) from the bromido ligand, allowing for two possible diastereomer conformers both with C_s-symmetry (SI section 9, Figure S18) For structure **3a**, the *syn*-conformer is computed to be more stable than

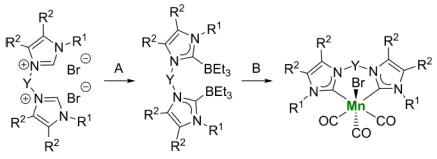

2 • 2 HBr | **2 • 2 BEt_3** 58 – 99 % yield | **3** 77 – 99 % yield

	R^1	R^2	Y		R^1	R^2	Y		R^1	R^2	Y
a	Me	H	CH_2	**e**	Bn	Me	CH_2	**h**	*i*Pr	Me	CH_2
b	*i*Pr	H	CH_2	**f**	Me	C_4H_4[b]	CH_2	**i**	Me	H	$(CH_2)_2$
c[a]	*t*Bu	H	CH_2	**g**	Me	Me	CH_2	**j**	Me	Me	$(CH_2)_2$
d	Ph	H	CH_2								

Scheme 1. Synthesis of bis(NHC) Mn^I complexes **3** from bis(imidazolium) bromides **2·2 HBr** via bis(NHC)-BEt_3 adducts **2·2 BEt_3**. Conditions A: 1) NaHMDS (2.1 eq.), 2) BEt_3 (2.1 eq.), THF, −78 C to rt, 16 h. Conditions B: $Mn(CO)_5Br$ (1.0 eq.), THF, reflux, 16 h. [a] **2c·2 BEt_3** and **3c** were not synthesized. [b] Benzimidazol/benzimidazolilydene.

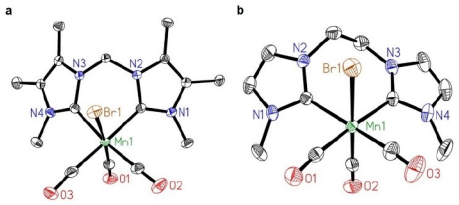

Figure 2. Molecular structures of a) complex **3g** and b) complex **3i** in the solid state. Displacement ellipsoids set at 50% probability level. Hydrogen atoms and solvent molecules omitted for clarity. For the structure of **3i** only one of the two molecules of the asymmetric unit is shown.[22]

the *anti*-conformer by 1.69 kcal/mol, and the ring inversion barrier is 13.52 and 11.83 kcal/mol for the forward and backward inversion, respectively, indicating an equilibrium of the two conformers and the reversibility of the ring inversion at room temperature.

For ethylene-bridged complexes (Y=$(CH_2)_2$), there are also such *syn*- and *anti*-conformations regarding the position of the ethylene-bridge and the bromido ligand. Additionally, the ethylene-bridge can adopt either an eclipsed or staggered conformation, giving four conformers in total (SI section 9, Figure S19). DFT calculations show that the different conformers are close in energy, therefore we assume that interconversion leads to broad signals in the NMR spectra at room temperature. At elevated temperatures (373 K) sharper peaks are observed; however, a clear assignment of resonances was not possible in most cases. As an exception, complexes **3a** and **3g** with methyl substituents at the wing tips (R^1=Me) show sharp NMR resonances at room temperature. We assume that for these substituents interconversion between the conformers is fast due to less steric repulsion between R^1 and the CO ligands. The IR spectra of complexes **3** feature strong absorption bands of the CO ligands. According to their C_s symmetry, methylene-bridged complexes show three CO absorptions, typically between 2000 and 1860 cm^{-1}. For complex **3i** four absorption maxima are observed, likely due to the presence of different conformers as discussed above (compare Supporting Information section 9, Figure S19). In contrast, complex **3j**, for which only the staggered *syn*- and *anti*-conformer in close energy (0.09 kcal/mol) were computed to be stable, only exhibits three CO bands. Ionization of complexes **3** by ESI took place under cleavage of the bromido ligand and the resulting positive fragment was detected by HRMS.

Catalytic Hydrogenation of Esters

Having a small library of synthesized bis(NHC) Mn^I complexes **3** in hand, we tested them for ester hydrogenation using methyl benzoate **5a** and decyl decanoate **5v** as model substrates for aromatic and aliphatic esters, respectively (Scheme 2). In these experiments, 1 mol% of $KHBEt_3$ was added to activate the precatalysts. To differentiate the performance from most previously known manganese-based hydrogenation catalysts, we applied low metal loading (0.5 mol%) at comparably low temperatures of 60–80 C for both benchmark reactions.

For the hydrogenation of methyl benzoate **5a**, complexes **3g** and **3h** with a 4,5-dimethyl-imidazol backbone (R^2=Me) showed the best activity with almost full conversion and yield. In comparison to **3g**, the activity decreased for complex **3a** with a less electron-donating imidazole backbone (R^2=H) and almost no conversion was observed for complex **3f** with the benzimidazole backbone. For the wing tip substituent R^1, also increasing catalytic activity with increasing electron-donation of the substituent in the order of Ph < Me < Bn < *i*Pr (**3d** ≪ **3a** < **3e** < **3b**) is observed. Ethylene-bridged complexes **3i** and **3j** showed worse catalytic activity than their methylene bridged congeners **3a** and **3g**, which we assign to changes in the complex geometry rather than the electronic properties of the present bis(NHC) ligands.

In contrast, the hydrogenation of decyl decanoate **5v** using ethylene-bridged complexes **3i** and **3j** proceeded better than with methylene-bridged analogues leading to high conversions and yields of the desired product. Regarding wing tip substituent R^1, the same trend as for methyl benzoate has been observed and catalytic activity enhanced with increasing electron donation of the substituent (**3d** < **3a** < **3e** < **3b**). Dimethylation of the ligand backbone had almost no effect on the catalytic performance leading to similar results for complexes **3a** and **3g** as well as **3b** and **3h**, respectively. In case of complex **3f** bearing a benzimidazole backbone, no hydrogenation was observed. Overall, the best results were obtained with complex **3g** for the hydrogenation of methyl benzoate **5a** and with complex **3i** for the hydrogenation of decyl decanoate **5v**.

Generally, the catalytic activity of complexes **3** correlates with the electron donator strength of the corresponding bis(NHC) ligand, which interestingly is in agreement with observations using palladium complexes.[27]

In general, molecularly defined ester hydrogenation catalysts require the addition of significant amounts of strong basic reagents, e.g. 2–75 mol% of KO*t*Bu.[5] Hence, the influence of the used additive and additive loading was explored in more detail. Also, other crucial parameters such as reaction temperature, catalyst loading, and hydrogen pressure were investigated, too (Table 1). While applying only 1 mol% of $KHBEt_3$ as additive led to almost full conversion of **5a** and high yield of **6a** (entry 1), KO*t*Bu, KHMDS and KH at the same additive loading showed significantly lower conversions and yields (entries 2, 4 and 5). At an increased additive loading of 20 mol% of KO*t*Bu, 92% conversion of **5a** but a yield of only 74% of **6a** were obtained. In this case, a white precipitate was obtained which was identified as benzoic acid after acidic workup (see SI, section 6). This observed side reaction might explain the need of higher additive loadings to reach full conversion as well as the difference between conversion and yield. Furthermore, the influence of the cation was investigated by using $NaHBEt_3$ and $LiHBEt_3$ as additives (entries 8 and 9).

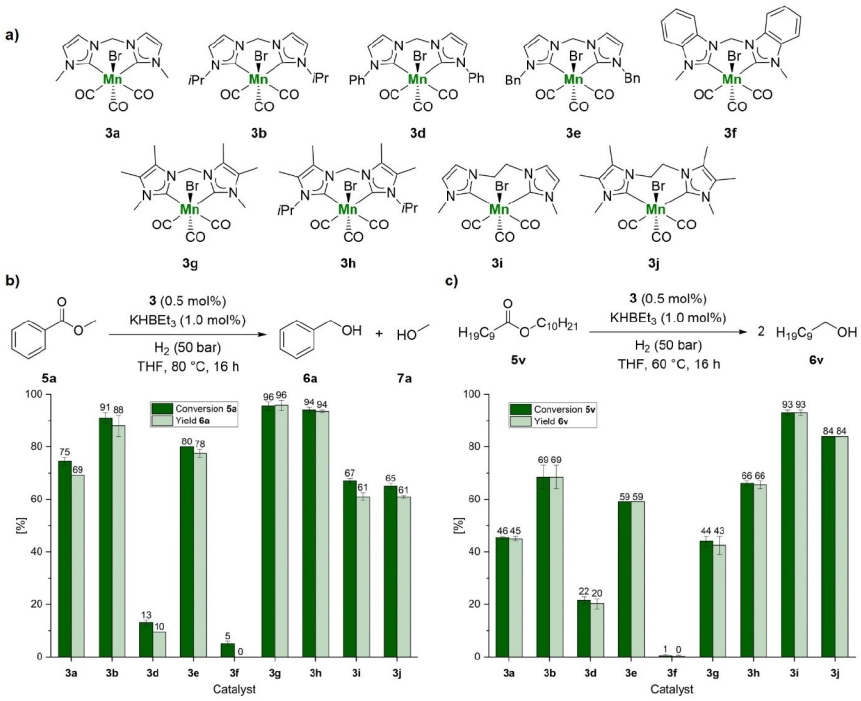

Scheme 2. Catalytic performance of bis(NHC) Mn^{I} complexes **3** for the hydrogenation of esters. a) Lewis structures of bis(NHC) Mn^{I} complexes **3**. Catalyst comparison for the hydrogenation of b) methyl benzoate **5a** and c) decyl decanoate **5v**. Values represent the average of two experiments. Error bars represent the standard deviation. Reaction conditions: 1 mmol methyl benzoate **5a** or decyl decanoate **5v**, 5 µmol **3** (0.5 mol%), 10 µmol $KHBEt_3$ (1.0 mol%), 4.0 ml THF, 50 bar H_2, 80 °C (methyl benzoate **5a**) or 60 °C (decyl decanoate **5v**), 16 h. Conversion of methyl benzoate **5a** or decyl decanoate **5v** and yield of benzyl **6a** alcohol or 1-decanol **6v** were determined by GC using hexadecane as internal standard. The differences of conversion and yield in the case of methyl benzoate **5a** are mainly due to the formation of benzyl benzoate via transesterification.

In comparison to $KHBEt_3$ only a slight decrease in performance was observed with $NaHBEt_3$ whereas $LiHBEt_3$ gave much lower conversion and yield. As control experiments the reaction was performed without any additive (entry 10) as well as without manganese complex **3g** (entry 11) showing only very small reactivity. Lowering of the reaction temperature (entry 12) or catalyst loading (entry 13) led to a decreased catalytic performance. Applying 30 bar of hydrogen pressure only slightly decreased conversion and yield (entry 14).

To investigate the scope of the reaction various aromatic and aliphatic esters were exposed to our hydrogenation conditions applying complex **3g** (for aromatic esters) or **3i** (for aliphatic esters) as (pre)catalyst (Scheme 3). Methyl benzoate **5a** and benzyl benzoate **5b** are readily converted to their corresponding alcohols with very good yields. Sterically more hindered isopropyl benzoate **5c** gave the desired product, too, albeit slightly higher temperature and catalyst loading are required, while *tert*-butyl benzoate **5d** showed low conversion under these conditions. Phenyl benzoate **5e** provided moderate yields of phenol and the formed benzyl alcohol underwent full transesterification to form benzyl benzoate. In this case, we assign the lower conversion to the high acidity of phenol and the formation of phenoxide complexes. In contrast, electron-rich aromatic esters (**5f**, **5g**, **5l**, and **5p**) are smoothly converted to their corresponding alcohols. Remarkably, tertiary (**5l**) and even primary amines (**5p**) are tolerated by this hydrogenation procedure. Notably, alcohols formed from esters with electron-withdrawing groups can inhibit the active catalyst species by the formation of the corresponding alkoxide complexes in a similar manner to phenol mentioned above. Nevertheless, esters **5h**, **5i**, **5j**, **5k**, **5n** and **5o** provided the desired alcohols at somewhat higher temperature and/or higher catalyst loading. Interestingly, halogenated esters displayed varying activity. While methyl *p*-chlorobenzoate

Table 1: Screening of reaction conditions for the Mn-catalyzed hydrogenation of methyl benzoate **5a**.[a]

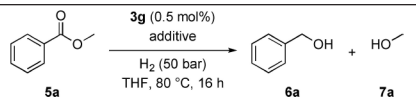

5a **6a** **7a**

#	additive	Add. load. [mol%]	Conv. **5a**[b] [%]	Yield **6a**[b] [%]	Yield **8a**[b] [%]
1	$KHBEt_3$	1.0	96(2)	94(2)	2(1)
2	KO*t*Bu	1.0	2	2	0
3	KO*t*Bu	20.0	92	74[d]	3[d]
4	KHMDS	1.0	2	2	0
5	KH	1.0	15	5	8
6	$KHBEt_3$	0.5	70	70	1
7	$KHBEt_3$	2.0	90	88	4
8	$NaHBEt_3$	1.0	91	84	4
9	$LiHBEt_3$	1.0	49	31	16
10	none	–	0	0	0
11	$KHBEt_3$[e]	1.0	6	0	0
12	$KHBEt_3$[f]	1.0	53	49	4
13	$KHBEt_3$[g]	0.6	52	50	3
14	$KHBEt_3$[h]	1.0	92	91	3

[a] General reaction conditions: 1 mmol methyl benzoate **5a**, 5 µmol **3g** (0.5 mol%), 4.0 mL THF, 50 bar H_2, 80 C, 16 h. [b] Conversion of methyl benzoate **5a** and yield of benzyl alcohol **6a** and benzyl benzoate **8a** were determined by GC analysis using hexadecane as internal standard. [c] Average of two experiments given. Values in parentheses represent the standard deviation. [d] Formation of potassium benzoate observed. No *tert*-butyl benzoate detected via GC analysis. [e] Without complex **3g**. [f] Reaction performed at 60 C. [g] 3 µmol **3g** (0.3 mol%) used. [h] Reaction performed with 30 bar H_2.

5j and methyl *p*-bromobenzoate **5k** are readily hydrogenated at 100 C applying 1 mol% of **3g** and 2 mol% $KHBEt_3$, surprisingly, the fluorinated congener **5h** showed no conversion under these conditions. Yet, a fluoro substituent in *meta*-position (**5i**) is tolerated much better, giving the corresponding alcohol in 56% and with increased catalyst loading even in 83% isolated yield. Presumably, the fluorinated position is susceptible to nucleophilic aromatic substitution with $KHBEt_3$ or a manganese hydrido complex, which is facilitated by the conjugated ester group. Increasing the loading of $KHBEt_3$ to 10 mol% leads to full conversion for methyl *p*-fluorobenzoate as well as an isolated yield of 78% of the alcohol. An iodo substituent (**5n**) resulted in lower activity than chloro and bromo substituents, nevertheless, its alcohol was isolated in 78% yield after applying 2 mol% of **3g**. Furthermore, hydrogenation of the naphthyl ester **5q** gave the corresponding alcohol in good yield. Although lactones and diesters are challenging substrates due to potential side reactions like oligomerization, the corresponding diols from five-membered lactone **5r** and diester **5s** were isolated in good to very good yields. Interestingly, in case of quinoline-derived ester **5v** reduction of either the ester function or the quinoline ring occurred to a similar extent. Here, 37% of the corresponding alcohol and 20% of 1,2,3,4-tetrahydroquinoline-6-carboxylate were isolated. As an example, for heterocyclic esters, the hydrogenation of the niacin-derived ester **5w** proceeded easily and the desired alcohol was isolated in good yield. Similarly, tertiary and secondary amines in the pharmaceutical substrates, trimebutine **5t** and tetracaine **5u**, were well tolerated by our hydrogenation procedure and the corresponding alcohols were isolated in good to very good yield.

Next, we tested the hydrogenation of various aliphatic esters applying (pre)catalyst **3i**. Esters containing different aliphatic chains (**5x**, **5y**, and **5z**) were smoothly hydrogenated already at low temperatures (60 or 80 C) and low catalyst loadings (0.5 or 1.0 mol%). Sterically more demanding esters containing branched alkyl chains or substituents in closer proximity to the ester group (**5aa**, **5ab** and **5ac**) gave slightly lower yields. Steric hindrance appears to be more problematic in R^1 than in R^2, since cyclohexyl acetate **5ad** was easily hydrogenated whereas methyl cyclohexanecarboxylate **5ae** provided only moderate yield of cyclohexylmethanol. Lactones with larger ring size could be smoothly hydrogenated, e.g. the 16-membered lactone **5af** was converted to the corresponding diol. Interestingly, this catalyst system showed some activity for the hydrogenation of non-activated olefins, which has yet only rarely been observed for homogeneous Mn complexes.[11c] For example, the internal C=C double bond in **5ag** was partially hydrogenated and next to the ester function in compound **5ai** also the terminal alkene moiety was hydrogenated and undecane-1-ol was isolated in 63% yield. For the sterically more hindered C=C double bond in citronellyl acetate **5an**, no hydrogenation occurred at the standard conditions and citronellol was isolated in excellent yield. Esters **5aj** and **5ak** containing a hydroxy or a bromide functional group were reduced to their corresponding alcohols with good yields. Furthermore, the natural terpenes menthyl acetate **5al** and bornyl acetate **5am** yielded (±)-menthol and (−)-borneol in 76% and 94% yield, respectively.

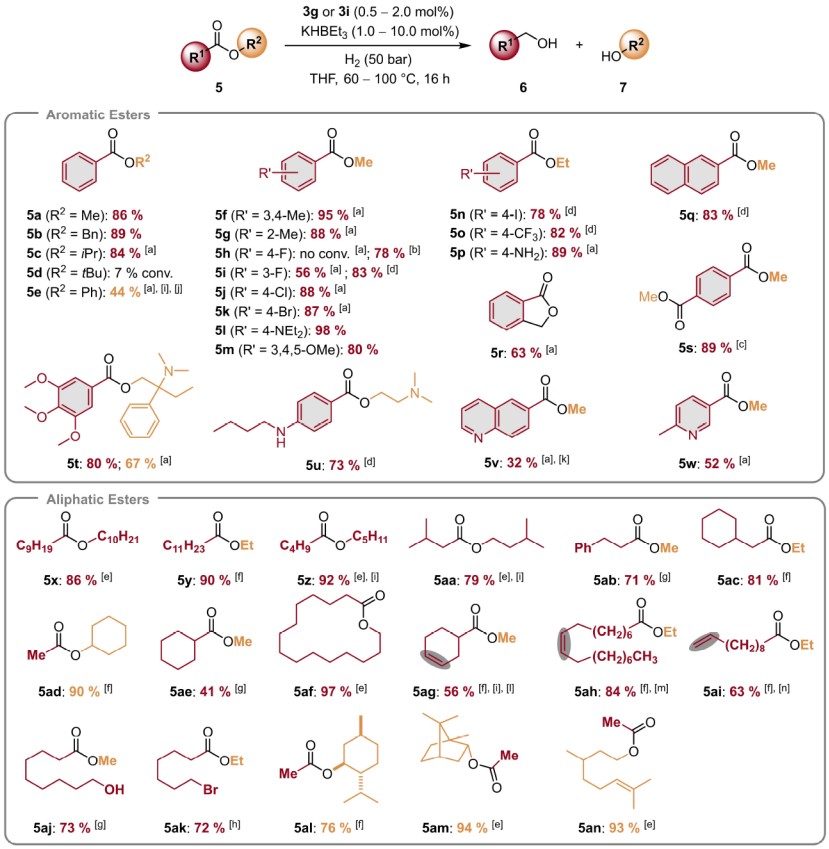

Scheme 3. Mn-catalyzed hydrogenation of various aromatic and aliphatic esters **5** to their corresponding alcohols **6** and **7**. Values below the Lewis structures of esters **5** represent the isolated yields of the corresponding alcohols **6** (red) and/or **7** (orange). Standard conditions: 1 mmol of ester **5**, 0.5 mol% **3g**, 1 mol% $KHBEt_3$, 50 bar H_2, 4 mL THF, 80 C, 16 h. [a] 100 C, 1 mol% **3g**, 2 mol% $KHBEt_3$; [b] 100 C, 1 mol% **3g**, 10 mol% $KHBEt_3$; [c] 80 C, 2 mol% **3g**, 4 mol% $KHBEt_3$; [d] 100 C, 2 mol% **3g**, 4 mol% $KHBEt_3$; [e] 60 C, 0.5 mol% **3i**, 1 mol% $KHBEt_3$; [f] 80 C, 1 mol% **3i**, 2 mol% $KHBEt_3$; [g] 100 C, 1 mol% **3i**, 2 mol% $KHBEt_3$; [h] 100 C, 2 mol% **3i**, 4 mol% $KHBEt_3$; [i] Yield determined by GC analysis using hexadecane as internal standard; [j] 22% benzyl benzoate observed by GC analysis. Formed benzyl alcohol undergoes transesterification with phenyl benzoate and liberates phenol, so only 22% of ester are converted; [k] 20% methyl 1,2,3,4-tetrahydroquinoline-6-carboxylate isolated; [l] 13% cyclohexylmethanol, 5% cyclohex-2-enylmethanol, 3% cyclohex-1-enylmethanol and 5% methyl cyclohexanecarboxylate observed by GC analysis; [m] The isolated material was an inseparable mixture of regioisomers and diastereomers with an overall *(Z)* : *(E)* ratio of 55 : 45 according to GC analysis; [n] 1-undecanol was isolated.

Since we observed the reduction of other moieties like alkenes (**5ae** or **5ag**) and N-heteroarenes (**5r**) next to ester groups, we were curious about the applicability of our catalytic protocol to other substrate classes. Therefore, we investigated the hydrogenation of ketones **8**, nitriles **10**, N-heteroarenes **12** and alkenes **14** (Scheme 4). Aromatic and aliphatic ketones are readily converted to the corresponding alcohols (**8a**, **8b**, **8c** and **8d**). For the steroid dehydroepiandrosterone **8c** a 60:40 mixture of diastereomers was obtained. Interestingly, at temperatures below 60 C only low activity is observed, which we assign to the energy required for catalyst activation. In case of isophorone **8e**, partial hydrogenation of the conjugated C=C double bond takes place. Moreover, aromatic nitriles with electron-donating groups and aliphatic nitriles (**10a–e**) are hydrogenated at 120 C using 2 mol% of **3g** as (pre)catalysts and

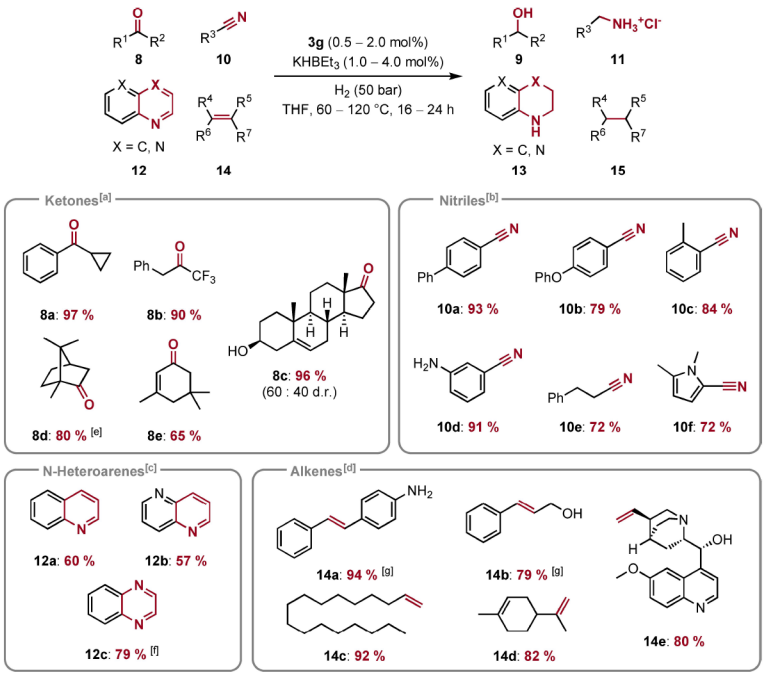

Scheme 4. Mn-catalyzed hydrogenation of ketones **8**, nitriles **10**, N-heteroarenes **12** and alkenes **14** to alcohols **9**, amines **11**, tetrahydro-N-heteroarenes **13** and alkanes **15**, respectively. Values below the Lewis structures represent isolated yields. [a] Standard conditions: 1 mmol of ketone **8**, 1 mol% **3g**, 2 mol% $KHBEt_3$, 50 bar H_2, 4 mL THF, 80 °C, 16 h; [b] Standard conditions: 0.5 mmol of nitrile **10**, 2 mol% **3g**, 4 mol% $KHBEt_3$, 50 bar H_2, 2 mL THF, 120 °C, 24 h. Corresponding amines were isolated as the hydrochloride salts; [c] Standard conditions: 0.5 mmol of N-heteroarene **12**, 2 mol% **3g**, 4 mol% $KHBEt_3$, 50 bar H_2, 2 mL THF, 120 °C, 24 h; [d] Standard conditions: 1 mmol of alkene **14**, 0.5 mol% **3g**, 1 mol% $KHBEt_3$, 50 bar H_2, 4 mL THF, 80 °C, 16 h; [e] 60 °C, 0.5 mol% **3g**, 1 mol% $KHBEt_3$; [f] 1 mol% **3g**, 2 mol% $KHBEt_3$; [g] 100 °C, 1 mol% **3g**, 2 mol% $KHBEt_3$.

were isolated in good to very good yields. Electron-poor nitriles showed only low conversion under these conditions, likely due to catalyst inhibition by substrate coordination. The N-heterocyclic nitrile **10f** is readily converted to the corresponding amine and was isolated in 72 % yield. Additionally, several N-heteroarenes like quinoline **12a**, 1,5-naphtyridine **12b** or quinoxaline **12c** are hydrogenated by the presented catalytic system. Moreover, various alkenes including aromatic (**14a**, **14b**) and aliphatic (**14c**, **14d**, **14e**) substituents were hydrogenated at 80 °C or 100 °C applying a catalyst loading of 1 mol%. Functional groups such as amines (e.g. in quinine **14e**) and alcohols (e.g. in cinnamyl alcohol **14b**) are readily tolerated by the catalytic procedure. Interestingly, no reduction of the more substituted C=C double bond in limonene **14d** was observed.

Overall, the presented catalytic systems show high efficiency and rank among the best known manganese catalysts for ester hydrogenation.[5] In particular, the hydrogenation of various aliphatic esters at only 60 °C and 0.5 mol% catalyst loading is remarkable. The scope is relatively broad and different classes of substrates including ketones, nitriles, N-heteroarenes and, most impressively, alkenes are shown to be hydrogenated efficiently aside from esters. Functional groups like halides, alcohols and tertiary, secondary, and even primary amines are tolerated. However, the high activity as well as the ability to hydrogenate different functional groups results in diminished selectivity in certain cases (substrates **5v**, **5ag**, **5ah**, **5ai** or **8e**). Further limitations of the catalytic system remain heteroaromatic substrates, which are only partially tolerated, as well as lactones with a small ring size.

Mechanistic Investigations

Since the presented catalytic systems represent the first examples of bis(NHC)-based manganese complex catalyzed hydrogenation of carboxylic acid esters, a deeper under-

standing of the mechanism is important. As a starting point of our mechanistic investigations, hydrido complex **4a** was prepared in almost quantitative yield by the reaction of bromido complex **3a** with one equivalent of $KHBEt_3$ at room temperature over 24 h (Scheme 5). The ^1H NMR spectrum of **4a** shows a hydride resonance at −6.79 in THF-d_8. The carbonyl vibrations observed by IR spectroscopy are shifted to lower wave numbers (1962, 1866, 1823 cm^{-1} for **4a**;) in comparison to the corresponding bromido complex (1998, 1917, 1879 cm^{-1} for **3a**). This observation agrees with the higher electron donation of the hydrido ligand compared to the bromido ligand. Similar shifts between **3a** and **4a** have been found by DFT calculations (SI, section 9.1). As in case of structure **3a**, structure **4a** also exhibits a *syn*- and *anti*-conformer, and the former is more stable by 3.84 kcal/mol and should be the major conformer (99.8 %).

Interestingly, hydrido complex **4a** without additive present does not show any catalytic activity in the hydrogenation of methyl benzoate (Table 2, entry 2), but in the presence of complex **4a** and $KHBEt_3$ (entry 3) hydrogenation of methyl benzoate takes place. Obviously, $KHBEt_3$ is not only responsible for formation of hydrido complex **4a**, but also necessary for the catalytic activity. Therefore, we assume that BEt_3 liberated during hydrido complex formation plays a crucial role in the catalytic system. A control experiment applying **4a** and BEt_3 (entry 4) confirmed this assumption. Also, other borane-based additives have been tested with **4a** and comparable activity was found for 9-borabicyclo(3.3.1)nonane (9-BBN) (see Supporting Information section 11.3 for details). In contrast, the combination of bromido complex **3a** and BEt_3 does not catalyze the model reaction (entry 5). Furthermore, the presence of strongly coordinating, monodentate ligands such as CO or PMe_3 results in a complete shutdown of the reaction (entries 6 and 7).

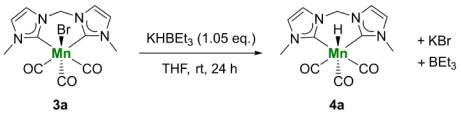

3a **4a**

Scheme 5. Synthesis of bis(NHC) manganese hydrido complex **4a** from bromido complex **3a** with $KHBEt_3$.

Moreover, the reaction of **4a**, BEt_3 and methyl benzoate (in a 1:1:2 ratio) was investigated by NMR spectroscopy (see Supporting Information for details), but no transformation was observed after heating the sample at 80 C for 16 h without H_2. However, if the mixture was heated in an autoclave to 80 C under 50 bar of H_2 pressure for 3 h, a clear, light-yellow solution with a blue precipitate was obtained. NMR spectroscopic analysis of the solution confirms quantitative conversion of methyl benzoate to benzyl alcohol and methanol. In addition, the presence of hydrido complex **4a** and another, unidentified manganese complex as well as decomposition of BEt_3 to unidentified products is observed (SI section 11). IR analysis of the blue reaction residue shows two absorption bands in the carbonyl area at 1854 and 1781 cm^{-1}, respectively, indicative for an electron-rich manganese species containing only two CO ligands (SI section 11.2). The reaction residue was also tested for catalytic activity in the presence and absence of $KHBEt_3$, but no reaction was observed (SI, section 11.2.2). Therefore, we conclude that the species is not involved in the catalytic cycle.

To gain further insight into the mechanism of the hydrogenation of methyl benzoate (**5a**), we performed DFT calculations (see Supporting Information for details). Under the H_2 rich conditions, we started our computations by substituting one equatorial CO ligand in **4a** by a molecular hydrogen (**4a-H_2**). However, many attempts to get such a complex via an energetic favourable way failed, either via direct CO dissociation (38.50 kcal/mol) nor O*t*Bu mediated H_2 hydrogenolysis (30.96 kcal/mol) as well as BEt_3 mediated exchange and CO insertion forming propionaldehyde

Table 2: Control experiments and mechanistic investigations.[a]

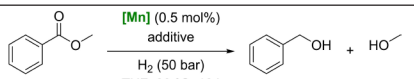

5a **6a** **7a**

#	[Mn]	additive	additive load. [mol %]	Conv. **5a**[b] [%]	Yield **6a**[b] [%]
1	**3a**	$KHBEt_3$	1.0	75(2)[c]	69(0)[c]
2	**4a**	–	–	2(0)[c]	1(1)[c]
3	**4a**	$KHBEt_3$	0.5	73	64
4	**4a**	BEt_3	1.0	61(1)[c]	59(1)[c]
5	**3a**	BEt_3	1.0	0	0
6[d]	**3a**	$KHBEt_3$	1.0	0	0
7[e]	**3g**	$KHBEt_3$	1.0	0	0

[a] Reaction conditions: 1 mmol methyl benzoate **5a**, 5 µmol **[Mn]** (0.5 mol%), 4.0 ml THF, 50 bar H_2, 80 C, 16 h. [b] Conversion of methyl benzoate **5a** and yield of benzyl alcohol **6a** were determined by GC using hexadecane as internal standard. [c] Average of two experiments given. Values in parentheses represent the standard deviation. [d] The autoclave was charged with 10 bar of CO and 50 bar of H_2. [e] Reaction was performed in the presence of 5 mol% PMe_3.

(29.06 kcal/mol). Therefore, from a computational as well as an experimental perspective, it is unclear how exactly a CO ligand is lost.

Starting from **4a**-H_2 and **5a** based on the inner-sphere mechanisms, we found a two-step pathway (Scheme 6). The first step is the Mn–H transfer to the coordinated methyl benzoate via transition state **I** followed by the formation of a more stable bidentate complex of the formed methoxy-(phenyl)methanolate via the C–H and C–OMe exchange (**II** to **III**). The second step is the hydrogenolysis of the methoxy(phenyl)methanolate **IV** via transition state **V** to methoxy(phenyl)methanol **VI** as the first intermediate, which is the rate determining step with an apparent Gibbs free energy barrier of 20.24 kcal/mol. Due to the face-coordination of **5a**, we computed the (*R*)- and (*S*)-configurations and found that the formation of (*S*)-methoxy-(phenyl)methanol has a lower Gibbs free energy barrier than (*R*)-methoxy(phenyl)methanol (20.10 vs. 25.12 kcal/mol). Methoxy(phenyl)methanol (**VI**) can decompose to benzaldehyde (**VII**) and methanol (**7a**). In a similar way, we also computed the hydrogenation of benzaldehyde (**VII**) following the inner-sphere mechanism. Starting from the complex of benzaldehyde (**VIII**), it is not possible to locate the corresponding Mn–H transfer transition state and all attempts resulted in the formation of the C–H agostic interacted intermediate **IX**, which undergoes further isomerisation to intermediate **X**. Hydrogenolysis via transition state **XII** results in benzyl alcohol (**6a**). As expected, a much lower apparent Gibbs free energy barrier (6.88 kcal/mol, SI) for the hydrogenolysis step (**XII**) of alkoxide **XI** has been found.

Based on the control experiments, spectroscopic investigations and DFT calculations, we propose the following mechanism: Initially, one CO ligand is cleaved from hydrido complex **4a** to create a vacant coordination site, which is supported by 1) strongly coordinating, monodentate ligands (including strongly coordinating substrates) inhibiting the hydrogenation and 2) the observation of only two CO stretches in the reaction residue. We speculate, that the CO cleavage might be facilitated by BEt_3, which was shown to form a catalytically active species with hydrido complex **4a**. However, the detailed role of $KHBEt_3$/BEt_3 for the catalytic system is not clear and requires further investigation. Subsequently, substrate coordination to the Mn center occurs, followed by an inner-sphere hydride transfer to the substrate and liberation of the product by hydrogenolysis.

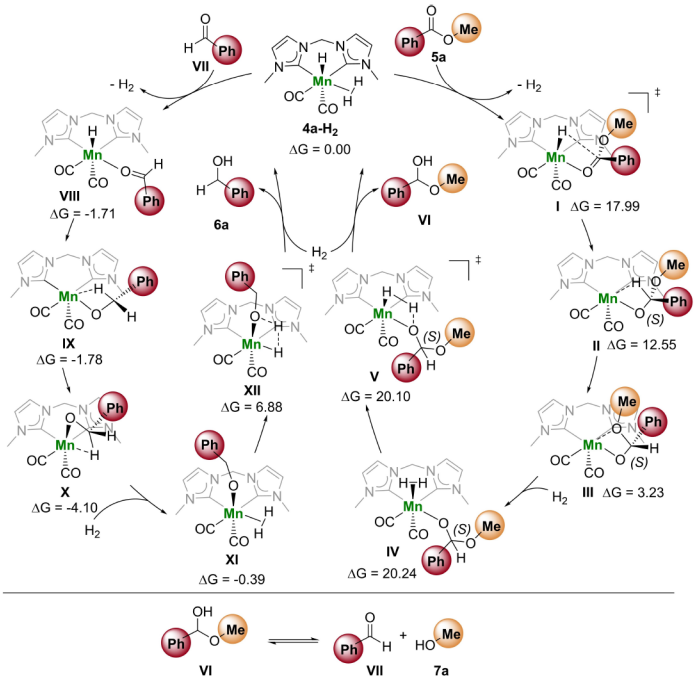

Scheme 6. Mechanistic proposal for the Mn-catalyzed hydrogenation of methyl benzoate. Gibbs free energies (M06L-SCRF) are given in kcal mol^{-1} and referred to **4a**-H_2.

Conclusion

In summary, we present a novel catalytic system for the efficient hydrogenation of carboxylic acid esters based on Mn^I complexes bearing simple phosphine-free, non-bifunctional bis(NHC) ligands. An improved synthetic access to these bis(NHC) Mn^I complexes **3** utilizing bis(NHC)-borane adducts has been developed. Complexes **3** have successfully been applied as (pre)catalyst with $KHBEt_3$ as cocatalyst in the hydrogenation of various aromatic and aliphatic esters at low temperatures and low catalyst loadings. The general applicability was further demonstrated by the hydrogenation of other substrate classes such as ketones, nitriles, N-heteroarenes and alkenes. Control experiments reveal the essential role of BEt_3 as cocatalyst and indicate an inner-sphere mechanism. This mechanistic proposal is further supported by DFT calculations. Overall, we present rare examples of Mn-based hydrogenation catalysts containing simple phosphine-free, non-bifunctional ligands. We believe that the use of simpler ligand frameworks is a great improvement in the field of homogeneous Mn catalysis.

Author Contributions

N.B. conceptualized the work. H.J., K.J and M.B contributed to the further drafting of the project. N.B. performed synthetic and catalytic experiments for data collection. A.S. measured SC-XRD data and solved molecular structures. H.J. performed DFT calculations. N.B. wrote the first draft of the manuscript. A.S., H.J. and K.J. wrote sections of the manuscript. All authors contributed to manuscript revision, read, and approved the submitted version.

Acknowledgements

We thank Katja Andres for her support with the syntheses of bis(imidazolium) salts and bis(NHC)-BEt_3 adducts. Furthermore, the authors thank Astrid Lehmann for performing elemental analyses, Dr. Marcus Klahn for HRMS measurements, Andreas Koch for VT NMR measurements, and PD Dr. Wolfgang Baumann, Dr. Dilver Peña Fuentes and Susann Buchholz for NMR measurements. We are also grateful to Johannes Fessler for helpful discussions. Open Access funding enabled and organized by Projekt DEAL.

Conflict of Interest

The authors declare no conflict of interest.

Data Availability Statement

The data that support the findings of this study are available in the supplementary material of this article.

Keywords: Carbene Ligands · Esters · Homogeneous Catalysis · Hydrogenation · Manganese

[1] a) U. R. Kreutzer, *J. Am. Oil Chem. Soc.* **1984**, *61*, 343–348; b) R. D. Rieke, D. S. Thakur, B. D. Roberts, G. T. White, *J. Am. Oil Chem. Soc.* **1997**, *74*, 341–345.
[2] M. A. Sánchez, G. C. Torres, V. A. Mazzieri, C. L. Pieck, *J. Chem. Technol. Biotechnol.* **2017**, *92*, 27–42.
[3] a) J. Zhang, G. Leitus, Y. Ben-David, D. Milstein, *Angew. Chem. Int. Ed.* **2006**, *45*, 1113–1115; b) L. A. Saudan, C. M. Saudan, C. Debieux, P. Wyss, *Angew. Chem. Int. Ed.* **2007**, *46*, 7473–7476; c) W. Kuriyama, T. Matsumoto, O. Ogata, Y. Ino, K. Aoki, S. Tanaka, K. Ishida, T. Kobayashi, N. Sayo, T. Saito, *Org. Process Res. Dev.* **2012**, *16*, 166–171; d) D. Spasyuk, S. Smith, D. G. Gusev, *Angew. Chem. Int. Ed.* **2012**, *51*, 2772–2775; e) Y. Shaalan, L. Boulton, C. Jamieson, *Org. Process Res. Dev.* **2020**, *24*, 2745–2751.
[4] a) K. Junge, B. Wendt, H. Jiao, M. Beller, *ChemCatChem* **2014**, *6*, 2810–2814; b) T. P. Brewster, N. M. Rezayee, Z. Culakova, M. S. Sanford, K. I. Goldberg, *ACS Catal.* **2016**, *6*, 3113–3117.
[5] a) S. Elangovan, M. Garbe, H. Jiao, A. Spannenberg, K. Junge, M. Beller, *Angew. Chem. Int. Ed.* **2016**, *55*, 15364–15368; b) M. B. Widegren, G. J. Harkness, A. M. Slawin, D. B. Cordes, M. L. Clarke, *Angew. Chem. Int. Ed.* **2017**, *56*, 5825–5828; c) N. A. Espinosa-Jalapa, A. Nerush, L. J. Shimon, G. Leitus, L. Avram, Y. Ben-David, D. Milstein, *Chem. Eur. J.* **2017**, *23*, 5934–5938; d) R. Van Putten, E. A. Uslamin, M. Garbe, C. Liu, A. Gonzalez-de-Castro, M. Lutz, K. Junge, E. J. Hensen, M. Beller, L. Lefort, *Angew. Chem. Int. Ed.* **2017**, *56*, 7531–7534; e) V. Zubar, N. Lichtenberger, M. Schelwies, T. Oeser, A. S. K. Hashmi, T. Schaub, *ChemCatChem* **2022**, *14*, e202101443; f) W. Yang, T. Y. Kalavalapalli, A. M. Krieger, T. A. Khvorost, I. Y. Chernyshov, M. Weber, E. A. Uslamin, E. A. Pidko, G. A. Filonenko, *J. Am. Chem. Soc.* **2022**, *144*, 8129–8137; g) X. G. Li, F. Li, Y. Xu, L. J. Xiao, J. H. Xie, Q. L. Zhou, *Adv. Synth. Catal.* **2022**, *364*, 744–749; h) Z. Wei, H. Li, Y. Wang, Q. Liu, *Angew. Chem. Int. Ed.* **2023**, *62*, e202301042.
[6] a) S. Werkmeister, K. Junge, B. Wendt, E. Alberico, H. Jiao, W. Baumann, H. Junge, F. Gallou, M. Beller, *Angew. Chem. Int. Ed.* **2014**, *53*, 8722–8726; b) T. Zell, Y. Ben-David, D. Milstein, *Angew. Chem. Int. Ed.* **2014**, *53*, 4685–4689; c) S. Chakraborty, H. Dai, P. Bhattacharya, N. T. Fairweather, M. S. Gibson, J. A. Krause, H. Guan, *J. Am. Chem. Soc.* **2014**, *136*, 7869–7872; d) S. Elangovan, B. Wendt, C. Topf, S. Bachmann, M. Scalone, A. Spannenberg, H. Jiao, W. Baumann, K. Junge, M. Beller, *Adv. Synth. Catal.* **2016**, *358*, 820–825; e) P. Gajewski, A. Gonzalez-de-Castro, M. Renom-Carrasco, U. Piarulli, C. Gennari, J. G. de Vries, L. Lefort, L. Pignataro, *ChemCatChem* **2016**, *8*, 3431–3435.
[7] a) D. Srimani, A. Mukherjee, A. F. Goldberg, G. Leitus, Y. Diskin-Posner, L. J. Shimon, Y. Ben David, D. Milstein, *Angew. Chem. Int. Ed.* **2015**, *54*, 12357–12360; b) T. J. Korstanje, J. Ivar van der Vlugt, C. J. Elsevier, B. de Bruin, *Science* **2015**, *350*, 298–302; c) K. Junge, B. Wendt, A. Cingolani, A. Spannenberg, Z. Wei, H. Jiao, M. Beller, *Chem. Eur. J.* **2018**, *24*, 1046–1052.
[8] B. M. Zimmermann, T. T. Ngoc, D.-I. Tzaras, T. Kaicharla, J. F. Teichert, *J. Am. Chem. Soc.* **2021**, *143*, 16865–16873.
[9] P. Schlichter, C. Werlé, *Synthesis* **2022**, *54*, 517–534.
[10] J. R. Khusnutdinova, D. Milstein, *Angew. Chem. Int. Ed.* **2015**, *54*, 12236–12273.
[11] a) S. Weber, B. Stöger, K. Kirchner, *Org. Lett.* **2018**, *20*, 7212–7215; b) J. A. Garduño, J. J. García, *ACS Catal.* **2018**, *9*, 392–401; c) S. Weber, B. Stöger, L. F. Veiros, K. Kirchner, *ACS Catal.* **2019**, *9*, 9715–9720; d) S. Weber, L. F. Veiros, K.

Kirchner, *Adv. Synth. Catal.* **2019**, *361*, 5412–5420; e) S. Kostera, S. Weber, M. Peruzzini, L. F. Veiros, K. Kirchner, L. Gonsalvi, *Organometallics* **2021**, *40*, 1213–1220; f) S. Weber, J. Brünig, L. F. Veiros, K. Kirchner, *Organometallics* **2021**, *40*, 1388–1394.

[12] a) R. Buhaibeh, O. A. Filippov, A. Bruneau-Voisine, J. Willot, C. Duhayon, D. A. Valyaev, N. Lugan, Y. Canac, J. Sortais, *Angew. Chem. Int. Ed.* **2019**, *58*, 6727–6731; b) R. Buhaibeh, C. Duhayon, D. A. Valyaev, J. Sortais, Y. Canac, *Organometallics* **2021**, *40*, 231–241; c) W. Yang, I. Y. Chernyshov, R. K. A. van Schendel, M. Weber, C. Müller, G. A. Filonenko, E. A. Pidko, *Nat. Comm.* **2021**, *12*, 12; d) R. Kumar, M. K. Pandey, A. Bhandari, J. Choudhury, *ACS Catal.* **2023**, *13*, 4824–4834.

[13] a) V. Charra, P. de Fremont, P. Braunstein, *Coord. Chem. Rev.* **2017**, *341*, 53–176; b) M. G. Gardiner, C. C. Ho, *Coord. Chem. Rev.* **2018**, *375*, 373–388.

[14] F. Franco, M. F. Pinto, B. Royo, J. Lloret-Fillol, *Angew. Chem. Int. Ed.* **2018**, *57*, 4603–4606.

[15] a) S. C. Sousa, C. J. Carrasco, M. F. Pinto, B. Royo, *ChemCatChem* **2019**, *11*, 3839–3843; b) S. C. Sousa, S. Realista, B. Royo, *Adv. Synth. Catal.* **2020**, *362*, 2437–2443.

[16] a) X.-B. Lan, Z. Ye, M. Huang, J. Liu, Y. Liu, Z. Ke, *Org. Lett.* **2019**, *21*, 8065–8070; b) M. Huang, Y. Li, Y. Li, J. Liu, S. Shu, Y. Liu, Z. Ke, *Chem. Commun.* **2019**, *55*, 6213–6216.

[17] K. Ganguli, A. Mandal, S. Kundu, *ACS Catal.* **2022**, *12*, 12444–12457.

[18] F. A. Westerhaus, B. Wendt, A. Dumrath, G. Wienhöfer, K. Junge, M. Beller, *ChemSusChem* **2013**, *6*, 1001–1005.

[19] K. Azouzi, L. Pedussaut, R. Pointis, A. Bonfiglio, R. K. Riddhi, C. Duhayon, S. Bastin, J. Sortais, *Organometallics* **2023**, https://doi.org/10.1021/acs.organomet.3c00137.

[20] a) M. G. Gardiner, W. A. Herrmann, C.-P. Reisinger, J. Schwarz, M. Spiegler, *J. Organomet. Chem.* **1999**, *572*, 239–247; b) W. A. Herrmann, J. Schwarz, M. G. Gardiner, *Organometallics* **1999**, *18*, 4082–4089.

[21] a) Y. Yamaguchi, T. Kashiwabara, K. Ogata, Y. Miura, Y. Nakamura, K. Kobayashi, T. Ito, *Chem. Commun.* **2004**, 2160–2161; b) K. Ogata, Y. Yamaguchi, Y. Kurihara, K. Ueda, H. Nagao, T. Ito, *Inorg. Chim. Acta* **2012**, *390*, 199–209.

[22] Deposition numbers 2268051 (**3g**) and 2268052 (**3i**) contain the supplementary crystallographic data for this paper. These data are provided free of charge by the joint Cambridge Crystallographic Data Centre and Fachinformationszentrum Karlsruhe Access Structures service.

[23] a) W. P. Fehlhammer, T. Bliss, U. Kernbach, I. Brüdgam, *J. Organomet. Chem.* **1995**, *490*, 149–153; b) W. A. Herrmann, C.-P. Reisinger, M. Spiegler, *J. Organomet. Chem.* **1998**, *557*, 93–96; c) M. Heckenroth, A. Neels, H. Stoeckli-Evans, M. Albrecht, *Inorg. Chim. Acta* **2006**, *359*, 1929–1938; d) M. Heckenroth, A. Neels, M. G. Garnier, P. Aebi, A. W. Ehlers, M. Albrecht, *Chem. Eur. J.* **2009**, *15*, 9375–9386.

[24] J. A. Mata, A. R. Chianese, J. R. Miecznikowski, M. Poyatos, E. Peris, J. W. Faller, R. H. Crabtree, *Organometallics* **2004**, *23*, 1253–1263.

[25] M. Albrecht, J. R. Miecznikowski, A. Samuel, J. W. Faller, R. H. Crabtree, *Organometallics* **2002**, *21*, 3596–3604.

[26] K. Öfele, W. A. Herrmann, D. Mihalios, M. Elison, E. Herdtweck, T. Priermeier, P. Kiprof, *J. Organomet. Chem.* **1995**, *498*, 1–14.

[27] Q. Teng, H. V. Huynh, *Inorg. Chem.* **2014**, *53*, 10964–10973.

Manuscript received: June 7, 2023
Accepted manuscript online: July 3, 2023
Version of record online: July 18, 2023

7.2 Low-Valent Molybdenum PNP Pincer Complexes as Catalysts for the Semihydrogenation of Alkynes

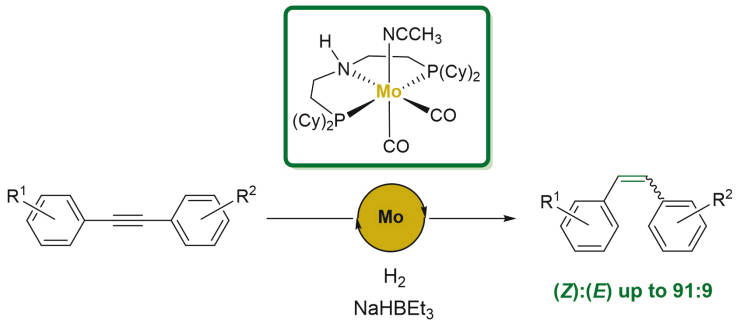

N. F. Both, A. Spannenberg, K. Junge, M. Beller, *Organometallics* **2022**, *41*, 1797–1805.
DOI: 10.1021/acs.organomet.1c00709. Electronic supporting information is available online.

Author's Contribution

The author performed the experimental work including synthesis of the utilized Mo complexes, optimization of the reaction conditions, investigation of the substrate scope and catalytic experiments for mechanistic studies. Furthermore, the author evaluated all analytical data, except for the data from single crystal X-ray diffraction, wrote the initial draft of the manuscript and the supporting information. The author's contribution approximately accounts 80 %.

Niklas F. Both	Prof. Matthias Beller
(PhD student)	(supervisor)

ORGANOMETALLICS

pubs.acs.org/Organometallics Article

Low-Valent Molybdenum PNP Pincer Complexes as Catalysts for the Semihydrogenation of Alkynes

Niklas F. Both, Anke Spannenberg, Kathrin Junge,* and Matthias Beller*

Cite This: *Organometallics* 2022, 41, 1797–1805 Read Online

ACCESS | Metrics & More | Article Recommendations | Supporting Information

ABSTRACT: Low-valent molybdenum PNP pincer complexes were studied as catalysts for the semihydrogenation of alkynes. For that purpose, *t*Bu-substituted PNP complexes $PNP^{tBu}Mo(CO)_2$ (**6a**) and $PNP^{tBu}Mo(CO)_3$ (**6c**) and the NNP complex $NNP^{iPr}Mo(CO)_2(PPh_3)$ ((*rac*)-**7**) were synthesized and characterized. By utilizing the cyclohexyl-substituted complex $PNP^{Cy}Mo(CO)_2(CH_3CN)$ (**5a**), several diphenylacetylene derivatives are transformed to the corresponding (*Z*)-alkenes with good to very good diastereoselectivities (up to 91:9). Mechanistic experiments indicate an outer-sphere mechanism including metal−ligand cooperativity.

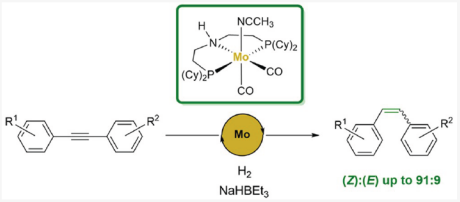

INTRODUCTION

The conversion of alkynes to alkenes plays an important role in the bulk and fine chemical industry as well as in basic chemical research.[1,2] Although numerous methods for the synthesis of alkenes have been developed in the past, the catalytic semihydrogenation of alkynes with dihydrogen is arguably one of the most efficient and atom economic approaches in this respect. However, it continues to be challenging due to the required control of stereo- ((*Z*)/(*E*)-isomers) and chemoselectivity (alkynes vs alkenes).

Typically, in this transformation heterogeneous systems based on noble metals, in particular Pd,[3,4] are utilized such as the well-known Lindlar's catalyst (Pb-poisoned $Pd/CaCO_3$).[5] With growing importance of sustainability and resource scarcity, over the past decade many efforts were made to develop catalysts derived from more available and cheaper non-noble metals, especially from the first-row transition metals.[6] More specifically, both heterogeneous and homogeneous systems based on Cr,[7] Fe,[8−11] Mn,[12,13] Co,[14−16] Ni,[17−19] and Cu[20] have been studied for this transformation.

For homogeneous, non-noble metal systems, the first report dates back to 1989, when Bianchini and co-workers discovered that iron(II) complex **I** with a tetradentate phosphine ligand is capable of selectively hydrogenating terminal alkynes to the corresponding alkenes (Figure 1).[8,9] In 2013, the group of Milstein described acridine-based PNP iron(II) pincer complex **II** with an amidoborane coligand for the (*E*)-selective semihydrogenation of alkynes.[10] Initially, in this process the (*Z*)-alkene is formed which is rapidly isomerized to its (*E*)-isomer. Later, Fout and co-workers reported cobalt(I) dihydrogen complex **III** bearing a CCC pincer ligand with two NHC moieties for the (*E*)-selective semihydrogenation of a broad scope of alkynes.[14] As in the case of iron complex **II**, the

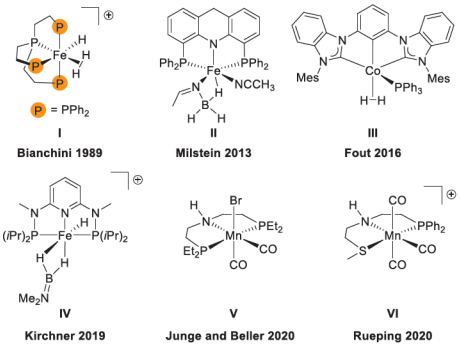

Figure 1. Selected examples of homogeneous, non-noble metal (pre)catalysts for the semihydrogenation of alkynes.

(*Z*)-alkene is formed first and then isomerized. Cationic PNP iron(II) complex **IV** published by the group of Kirchner efficiently hydrogenates internal alkynes to (*Z*)-alkenes under mild conditions.[11] Recently, our group published the first homogeneous manganese complex for the semihydrogenation

Special Issue: Sustainable Organometallic Chemistry

Received: December 21, 2021
Published: March 15, 2022

of alkynes.[12] Here, PNP manganese(I) complex **V** reduces diphenylacetylene derivates under mild conditions with excellent (*Z*)-selectivity. Mechanistic investigations revealed that hydrogenation proceeds via an outer-sphere mechanism utilizing the amino moiety in the ligand backbone for metal–ligand cooperativity[21] as it is often observed for these systems. No isomerization of the formed alkene takes place under the chosen conditions. Shortly after, Rueping and co-workers reported a similar cationic PNS manganese(I) complex **VI**.[13] This air-stable complex hydrogenates a variety of alkynes to the (*Z*)-alkenes under mild conditions.

Besides first-row transition metals, molybdenum also represents an attractive substitute for noble metals due to its low costs and toxicity.[22] Indeed, heterogeneous molybdenum catalysts are widely used for hydrogenation reactions[23] and homogeneous molybdenum complexes were studied for hydrogenations, particularly of N_2 and CO_2.[24−31] However, reports on catalytic hydrogenations with molybdenum complexes remain scarce in comparison to first-row transition metals.[32−38]

Our group has recently developed a series of structurally related low-valent molybdenum complexes as catalysts for the hydrogenation of ketones,[39] alkenes,[39] formamides,[40] and nitriles.[41] Based on this work, we became interested to explore their potential as catalysts for the semihydrogenation of alkynes.

RESULTS AND DISCUSSION

Synthesis and Characterization of Mo Complexes. Initially, a series of low-valent molybdenum complexes have been prepared starting from $Mo(CH_3CN)_2(CO)_2(PPh_3)_2$ (**1**) and the corresponding PNP ligands (Scheme 1, Figure 2)

Scheme 1. General Synthesis of Low-Valent PNP Molybdenum Complexes Used in This Work

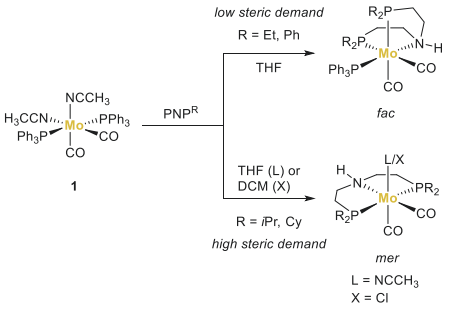

according to previous protocols.[39−41] Sterically low demanding substituents (Ph, Et) on the phosphines of the pincer ligand lead to complexes with a facial coordination mode of the PNP ligand. In these complexes a PPh_3 ligand remains besides the two strongly bound CO ligands on the Mo atom.

Increased steric demand on the phosphines (*i*Pr, Cy) causes a meridional arrangement of the PNP ligand, leading to the formation of more classical pincer complexes. Due to the structure of **1**, in which the weak-field CH_3CN ligands are located *trans* to the strong-field CO ligands, a meridional coordination of the PNP ligand inevitably results in the preservation of one CH_3CN ligand in the complex sphere. If

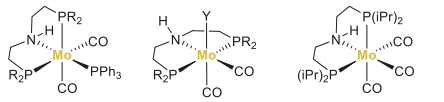

R = Et; **2** [41]
R = Ph; **3** [41]

R = *i*Pr; Y = $NCCH_3$; **4a** [39]
R = Cy; Y = $NCCH_3$; **5a** [41]
R = *t*Bu; Y = none; **6a**
R = *i*Pr; Y = Cl; **4b** [39]
R = Cy; Y = Cl; **5b** [41]
R = *t*Bu; Y = Cl; **6b**

4c [39]
$PNP^{Cy}Mo(CO)_3$
5c
$PNP^{tBu}Mo(CO)_3$
6c

Figure 2. Series of molybdenum complexes tested in this work as catalysts for the semihydrogenation of alkynes.

the synthesis of these complexes is performed in DCM as a solvent, chlorinated molybdenum(I) complexes are obtained, in which the neutral CH_3CN ligand is replaced by a formally anionic Cl ligand.[39,41] The facially coordinated Ph-substituted complex **3** is more stable to chlorination and therefore can be prepared in DCM at room temperature. However, refluxing in DCM yields a heptacoordinated Mo(II) complex bearing two Cl ligands.[41] The reaction of the PNP^{Et} ligand and **1** in DCM leads to product mixtures even at −20 °C.[41]

The new complex **6a** was prepared according to Scheme 2. In contrast to the known *i*Pr- and Cy-substituted congeners,

Scheme 2. Synthesis of *t*Bu-Substituted PNP Molybdenum Complexes 6a, 6b, and 6c

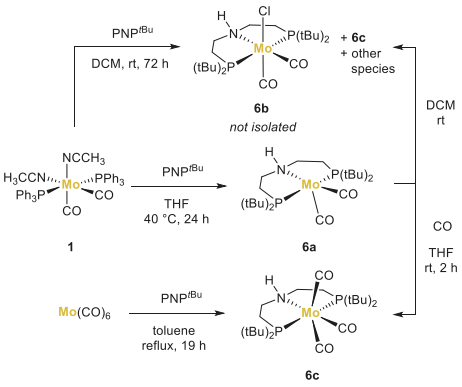

the conversion is not complete after stirring a solution of **1** and the PNP^{tBu} ligand at room temperature overnight, but increased temperature and/or longer reaction times were necessary (e.g., 40 °C for 24 h). Compound **6a** is sparingly soluble in common solvents (toluene, THF, acetonitrile, methanol, DMSO), and therefore, no crystals of the complex nor a meaningful NMR spectrum was obtained. Hence, **6a** could only be analyzed by IR spectroscopy and elemental analysis. The IR spectrum of **6a** features strong CO absorption bands at similar energies as observed for its *i*Pr- and Cy-substituted congeners **4a** and **5a**. However, no CN-stretch of a potential CH_3CN ligand was detected. Elemental analysis of the obtained material also pointed toward the absence of a CH_3CN ligand. This might be rationalized by the high steric

https://doi.org/10.1021/acs.organomet.1c00709
Organometallics 2022, 41, 1797−1805

demand of the *t*Bu-groups leaving little space in the coordination sphere.

If compound **1** is reacted with the PNP^{tBu} ligand in DCM or **6a** is dissolved in this solvent, formation of another complex was observed by IR spectroscopy, which proofed as a useful tool due to the strong CO absorption bands that all these complexes exhibit (see Supporting Information (SI) for details). However, attempts to isolate this compound in analytical purity remained unsuccessful. Most likely, molybdenum(I) complex **6b** is formed, as can be concluded from the observed reactivity of the analogous complexes **4a** and **5a** in DCM and the similarity of the IR spectrum of the formed complex with these of complexes **4b** and **5b**. In solution (THF, DCM, DMSO) **6a** and **6b** slowly form the tri(carbonyl)complex **6c** and other unidentified species.

Complex **6c** could be separately prepared by refluxing $Mo(CO)_6$ with a slight excess of PNP^{tBu} in toluene for 19 h. Furthermore, **6c** is obtained by the exposure of a suspension of complex **6a** in THF to CO gas, visible by a color change from brown red to yellow in a couple of minutes (see SI for images). The complex crystallizes as fine yellow needles from DCM/heptane, which were suitable for single crystal X-ray diffraction analysis. In the solid state of **6c** (Figure 3) the PNP ligand

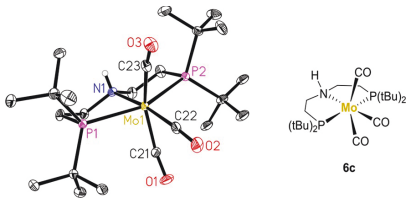

Figure 3. Molecular structure of **6c** in the solid-state. Displacement ellipsoids set at 30% probability level, carbon-bound hydrogen atoms and lower occupied atoms of the disordered *t*Bu-group are omitted for clarity. Selected bond lengths [Å] and angles [deg]: Mo1−N1 2.3582(14), Mo1−P1 2.5182(4), Mo1−C21 1.9963(19), Mo1−C22 1.9289(18), Mo1−C23 2.0042(19), C21−O1 1.166(2), C22−O2 1.179(2), C23−O3 1.161(2), N1−Mo1−C21 93.88(7), N1−Mo1−C22 168.91(7), N1−Mo1−C23 112.31(6), P1−Mo1−P2 154.23(2), C21−Mo1−C23 153.79(8).

coordinates meridionally to the molybdenum center, forcing two CO ligands in a *trans* position. This leaves the complex in a strongly distorted octahedral geometry with a C21−Mo1−C23 angle of 153.79(8)°, far from linearity.

The meridional structure of **6c** contrasts with the solid-state structure of the *i*Pr-substituted tri(carbonyl)molybdenum complex **4c**, which was found to have a facial ligand geometry.[39] The NMR spectra of complexes **4c**, **5c**, and **6c** show the presence of two different species whose ratio is solvent dependent.[42] Likely, in solution an equilibrium exists between the facial and the meridional complexes.

The resonance of the *t*Bu-groups of **6c** in the ^1H NMR spectrum shows a complex coupling pattern due to $^1H-^{31}P$ coupling. Decoupling of ^{31}P simplifies the resonances to two singlets in accordance with the C_S symmetry of the complex.

Next to Mo PNP pincer compounds, the coordination of NNP ligands to molybdenum was studied. Complex (*rac*)-**7** can easily be prepared by stirring **1** with a slight excess of the NNP ligand in THF at room temperature. In contrast to the symmetric PNP pincer complexes, which all feature a mirror plane, (*rac*)-**7** exhibits helical chirality due to the unsymmetric NNP ligand. In the solid state, the NNP ligand coordinates facially to the molybdenum center with the phosphine moiety being located *trans* to the one remaining PPh_3 ligand (Figure 4). The facial structure can be explained by the low steric

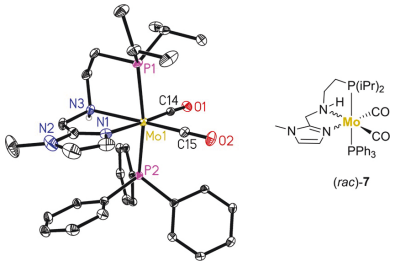

Figure 4. Molecular structure of (*rac*)-**7** in the solid-state. Displacement ellipsoids set at 30% probability level; carbon-bound hydrogen atoms omitted for clarity. Selected bond lengths [Å] and angles [deg]: Mo1−N1 2.2619(15) Mo1−N3 2.3839(14), Mo1−P1 2.4519(5), Mo1−P2 2.4347(5), Mo1−C14 1.9203(18), Mo1−C15 1.9202(17), C14−O1 1.190(2), C15−O2 1.185(2), N1−Mo1−N3 72.92(5), P1−Mo1−P2 168.83(2), N1−Mo1−C14 176.41(6), N3−Mo1−C15 169.17(6).

demand of the *N*-methylimidazolyl group (compare Scheme 1). Interestingly, in (*rac*)-**7** the PPh_3 ligand is located *trans* to the phosphine of the NNP ligand, whereas in **2** and **3** it opposes the amino functionality of the PNP ligand. However, heating a solution of **3** in toluene-d_8 to 80 °C leads to a mixture of complexes as indicated by NMR experiments. One of the formed complexes likely is a complex (*iso*)-**3** in which the PPh_3 ligand is opposing a phosphine of the PNP ligand in analogy to the solid-state structure of (*rac*)-**7** (see SI for details). Also, resonances that can be assigned to meridional complexes were observed, indicating that *fac-mer* isomerization takes places at elevated temperatures. Due to the helical chirality of (*rac*)-**7**, protons bound to the same carbon atom in the methylene and ethylene linker in the ligand backbone as well as the two *i*Pr-groups are diastereotopic to each other. Together with the limited solubility of (*rac*)-**7**, this leads to a low intensity of the resonances of these protons in the ^1H NMR spectrum. As expected, the ^{31}P NMR spectrum of (*rac*)-**7** in CD_3CN exhibits two doublets at 67.24 and 55.54 ppm, respectively. Furthermore, some free PPh_3 is observed which originates from the complex, since no resonance for free PPh_3 is found for a suspension of (*rac*)-**7** in toluene-d_8, in which (*rac*)-**7** itself is insoluble. This implies that PPh_3 is not strongly bound in (*rac*)-**7**.

The IR spectrum of (*rac*)-**7** exhibits two strong CO absorption bands at 1778 and 1697 cm^{-1}. The very low energy of the absorptions—being in the area typically observed for C=O double bonds—displays the strong π-backbonding to the CO ligands and the electron richness of the complex. For comparison, complexes **2** and **3** show CO absorptions at higher energies (1812, 1730 cm^{-1} and 1827, 1743 cm^{-1}, respectively)[41] which illustrates the weaker electron-donating ability of the phosphines compared with the *N*-methylimida-

https://doi.org/10.1021/acs.organomet.1c00709
Organometallics 2022, 41, 1797−1805

zolyl group. Liu and co-workers observed similar ligand properties with analogous manganese complexes.[43]

Catalytic Hydrogenation of Diphenylacetylene with Low-Valent Molybdenum Complexes. We started our catalytic experiments by investigating the different molybdenum(0) and molybdenum(I) complexes as catalysts for the hydrogenation of alkynes (Table 1). Diphenylacetylene was reacted as a model substrate under 30 bar of H_2 pressure at 80 °C using 5 mol % catalyst and 5 mol % $NaHBEt_3$ as base, since $NaHBEt_3$ has significantly affected catalyst activity in previous works.[39−41]

Table 1. Molybdenum-Catalyzed Hydrogenation of Diphenylacetylene[a]

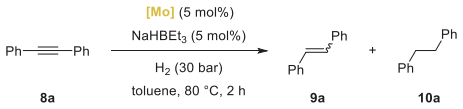

Entry	[Mo]	Conv[b]	Yield **9a** (%)	(*Z*)/(*E*)	Yield **10a** (%)
1	**2**	17	15	36:64	2
2	**3**	54	51	57:43	3
3	**4a**	68	65	75:25	3
4	**4b**	14	7	76:24	7
5	**5a**	93	89	85:15	4
6	**5b**	7	2	n.d.	5
7	**6a**	1	1	n.d.	0
8	**6c**	3	2	n.d.	1
9	(*rac*)-**7**	19	15	77:23	4
10	**1**	21	13	33:67	8
11	none	1	1	n.d.	0

[a]Reaction conditions: 0.5 mmol of **8a**, a 0.5 M solution of $NaHBEt_3$ in toluene and 2 mL of toluene were used. [b]Conversion, yield, and (*Z*)/(*E*) ratio were determined by GC analysis using hexadecane as internal standard.

The facial complexes **2** and **3** showed mediocre conversions and diastereoselectivities (Table 1, entries 1−2), whereas the meridional complexes **4a** and **5a** performed better especially regarding the diastereoselectivity (Table 1, entries 3 and 5). Complex **5a** gave the best results with nearly full conversion (93%) and a good diastereoselectivity of 85:15 in favor of the (*Z*)-diastereomer. In contrast, the chlorinated molybdenum(I) complexes **4b** and **5b** only showed low conversions.

Interestingly, the observed difference in catalytic activity between **4a** and **5a** was surprisingly large (93% to 68% conversion). Since the electronic properties of the *i*Pr- and the Cy-substituents are quite similar, we suggest that the improved catalytic activity might be caused by the increased steric demand.

To prove this assumption the *t*Bu-substituted PNP complexes **6a** and **6c** were tested in the semihydrogenation of diphenylacetylene. Unfortunately, both complexes, **6a** and **6c**, showed nearly no catalytic activity (Table 1, entries 7−8).

For related Mn-complexes, NNP-type ligands showed an improved catalytic activity in hydrogenation reactions in comparison to the PNP complexes.[43,44] Therefore, the respective Mo NNP pincer complex (*rac*)-**7** (*vide supra*) was tested under our standard conditions. However, complex (*rac*)-**7** showed moderate conversion and good diastereoselectivity (Table 1, entry 9). By applying complex **1**, moderate conversion and diastereoselectivity were obtained (Table 1, entry 10), and by just using $NaHBEt_3$ without a molybdenum complex, no conversion of diphenylacetylene was observed (Table 1, entry 11).

Variation of the Reaction Conditions and Substrate Scope of the Semihydrogenation. After identifying complex **5a** as the most promising precatalyst, we investigated the influence of different reaction parameters such as solvents and bases on the outcome of the reaction (Table 2). Polar solvents like THF, acetonitrile, or DCM led to poor conversions (<10%), whereas nonpolar, aprotic solvents like toluene, cyclohexane, and heptane are suitable for the reaction. Both toluene and cyclohexane provided high conversions and yields around 90% (Table 2, entries 1 and 3). In the base screening, $NaHBEt_3$ presented the best results under the tested conditions (Table 2, entry 1). For NaHMDS a slightly lower conversion and yield were observed (Table 2, entry 7). The weaker bases $NaHBH_3$, NaOH, and NaO*t*Bu gave only low conversions (≤10%) (Table 2, entries 8−10), which are comparable with the results obtained without addition of base (Table 2, entry 11).

Table 2. Influence of Solvent and Base on the Molybdenum-Catalyzed Hydrogenation of Diphenylacetylene[a]

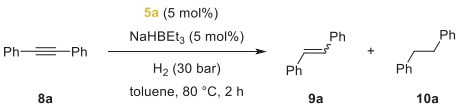

Entry	Deviation	Conv[b]	Yield **9a** (%)[b]	(*Z*)/(*E*)	Yield **10a** (%)[b]
1	–	93	89	85:15	4
2	THF	9	4	68:32	5
3	heptane	46	44	73:27	2
4	acetonitrile	1	1	n.d.	0
5	DCM	3	1	n.d.	2
6	cyclohexane	92	87	86:14	5
7	NaHMDS	79	75	87:13	4
8	$NaHBH_3$	9	5	58:42	4
9	NaOH	9	5	52:48	4
10	NaO*t*Bu	10	4	45:55	6
11	no base	9	4	43:57	5

[a]Reaction conditions: 0.5 mmol of **8a**, a 0.5 M solution of $NaHBEt_3$ in toluene and 2 mL of toluene were used. [b]Conversion, yield, and (*Z*)/(*E*) ratio were determined by GC analysis using hexadecane as internal standard.

Thus, a strong base seems to be needed to form the active catalyst species, likely an anionic amido complex which is generated by the deprotonation of the amine in the ligand backbone.[40] Interestingly, variation of the cation of the additive has a significant influence on the catalytic performance. While $LiHBEt_3$ showed lower activity (32% conv, 23% yield, 84:16 (*Z*)/(*E*)) in comparison to $NaHBEt_3$, $KHBEt_3$ produced comparable conversion and yield but lower diastereoselectivity (84% conv, 79% yield, 73:27 (*Z*)/(*E*)). The influence of the cation is further supported by experiments in the presence of 15-crown-5, which is known to selectively bind potassium ions (see SI for details). A similar effect was found for the addition of THF.

Furthermore, catalyst loading, reaction temperature, and the dihydrogen pressure were investigated (Table 3). Even a slight decrease of the catalyst loading resulted in a major loss in conversion and yield (Table 3, entries 2−3). At 60 °C the

https://doi.org/10.1021/acs.organomet.1c00709
Organometallics 2022, 41, 1797−1805

Table 3. Influence of Catalyst Loading, Temperature and Dihydrogen Pressure on the Molybdenum-Catalyzed Hydrogenation of Diphenylacetylene[a]

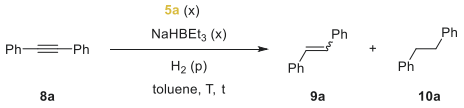

8a 9a 10a

Entry	x [mol %]	T [°C]	p [bar]	t [h]	Conv[b]	Yield **9a**[b] (%)	$(Z)/(E)$	Yield **10a**[b] (%)
1	5.0	80	30	2	93	89	85:15	4
2	4.0	80	30	2	64	61	86:14	3
3	2.5	80	30	2	11	7	51:49	4
4	5.0	60	30	2	71	68	85:15	3
5	5.0	60	30	6	98	96	86:14	3
6	5.0	80	20	2	81	79	86:14	2
7	5.0	80	10	2	39	32	84:16	7
8[c]	5.0	80	30	2	98	96	86:14	4

[a]Reaction conditions: 0.5 mmol of **8a**, a 0.5 M solution of $NaHBEt_3$ in toluene and 2 mL of toluene were used. [b]Conversion, yield, and $(Z)/(E)$ ratio were determined by GC analysis using hexadecane as internal standard. [c]1 mL instead of 2 mL of toluene as solvent.

reaction proceeded slower, but by applying longer reaction times, full conversion could be reached (Table 3, entries 4−5). Under 20 bar of dihydrogen pressure, a slight decrease in conversion and yield is obtained, and lowering the pressure to 10 bar results in much lower conversion and yield (Table 3, entries 6−7). Conversion and yield could be enhanced by running the reaction at higher concentrations (Table 3, entry 8). During all these variations of parameters, the diastereoselectivity was not influenced.

Next, various substituted diphenylacetylenes were reacted under the optimized reaction conditions (Scheme 3). While a methyl substitution in the para- (**8b**) or meta-position (**8c**) on one of the phenyl rings was well tolerated and showed no significant difference compared to diphenylacetylene **8a**, methylation in the ortho-position (**8d**) resulted in drastically lowered conversion but similar diastereoselectivity. Fluorine-containing substrate **8e** was smoothly converted to the corresponding alkene **9e** with good diastereoselectivity, whereas for the more reactive chloride **8f** and bromide **8g**, small amounts of hydrodehalogenation products were observed. Likely, the catalyst is deactivated by halogenation in these cases, resulting in lower conversions and yields.

Electron-rich substituted diphenylacetylenes (**8h−k**) including ethers, thioethers, and silanes were readily converted to the corresponding alkenes (**9h−k**). Under standard reaction conditions (80 °C, 2 h) in all cases small amounts (>10%) of alkane were observed. By applying lower temperatures at an increased reaction time (60 °C, 16 h), reduction to the alkane could mostly be suppressed and high yields (91−86%) as well as good diastereoselectivities (91:9−79:21) were obtained.

For diphenylacetylenes featuring electron-withdrawing substituents like nitriles and ketones as well as nitro, ester, or trifluoromethyl groups, only low conversions (≥10%) were observed (see SI for detailed results). Even when a strongly electron-donating methoxy group is present, a trifluoromethyl group on the other phenyl ring, like in substrate **8m**, resulted in a low conversion. A possible explanation might be that the catalyst is inhibited by the substrates through the formation of stable alkyne complexes. A similar effect was observed for the pyridine derivative **8q** (see SI). Diyne **8p** featuring two directly connected alkyne functionalities resulted in poor conversion and yield (see SI), whereas substrate **8n** could be easily converted to the corresponding diene with a selectivity of the (Z, Z)-diastereomer **9n** to the other diastereomers of 86:14. Although sulfur-containing compounds often completely block hydrogenation catalysts, the thiophene-containing substrate **8o** showed moderate conversion.

Besides aryl−aryl alkynes also terminal alkynes, as well as aryl-alkyl or alkyl−alkyl alkynes, were tested. Unfortunately, all these substrate classes showed only low conversions under the applied conditions in the presence of either **4a** or **5a** as catalyst (see SI).

Finally, a series of mechanistic control experiments were performed. To investigate if isomerization of the formed alkenes takes place during the reaction, (Z)- and (E)-stilbene were used as starting material, respectively (Scheme 4). When (E)-stilbene was used, no significant isomerization and only traces of alkane were observed. In the case of (Z)-stilbene, formation of 2% of the more stable (E)-isomer and of the alkane were detected, respectively. This clearly shows that isomerization reactions are no major pathway under these conditions. Next, to examine whether metal−ligand cooperativity (MLC) is involved, the free NH-moiety in the ligand backbone of **4a** was blocked by substitution. When the *N*-methylated derivative **4a-Me** was applied under standard conditions, no significant hydrogenation occurred indicating an outer-sphere mechanism including MLC. Also, when **5a** was used with 5 mol % of PPh_3 as an additive under standard conditions (see SI for details), no decrease in catalytic activity was found, as would be expected for an inner-sphere mechanism due to the blocking of a vacant coordination site. This further supports an outer-sphere mechanism for the described hydrogenation reactions.

SUMMARY AND CONCLUSIONS

Here, we describe novel homogeneous catalytic hydrogenation of alkynes using molybdenum complexes. The new *t*Bu substituted Mo PNP pincer complexes **6a** and **6c** as well as the NNP pincer complex (*rac*)-**7** have been prepared and characterized. These complexes as well as related complexes were tested as catalysts in the semihydrogenation of diphenylacetylene. The best performance was obtained in the presence of the cyclohexyl-substituted complex **5a** $PNP^{Cy}Mo(CO)_2(CH_3CN)$. Utilizing this catalyst, various internal diaryl alkynes are hydrogenated to the corresponding alkenes with good to very good chemo- and diastereoselectivity for the (Z)-

https://doi.org/10.1021/acs.organomet.1c00709
Organometallics 2022, 41, 1797−1805

Scheme 3. Molybdenum Catalyzed Semihydrogenation of Selected Alkyne Substrates[a]

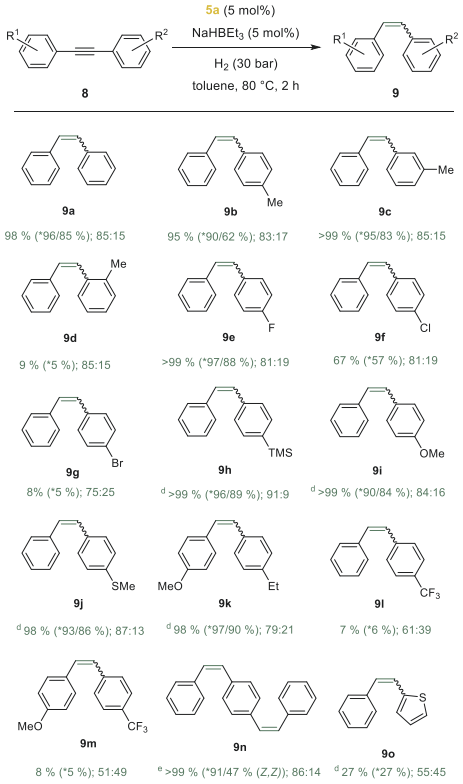

[a]Reaction conditions: 0.5 mmol of **8**, a 0.5 M solution of $NaHBEt_3$ in toluene and 1 mL of toluene were used. [b]Conversion and (*Z*)/(*E*) ratio were determined by GC analysis. [c]Yield determined by GC analysis; isolated yield given in brackets. [d]60 °C, 16 h. [e]GC yield for all diastereomers, isolated yield for (*Z*, *Z*) diastereomer, diastereomeric ratio of (*Z*, *Z*) to other diastereomers.

alkene and no significant isomerization taking place. However, the tolerance of this catalytic system toward substrates with electron-withdrawing substituents is limited, allowing for further improvement. Mechanistic experiments pointed toward an outer-sphere mechanism including MLC.

EXPERIMENTAL SECTION

General Information. All manipulations, except when indicated otherwise, were carried out under an argon atmosphere with exclusion of air and moisture using standard Schlenk and glovebox techniques. Solvents were dried over activated alumina columns using a solvent purification system (Innovative Technology PS-MD-6) and stored over molecular sieves (4 Å) under an argon atmosphere. Deuterated solvents were purchased from eurisotop, degassed by three successive freeze−pump−thaw cycles, and stored over molecular sieves (4 Å) under an argon atmosphere. NMR spectra were recorded on a Bruker Avance (300 MHz, 400 MHz) or Bruker Fourier (300 MHz)

Scheme 4. Mechanistic Experiments Performed for the Molybdenum Catalyzed Semihydrogenation of Alkynes[a]

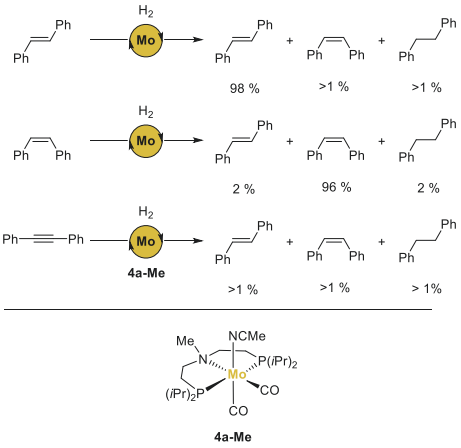

[a]Reaction conditions: 0.5 mmol of diphenylacetylene, (*Z*)-stilbene or (*E*)-stilbene as starting material, 5 mol % of molybdenum catalyst, a 0.5 M solution of $NaHBEt_3$ in toluene, 30 bar of dihydrogen pressure and 1 mL of toluene as a solvent were used at 80 °C for 2 h. [b]Yields were determined by GC analysis using hexadecane as an internal standard.

instrument. Chemical shifts (δ) are reported in parts per million (ppm) and are referenced to residual proton solvent signals or carbon resonances.[45,46] Infrared spectra were recorded in the solid state on a Nicolet iS 5 FT-IR spectrometer equipped with a PIKE Technologies GladiATR ATR. Elemental analyses were carried out in the Microanalysis Laboratory of the institute on a Leco TruSpec Micro CHNS device. GC analyses were carried out on an Agilent 7890A chromatograph using an HP-5 column (30 m × 0.25 m × 0.25 m). Bis[2-(diphenylphosphino)ethyl]ammonium chloride (15-7306), bis-[2-(di-isopropylphosphino)ethyl]amine (15-7304), and bis[2-(dicyclohexylphosphino)ethyl]amine (15-7310) were purchased from Strem Chemicals and used without further purification. Bis[2-(di-*tert*-butylphosphino)ethyl]amine (AB393139) was purchased from abcr and used without further purification. Bis[2-(diethylphosphino)ethyl]amine[47] and 2-(di-isopropylphosphino)-*N*-((1-methyl-1*H*-imidazol-2-yl)methyl)ethylamine[48] were synthesized according to literature. $NaHBEt_3$ was purchased from Sigma-Aldrich (227307). $Mo(CO)_6$ was purchased from Sigma-Aldrich (577766) with a metal purity of ≥99.9%. The complexes **1**,[49−51] **2**,[41] **3**,[41] **4a**,[39] **4a-Me**,[42] **4b**,[39] **5a**,[41] and **5b**[41] were synthesized according to literature procedures.

Synthesis of $Mo(CH_3CN)_2(CO)_2(PPh_3)_2$ (1). The procedure was adapted from literature.[49−51] In a 500 mL three-necked round-bottom equipped with a large stirring bar and a reflux condenser, $Mo(CO)_6$ (5.07 g, 19.2 mmol, 1.0 equiv) was suspended in 40 mL of acetonitrile and 40 mL of benzene and heated to reflux (95 °C oil bath temperature) for 4 h. The reaction mixture was allowed to cool to room temperature, and allylbromide (2.32 g, 19.2 mmol, 1.0 equiv) was added dropwise resulting in a color change from yellow to red. The mixture was heated to reflux for another 19 h, and an orange solid precipitated upon cooling to room temperature. The solution was filtered off at 0 °C, and the residue was suspended in 60 mL of acetonitrile. Triphenylphosphine (15.11 g, 57.61 mmol, 3.0 equiv) was added in one portion resulting in a color change to red. Upon heating to reflux for 2 h, a yellow solid precipitated. After cooling to room temperature, the solution was filtered off and the residue was

https://doi.org/10.1021/acs.organomet.1c00709
Organometallics 2022, 41, 1797−1805

thoroughly washed with acetonitrile (3 × 20 mL) and dried *in vacuo*, yielding **1** as a light-yellow solid (9.95 g, 68%). $^{31}P\{^{1}H\}$ NMR (161.99 MHz, DMSO-d_6, 295 K): δ [ppm] = 54.75 (s), 52.04 (s), 50.29 (s), 36.77 (s) 25.46 (s). Multiple resonances are observed because of ligand exchange with DMSO. Therefore, a resonance at −6.9 ppm is observed which is assigned to free PPh_3. A clear assignment of the resonances to the different formed complexes was not performed. Data are still provided for comparison. IR (ATR): ν [cm^{-1}] = 1806 (CO), 1734 (CO).

*Synthesis of $PNP^{Cy}Mo(CO)_3$ (**5c**).* In a 25 mL Schlenk tube $Mo(CO)_6$ (150.0 mg, 568 μmol, 1.0 equiv) and bis[2-(dicyclohexylphosphino)ethyl]amine (277.8 mg, 596.6 μmol, 1.05 equiv) were dissolved in 10 mL of toluene. The reaction mixture was heated to reflux for 19 h. The orange suspension was allowed to cool to room temperature. The solvent was filtered off, and the residue was washed with toluene (2 × 2 mL) and heptane (2 × 2 mL). The light-yellow solid was dried *in vacuo* (311.0 mg, 89%). ^{1}H NMR (400.13 MHz, CD_2Cl_2, 295 K): δ [ppm] = 3.22−3.05 (m, 2H), 2.77−1.10 (m, 49H), 0.84−0.68 (m, 2H). $^{31}P\{^{1}H\}$ NMR (161.99 MHz, CD_2Cl_2, 295 K): δ [ppm] = 65.67 (s), 41.43 (s). Elemental Analysis Calcd for $C_{31}H_{53}MoNO_3P_2$: C, 57.67; H, 8.27; N, 2.17. Found: C, 57.57; H, 8.64; N, 1.99. IR (ATR): ν [cm^{-1}] = 1897 (CO), 1795 (CO), 1761 (CO).

*Synthesis of $PNP^{tBu}Mo(CO)_2$ (**6a**).* In a 25 mL Schlenk tube $Mo(CH_3CN)_2(CO)_2(PPh_3)_2$ (199.9 mg, 263 μmol, 1.0 equiv) was suspended in 5 mL of THF, bis[2-(di-*tert*-butylphosphino)ethyl]amine (10 wt % in toluene, 100.0 mg, 277 μmol, 1.05 equiv) was added, and the reaction mixture was heated at 40 °C for 20 h. The reaction mixture was allowed to cool to room temperature, the solvent was filtered off, and the red-brown residue was washed with THF (4 × 2 mL). Drying in vacuo yielded **6a** as a red solid (145.1 mg, quant.). Elemental Analysis Calcd for $C_{22}H_{45}MoNO_2P_2$: C, 51.46; H, 8.83; N, 2.73. Found: C, 52.48; H, 8.59; N, 1.78. Although these results are outside the range viewed as establishing analytical purity, they are provided to illustrate the best values obtained to date. IR (ATR): ν [cm^{-1}] = 1769 (CO), 1677 (CO).

*Synthesis of $PNP^{tBu}Mo(CO)_3$ (**6c**).* **From 6a:** In a 25 mL Schlenk tube **6a** (110 mg, 214 μmol, 1.0 equiv) was suspended in 5 mL of THF. CO gas was introduced into the suspension, and a color change from brown red to yellow was observed within minutes. After 2 h, all volatiles were removed in vacuo yielding **6c** as a yellow solid (116 mg, quant.). **From $Mo(CO)_6$:** In a 25 mL Schlenk tube $Mo(CO)_6$ (148.3 mg, 562 μmol, 1.0 equiv) was dissolved in 10 mL of toluene and bis[2-(di-*tert*-butylphosphino)ethyl]amine (10 wt % in THF, 213.0 mg, 590 μmol, 1.05 equiv) was added. The reaction mixture was heated to reflux for 19 h. The red-brown suspension was allowed to cool to room temperature. The solvent was filtered off, and the residue was washed with toluene (2 × 1 mL). The residue was dissolved in DCM, and a yellow solid precipitated by adding heptane. The solvent was filtered off, and the residue was washed with heptane (2 × 2 mL). Drying *in vacuo* yielded **6c** as a yellow solid (190 mg, 63%). Yellow needles suitable for single-crystal X-ray diffraction were obtained by slow diffusion of heptane into a solution of **6c** in DCM at 0 °C. ^{1}H NMR (300.20 MHz, CD_2Cl_2, 295 K): δ [ppm] = 3.40−3.20 (m, 2H), 2.46−2.19 (m, 3H), 2.18−2.05 (m, 2H), 1.60−1.41 (m, 2H), 1.39−1.30 (m, 36H). $^{1}H\{^{31}P\}$ NMR (400.13 MHz, CD_2Cl_2, 295 K): δ [ppm] = 3.34−3.27 (m, 2H), 2.43−2.21 (m, 3H), 2.15−2.07 (m, 2H), 1.55−1.44 (m, 2H), 1.35 (s, 18H), 1.34 (s, 18H). $^{31}P\{^{1}H\}$ NMR (121.52 MHz, CD_2Cl_2, 295 K): δ [ppm] = 101.96 (s). Elemental Analysis Calcd for $C_{23}H_{45}MoNO_3P_2$: C, 51.01; H, 8.38; N, 2.59. Found: C, 51.08; H, 8.45; N, 2.41. IR (ATR): ν [cm^{-1}] = 1904 (CO), 1782 (CO), 1761 (CO).

*Synthesis of $NNP^{iPr}Mo(CO)_2(PPh_3)$ ((rac)-**7**).* In a 25 mL Schlenk tube $Mo(CH_3CN)_2(CO)_2(PPh_3)_2$ (569.3 mg, 750 μmol, 1.0 equiv) was suspended in 15 mL of THF, 2-(di-isopropylphosphino)-*N*-((1-methyl-1*H*-imidazol-2-yl)methyl)ethylamine (10 wt % in toluene, 210.8 mg, 826 μmol, 1.1 equiv) was added, and the reaction mixture was stirred at room temperature for 22 h. The solvent was filtered off, and the yellow residue was washed with hexane (5 × 5 mL). Drying *in vacuo* yielded (*rac*)-**7** as a yellow solid (403 mg, 80%). Red crystals suitable for single-crystal X-ray diffraction were obtained by slow diffusion of Et_2O into a solution of (*rac*)-**7** in acetonitrile at 0 °C. ^{1}H NMR (300.20 MHz, CD_3CN, 295 K): δ [ppm] = 7.61−7.52 (m, 6H), 7.33−7.21 (m, 9H), 6.62−6.58 (m, 2H), 3.32 (bs, 1H), 3.23 (s, 3H), 3.17−3.09 (m 1H), 2.86−2.61 (m, 3H), 2.40−2.56 (m, 1H), 1.82−1.68 (m, 1H), 1.39−1.17 (m, 10H), 1.09−0.99 (m, 4H). ^{31}P NMR (121.52 MHz, CD_3CN, 295 K): δ [ppm] = 67.24 (d, J = 141 Hz), 55.54 (d, J = 141 Hz). IR (ATR): ν [cm^{-1}] = 1778 (CO), 1697 (CO).

General Procedure for Hydrogenation Experiments. All hydrogenation reactions were carried out in a 300 mL autoclave (Parr Instrument Company). In a glovebox a 4 mL glass vial was charged with the corresponding molybdenum catalyst and a stirring bar. Solvent and $NaHBEt_3$ (0.5 M in toluene) were subsequently added, and the reaction mixture was stirred for approximately 10 min. The corresponding alkyne was added, and the vial was closed with a screw cap containing a septum. The septum of the vial was punctured with a needle to allow for the exchange of atmosphere, and the vial was transferred into an autoclave. The sealed autoclave was purged ten times with 10 bar of pressure of dihydrogen gas before the desired pressure was set. The autoclave was heated in a preheated aluminum block for the desired reaction time. Afterward, the autoclave was cooled in an ice bath and carefully depressurized. The reaction mixture was diluted with ethyl acetate, a known amount of hexadecane was added as an internal standard, and the mixture was filtered through a pad of Celite.

■ ASSOCIATED CONTENT

Supporting Information

The Supporting Information is available free of charge at https://pubs.acs.org/doi/10.1021/acs.organomet.1c00709.

Screening of reaction conditions. Results of hydrogenation experiments for alkynes **8p**−**8aa**. Analytical data and NMR spectra of isolated alkenes. Photographs of the reaction of **6a** with CO to **6c**. NMR and IR spectra of the material obtained by the reaction of **1** with ^{tBu}PNP in DCM. NMR and IR spectra of **1**, **5c**, **6a**, **6c**, and (*rac*)-**7**. Crystallographic details for molecular structures of **6c** and (*rac*)-**7**. (PDF)

Accession Codes

CCDC 2129493−2129494 contain the supplementary crystallographic data for this paper. These data can be obtained free of charge via www.ccdc.cam.ac.uk/data_request/cif, or by emailing data_request@ccdc.cam.ac.uk, or by contacting The Cambridge Crystallographic Data Centre, 12 Union Road, Cambridge CB2 1EZ, UK; fax: +44 1223 336033.

■ AUTHOR INFORMATION

Corresponding Authors

Matthias Beller − *Leibniz-Institut für Katalyse e.V., 18059 Rostock, Germany*; orcid.org/0000-0001-5709-0965; Email: matthias.beller@catalysis.de

Kathrin Junge − *Leibniz-Institut für Katalyse e.V., 18059 Rostock, Germany*; orcid.org/0000-0001-7044-8888; Email: kathrin.junge@catalysis.de

Authors

Niklas F. Both − *Leibniz-Institut für Katalyse e.V., 18059 Rostock, Germany*

Anke Spannenberg − *Leibniz-Institut für Katalyse e.V., 18059 Rostock, Germany*

Complete contact information is available at: https://pubs.acs.org/10.1021/acs.organomet.1c00709

https://doi.org/10.1021/acs.organomet.1c00709
Organometallics 2022, 41, 1797−1805

Notes

The authors declare no competing financial interest.

■ ACKNOWLEDGMENTS

We gratefully acknowledge the support from the Federal Ministry of Education and Research of Germany, the state of Mecklenburg Western Pomerania, and the European Research Council (EU project 670986-NoNaCat). We thank Helen Hornke for experimental support and PD Dr. Wolfgang Baumann, Dr. Thomas Leischner, Johannes Fessler, and Florian Bourriquen for helpful discussions. Furthermore, we thank the analytical department of the Leibniz-Institute for Catalysis for analytical measurements.

■ REFERENCES

(1) Crespo-Quesada, M.; Cárdenas-Lizana, F.; Dessimoz, A.-L.; Kiwi-Minsker, L. Modern Trends in Catalyst and Process Design for Alkyne Hydrogenations. *ACS Catal.* **2012**, *2*, 1773−1786.
(2) Chen, B.; Dingerdissen, U.; Krauter, J.; Rotgerink, H. L.; Möbus, K.; Ostgard, D.; Panster, P.; Riermeier, T.; Seebald, S.; Tacke, T. New Developments in Hydrogenation Catalysis Particularly in Synthesis of Fine and Intermediate Chemicals. *Appl. Catal. A: Gen.* **2005**, *280*, 17−46.
(3) Negishi, E.-i.; De Meijere, A. *Handbook of Organopalladium Chemistry for Organic Synthesis*; John Wiley & Sons: 2003.
(4) Vilé, G.; Albani, D.; Almora-Barrios, N.; López, N.; Perez-Ramirez, J. Advances in the Design of Nanostructured Catalysts for Selective Hydrogenation. *ChemCatChem.* **2016**, *8*, 21−33.
(5) Lindlar, H. Palladium Catalyst for Partial Reduction of Acetylenes. *Org. Synth.* **1966**, *46*, 89−92.
(6) Ludwig, J. R.; Schindler, C. S. Catalyst: Sustainable Catalysis. *Chem.* **2017**, *2*, 313−316.
(7) Gregori, B. J.; Nowakowski, M.; Schoch, A.; Pöllath, S.; Zweck, J.; Bauer, M.; von Wangelin, A. J. Stereoselective Chromium-Catalyzed Semi-Hydrogenation of Alkynes. *ChemCatChem.* **2020**, *12*, 5359−5363.
(8) Bianchini, C.; Meli, A.; Peruzzini, M.; Vizza, F.; Zanobini, F.; Frediani, P. A Homogeneous Iron(II) System Capable of Selectively Catalyzing the Reduction of Terminal Alkynes to Alkenes and Buta-1,3-dienes. *Organometallics* **1989**, *8*, 2080−2082.
(9) Bianchini, C.; Meli, A.; Peruzzini, M.; Frediani, P.; Bohanna, C.; Esteruelas, M. A.; Oro, L. A. Selective Hydrogenation of 1-Alkynes to Alkenes Catalyzed by an Iron(II) cis-Hydride η^2-Dihydrogen Complex. A Case of Intramolecular Reaction between η^2-H_2 and σ-Vinyl Ligands. *Organometallics* **1992**, *11*, 138−145.
(10) Srimani, D.; Diskin-Posner, Y.; Ben-David, Y.; Milstein, D. Iron Pincer Complex Catalyzed, Environmentally Benign, *E*-Selective Semi-hydrogenation of Alkynes. *Angew. Chem., Int. Ed.* **2013**, *52*, 14131−14134.
(11) Gorgas, N.; Brünig, J.; Stöger, B.; Vanicek, S.; Tilset, M.; Veiros, L. F.; Kirchner, K. Efficient *Z*-Selective Semihydrogenation of Internal Alkynes Catalyzed by Cationic Iron(II) Hydride Complexes. *J. Am. Chem. Soc.* **2019**, *141*, 17452−17458.
(12) Garbe, M.; Budweg, S.; Papa, V.; Wei, Z.; Hornke, H.; Bachmann, S.; Scalone, M.; Spannenberg, A.; Jiao, H.; Junge, K. Chemoselective Semihydrogenation of Alkynes Catalyzed by Manganese(I)-PNP Pincer Complexes. *Catal. Sci. Technol.* **2020**, *10*, 3994−4001.
(13) Zubar, V.; Sklyaruk, J.; Brzozowska, A.; Rueping, M. Chemoselective Hydrogenation of Alkynes to (*Z*)-Alkenes Using an Air-Stable Base Metal Catalyst. *Org. Lett.* **2020**, *22*, 5423−5428.
(14) Tokmic, K.; Fout, A. R. Alkyne Semihydrogenation with a Well-Defined Nonclassical Co−H_2 Catalyst: A H_2 Spin on Isomerization and *E*-selectivity. *J. Am. Chem. Soc.* **2016**, *138*, 13700−13705.
(15) Chen, F.; Kreyenschulte, C.; Radnik, J. r.; Lund, H.; Surkus, A.-E.; Junge, K.; Beller, M. Selective Semihydrogenation of Alkynes with N-Graphitic-Modified Cobalt Nanoparticles Supported on Silica. *ACS Catal.* **2017**, *7*, 1526−1532.
(16) Lapointe, S.; Pandey, D. K.; Gallagher, J. M.; Osborne, J.; Fayzullin, R. R.; Khaskin, E.; Khusnutdinova, J. R. Cobalt Complexes of Bulky PNP Ligand: H_2 Activation and Catalytic Two-Electron Reactivity in Hydrogenation of Alkenes and Alkynes. *Organometallics* **2021**, *40*, 3617−3626.
(17) Thiel, N. O.; Kaewmee, B.; Ngoc, T. T.; Teichert, J. F. A Simple Nickel Catalyst Enabling an *E*-Selective Alkyne Semi-hydrogenation. *Chem.—Eur. J.* **2020**, *26*, 1597.
(18) Murugesan, D. K.; Bheeter, C. B.; Linnebank, P. R.; Spannenberg, A.; Reek, J. N.; Jagadeesh, R. V.; Beller, M. Nickel-Catalyzed Stereodivergent Synthesis of *E*- and *Z*-Alkenes by Hydrogenation of Alkynes. *ChemSusChem* **2019**, *12*, 3363.
(19) Liu, Y.; Liu, X.; Feng, Q.; He, D.; Zhang, L.; Lian, C.; Shen, R.; Zhao, G.; Ji, Y.; Wang, D. Intermetallic Ni_xM_y (M= Ga and Sn) Nanocrystals: A Non-precious Metal Catalyst for Semi-Hydrogenation of Alkynes. *Adv. Mater.* **2016**, *28*, 4747−4754.
(20) Pape, F.; Thiel, N. O.; Teichert, J. F. Z-Selective Copper(I)-Catalyzed Alkyne Semihydrogenation with Tethered Cu−Alkoxide Complexes. *Chem.—Eur. J.* **2015**, *21*, 15934−15938.
(21) Alig, L.; Fritz, M.; Schneider, S. First-Row Transition Metal (De) Hydrogenation Catalysis Based On Functional Pincer Ligands. *Chem. Rev.* **2019**, *119*, 2681−2751.
(22) Bullock, R. M. *Catalysis Without Precious Metals*; John Wiley & Sons: 2011.
(23) Haber, J. *Studies in Inorganic Chemistry*; Elsevier: 1994; Vol. *19*.
(24) Zhang, Y.; Hanna, B. S.; Dineen, A.; Williard, P. G.; Bernskoetter, W. H. Functionalization of Carbon Dioxide with Ethylene at Molybdenum Hydride Complexes. *Organometallics* **2013**, *32*, 3969−3979.
(25) Zhang, Y.; Williard, P. G.; Bernskoetter, W. H. Synthesis and Characterization of Pincer-Molybdenum Precatalysts for CO_2 Hydrogenation. *Organometallics* **2016**, *35*, 860−865.
(26) Silantyev, G. A.; Förster, M.; Schluschaß, B.; Abbenseth, J.; Würtele, C.; Volkmann, C.; Holthausen, M. C.; Schneider, S. Dinitrogen Splitting Coupled to Protonation. *Angew. Chem., Int. Ed.* **2017**, *56*, 5872−5876.
(27) MacLeod, K. C.; Holland, P. L. Recent Developments in the Homogeneous Reduction of Dinitrogen by Molybdenum and Iron. *Nat. Chem.* **2013**, *5*, 559−565.
(28) McSkimming, A.; Suess, D. L. Dinitrogen Binding and Activation at a Molybdenum−Iron−Sulfur Cluster. *Nat. Chem.* **2021**, *13*, 666−670.
(29) Arashiba, K.; Miyake, Y.; Nishibayashi, Y. A molybdenum complex bearing PNP-type pincer ligands leads to the catalytic reduction of dinitrogen into ammonia. *Nat. Chem.* **2011**, *3*, 120−125.
(30) Arashiba, K.; Kinoshita, E.; Kuriyama, S.; Eizawa, A.; Nakajima, K.; Tanaka, H.; Yoshizawa, K.; Nishibayashi, Y. Catalytic Reduction of Dinitrogen to Ammonia by Use of Molybdenum−Nitride Complexes Bearing a Tridentate Triphosphine as Catalysts. *J. Am. Chem. Soc.* **2015**, *137*, 5666−5669.
(31) Liao, Q.; Saffon-Merceron, N.; Mézailles, N. Catalytic Dinitrogen Reduction at the Molybdenum Center Promoted by a Bulky Tetradentate Phosphine Ligand. *Angew. Chem., Int. Ed.* **2014**, *53*, 14206−14210.
(32) Chakraborty, S.; Berke, H. Homogeneous Hydrogenation of Nitriles Catalyzed by Molybdenum and Tungsten Amides. *ACS Catal.* **2014**, *4*, 2191−2194.
(33) Chakraborty, S.; Blacque, O.; Fox, T.; Berke, H. Hydrogenation of Imines Catalyzed by Trisphosphine-Substituted Molybdenum and Tungsten Nitrosyl Hydrides and Co-Catalytic Acid. *Chem.—Asian J.* **2014**, *9*, 2896−2907.
(34) Chakraborty, S.; Blacque, O.; Fox, T.; Berke, H. Highly Active, Low-Valence Molybdenum-and Tungsten-Amide Catalysts for Bifunctional Imine-Hydrogenation Reactions. *Chem.—Asian J.* **2014**, *9*, 328−337.

https://doi.org/10.1021/acs.organomet.1c00709
Organometallics 2022, 41, 1797−1805

(35) Chakraborty, S.; Blacque, O.; Berke, H. Ligand Assisted Carbon Dioxide Activation and Hydrogenation Using Molybdenum and Tungsten Amides. *Dalton Trans.* **2015**, *44*, 6560−6570.
(36) Chakraborty, S.; Blacque, O.; Fox, T.; Berke, H. Trisphosphine-Chelate-Substituted Molybdenum and Tungsten Nitrosyl Hydrides as Highly Active Catalysts for Olefin Hydrogenations. *Chem.—Eur. J.* **2014**, *20*, 12641−12654.
(37) Joannou, M. V.; Bezdek, M. J.; Chirik, P. J. Pyridine(diimine) Molybdenum-Catalyzed Hydrogenation of Arenes and Hindered Olefins: Insights into Precatalyst Activation and Deactivation Pathways. *ACS Catal.* **2018**, *8*, 5276−5285.
(38) Vielhaber, T.; Faust, K.; Topf, C. Group 6 Metal Carbonyl Complexes Supported by a Bidentate PN Ligand: Syntheses, Characterization, and Catalytic Hydrogenation Activity. *Organometallics* **2020**, *39*, 4535−4543.
(39) Leischner, T.; Spannenberg, A.; Junge, K.; Beller, M. Molecular Defined Molybdenum−Pincer Complexes and Their Application in Catalytic Hydrogenations. *Organometallics* **2018**, *37*, 4402−4408.
(40) Leischner, T.; Suarez, L. A.; Spannenberg, A.; Junge, K.; Nova, A.; Beller, M. Highly Selective Hydrogenation of Amides Catalysed by a Molybdenum Pincer Complex: Scope and Mechanism. *Chem. Sci.* **2019**, *10*, 10566−10576.
(41) Leischner, T.; Spannenberg, A.; Junge, K.; Beller, M. Synthesis of Molybdenum Pincer Complexes and Their Application in the Catalytic Hydrogenation of Nitriles. *ChemCatChem.* **2020**, *12*, 4543−4549.
(42) (a) Alberico, E.; Beller, M.; Spannenberg, A.; Baumann, W.; Seifert, J.; Sang, R.; Junge, K.; Junge, H.; Leischner, T.; Kammer, A. HCOOH Disproportionation to MeOH promoted by Molybdenum PNP Complexes. *Chem. Sci.* **2021**, *12*, 13101−13119. (b) Alberico, E.; Beller, M.; Spannenberg, A.; Baumann, W.; Seifert, J.; Sang, R.; Junge, K.; Junge, H.; Leischner, T.; Kammer, A. Correction for "HCOOH Disproportionation to MeOH promoted by Molybdenum PNP Complexes. *Chem. Sci.* **2021**, *12*, 15772−15774.
(43) Wang, Y.; Zhu, L.; Shao, Z.; Li, G.; Lan, Y.; Liu, Q. Unmasking the Ligand Effect in Manganese-Catalyzed Hydrogenation: Mechanistic Insight and Catalytic Application. *J. Am. Chem. Soc.* **2019**, *141*, 17337−17349.
(44) Papa, V.; Cabrero-Antonino, J. R.; Alberico, E.; Spanneberg, A.; Junge, K.; Junge, H.; Beller, M. Efficient and Selective Hydrogenation of Amides to Alcohols and Amines Using a Well-Defined Manganese−PNN Pincer Complex. *Chem. Sci.* **2017**, *8*, 3576−3585.
(45) Gottlieb, H. E.; Kotlyar, V.; Nudelman, A. NMR Chemical Shifts of Common Laboratory Solvents as Trace Impurities. *J. Org. Chem.* **1997**, *62*, 7512−7515.
(46) Fulmer, G. R.; Miller, A. J.; Sherden, N. H.; Gottlieb, H. E.; Nudelman, A.; Stoltz, B. M.; Bercaw, J. E.; Goldberg, K. I. NMR Chemical Shifts of Trace Impurities: Common Laboratory Solvents, Organics, and Gases in Deuterated Solvents Relevant to the Organometallic Chemist. *Organometallics* **2010**, *29*, 2176−2179.
(47) Elangovan, S.; Garbe, M.; Jiao, H.; Spannenberg, A.; Junge, K.; Beller, M. Hydrogenation of Esters to Alcohols Catalyzed by Defined Manganese Pincer Complexes. *Angew. Chem., Int. Ed.* **2016**, *128*, 15590−15594.
(48) Adam, R.; Alberico, E.; Baumann, W.; Drexler, H. J.; Jackstell, R.; Junge, H.; Beller, M. NNP-Type Pincer Imidazolylphosphine Ruthenium Complexes: Efficient Base-Free Hydrogenation of Aromatic and Aliphatic Nitriles under Mild Conditions. *Chem.—Eur. J.* **2016**, *22*, 4991−5002.
(49) Dieck, H. T.; Friedel, H. Über π-Allyl-Komplexe des Molybdäns II. Die Bildung von π-Allyldicarbonylmolybdän-Komplexen aus Molybdän-hexacarbonyl und seinen Derivaten. *J. Organomet. Chem.* **1968**, *14*, 375−385.
(50) Friedel, H.; Renk, I. W.; Dieck, H. T. Komplexchemie von Vierzentren-π-Systemen IV. Synthese und Eigenschaften hochsubstituierter Molybdän-Carbonyl-Derivate. *J. Organomet. Chem.* **1971**, *26*, 247−259.
(51) Anderson, S.; Cook, D. J.; Hill, A. F. Metallathiirenes. 3.1 Thiocarbamoyl and Alkoxythiocarbonyl Complexes of Molybdenum(II) and Tungsten(II). *Organometallics* **2001**, *20*, 2468−2476.

https://doi.org/10.1021/acs.organomet.1c00709
Organometallics 2022, 41, 1797−1805

7.3 Hydrogenation of Esters Catalyzed by Bis(N-Heterocyclic Carbene) Molybdenum Complexes

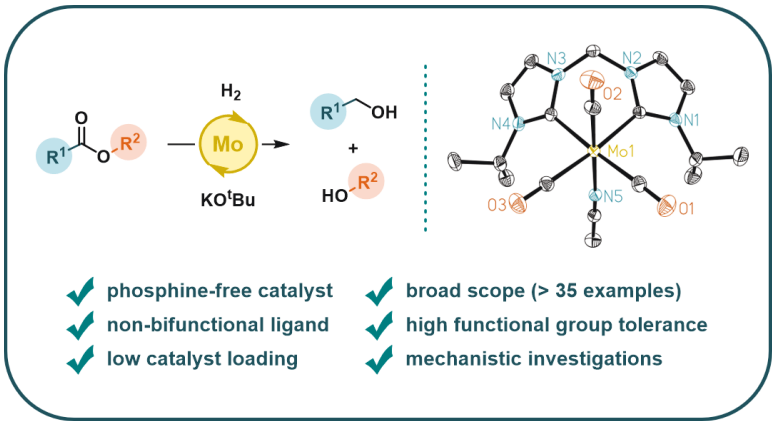

N. F. Both, J. Thaens, A. Spannenberg, H. Jiao, K. Junge, M. Beller, *ACS Catalysis* **2024**, *14*, 4082–4092.

Author's Contribution

The author initiated and conceptualized the project. The author performed most of the experimental work including synthesis and characterization of molybdenum complexes, screening of the reaction conditions, evaluation of the substrate scope as well as catalytic and spectroscopic experiments for mechanistic investigations. Furthermore, the author wrote the initial draft of the manuscript and most of the supporting information. The author's contribution approximately accounts 70 %.

Niklas F. Both	Prof. Matthias Beller
(PhD student)	(supervisor)

ACS Catalysis

Open Access

pubs.acs.org/acscatalysis

Research Article

Hydrogenation of Esters Catalyzed by Bis(*N*-Heterocyclic Carbene) Molybdenum Complexes

Niklas F. Both, Jannik Thaens, Anke Spannenberg, Haijun Jiao,* Kathrin Junge,* and Matthias Beller*

Cite This: *ACS Catal.* 2024, 14, 4082–4092

Read Online

ACCESS | Metrics & More | Article Recommendations | Supporting Information

ABSTRACT: A series of Mo complexes bearing inexpensive bidentate bis(NHC) ligands have been synthesized and characterized by NMR and IR spectroscopy as well as single crystal XRD analysis. These complexes proved to be efficient for the catalytic hydrogenation of aliphatic and aromatic esters (>35 examples) operating at low catalyst loadings (0.5–2 mol %) and temperatures (80–120 °C). Various functional groups, e.g., C═C double bonds, nitriles, alcohols, tertiary amines, halides, and acetals, as well as heteroaromatic substrates, lactones, and diesters, are tolerated by the optimal catalyst system. Based on NMR spectroscopic investigations, control experiments and DFT computations a non-bifunctional outer-sphere hydrogenation mechanism is proposed.

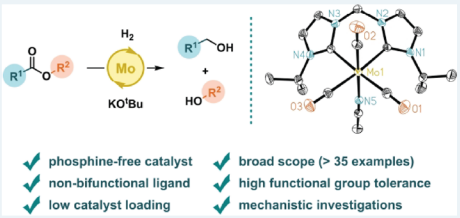

KEYWORDS: *homogeneous catalysis, molybdenum, N-heterocyclic carbenes, hydrogenation, esters, alcohols*

■ INTRODUCTION

Catalytic hydrogenation of carbonyl compounds represents an atom-efficient and sustainable approach for the synthesis of bulk and fine chemicals.[1] To date, many efficient homogeneous hydrogenation catalysts based on noble metals,[2] mainly Ru,[3] have been developed. Due to their costs and negative environmental impacts, many efforts over the past decade focused on the replacement of these metals by less expensive and environmentally more benign non-noble metals.[4] Especially, Mn, Fe, and Co attracted much attention and significant advances have been made in the development of hydrogenation catalysts based on these metals.[5] In comparison, the group 6 metals Cr, Mo, and W are much less studied with respect to their use in hydrogenation catalysis. Thereby, especially, Mo seems to have potential since it plays a vital role in the active centers of various redox-active enzymes[6] and is likewise inexpensive, environmentally benign, and, furthermore, offers a rich coordination chemistry.[7]

Among group 6 metals, Mo has been the most explored (Figure 1). In the 1980s, the groups of Darensbourg,[8] Markó,[9] and Fuchikami[10] investigated the reactivity of anionic metal carbonyl hydrides $[HM(CO)_5]^-$ or binuclear complexes $[(\mu\text{-}H)M_2(CO)_{10}]^-$ (M = Cr, Mo, W) and their use as hydrogenation catalysts. In the early 2000s, Bullock and Voges studied different Mo and W half sandwich complexes regarding their activity in catalytic ionic hydrogenations (e.g., Figure 1, complex **I**; used with $Ph_3C^+BArF_{24}^-$ as cocatalyst for hydride abstraction).[11] Recently, the Berke group synthesized Mo nitrosyl complexes featuring sterically demanding bidentate[12] or tridentate phosphine ligands[13] (e.g., complex

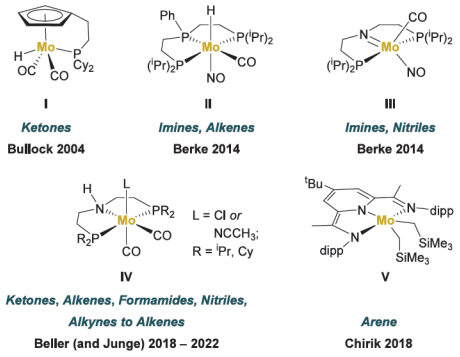

Figure 1. Selected examples of Mo-based homogeneous (pre)catalysts for hydrogenation reactions.

II), which are catalytically active in the hydrogenation of imines and olefins after formation of the cationic complexes by hydride abstraction similar to the complexes of Bullock and

Received: January 2, 2024
Revised: February 19, 2024
Accepted: February 21, 2024
Published: March 1, 2024

https://doi.org/10.1021/acscatal.4c00019
ACS Catal. 2024, 14, 4082–4092

Voges.[11] Furthermore, the same group developed Mo and W amido complexes (e.g., complex **III**) bearing nitrosyl and PNP pincer ligands.[14] These complexes can activate molecular hydrogen via metal ligand cooperativity (MLC)[5c,15] and were successfully applied in the catalytic hydrogenation of imines and nitriles, although relatively harsh reaction conditions were required (140 °C, 60 bar of H_2, 5 mol % catalyst loading).

Our group investigated Mo(I) chloride and Mo(0) acetonitrile PNP pincer complexes **IV** with a carbonyl instead of a nitrosyl ligand for the hydrogenation of ketones,[16] alkenes,[16] formamides,[17] and nitriles,[18] as well as the semihydrogenation of alkynes.[19] However, relatively high catalyst loadings (5 mol %) and the need of equimolar amounts of $NaHBEt_3$ for catalyst activation, restricting the functional group tolerance, limited the practicability of these systems. Remarkably, Chirik and co-workers developed PDI-based Mo complexes (e.g., complex **V**) as catalysts for arene hydrogenation.[20] In a consecutive work, replacement of one imino-moiety by a chiral oxazolyl-unit enabled asymmetric hydrogenation of (hetero)arenes.[21] Moreover, cyclohexadienyl hydride complexes with related phosphino(imino)pyridine- and phosphino(oxazoline)pyridine-ligands were isolated and their role as catalytic intermediates has been investigated.[22] Overall, Mo complexes have been successfully applied as hydrogenation catalysts, even though in most cases higher metal loadings and relatively harsh reaction conditions in comparison to well-established first-row transition metal catalysts made their utilization less attractive.

Recently, the group of Ke reported hydrogen borrowing reactions catalyzed by bis(NHC)$Mo(CO)_4$ complexes **2** and bis(NHC)$Cr(CO)_4$ complexes featuring strongly electron-donating, bidentate bis(NHC) ligands.[23,24] Given that Mn complexes bearing these bis(NHC) ligands catalyze the hydrogenation of esters,[25] we conjectured that comparable Mo complexes could also act as hydrogenation catalysts. In this respect, it is worth noting that very recently, the first molecular W-based system for the hydrogenation of esters has been reported by Topf and co-workers.[26] Nevertheless, to the best of our knowledge, no Mo-based homogeneous catalysts are known for this transformation. In line with these findings and based on our previous work,[25b,27] we became interested in the development of Mo-based catalysts for the reduction of carboxylic acid esters.

RESULTS AND DISCUSSION

Precatalyst Synthesis and Characterization. We started our work with the synthesis of bis(NHC) Mo complexes **2** and **3** by the reaction of $Mo(CO)_6$ or $Mo(CO)_3(CH_3CN)_3$ with bis(NHC)-BEt_3 adducts **1** (Scheme 1), which are obtained from their corresponding bis(imidazolium) salts.[25b,28] Using $Mo(CO)_6$ as the Mo precursor allows the isolation of the expected tetracarbonyl complexes **2** in very good yields as already reported for ethylene-, propylene-, and xylene-bridged bis(NHC) ligands.[28] These compounds have previously been synthesized directly from bis(imidazolium) salts, KO^{t}Bu, and $Mo(CO)_6$.[23] The reaction of bis(NHC)-BEt_3-adducts **1** with $Mo(CH_3CN)_3(CO)_3$ yields complexes **3** containing three CO ligands and one labile CH_3CN ligand in addition to the chelating bis(NHC) ligand. In contrast to complexes **2**, complexes **3** are much less soluble (e.g., THF or CH_3CN) or instable (e.g., DCM) in common organic solvents. Therefore, the direct synthesis from (bis)imidazolium salts is more challenging due to their tedious separation from the salts formed during deprotonation of the imidazolium units.

Scheme 1. General Syntheses of Bis(NHC) Mo Complexes 2 and 3[a]

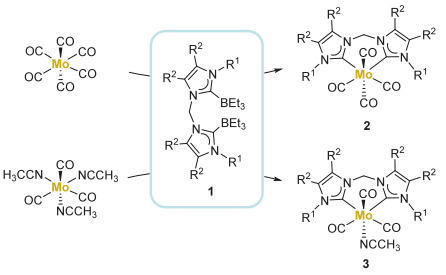

[a]Reaction conditions: For **2**: toluene (56 mM), 90 °C, 16 h; for **3**: CH_3CN (75 mM), 65 °C, 16 h.

Complexes **3** were characterized by ^1H, ^{13}C NMR and IR spectroscopy. Additionally, the structure of compound **3b** is confirmed by SC-XRD. As shown in Figure 2, the ligand

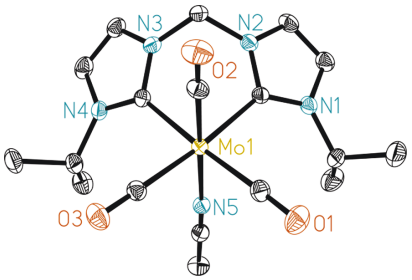

Figure 2. Molecular structure of complex **3b**. Displacement ellipsoids set at 50% probability. Hydrogen atoms and the solvent molecule are omitted for clarity. Only one of the two molecules of the asymmetric unit is shown.

backbone is bent, resulting in a boat-shaped conformation of the bis(NHC) ligand as commonly observed for various transition metal complexes of these ligands.[25b,29] The methylene-bridge in **3b** can point toward (*syn*) or away (*anti*) from the CH_3CN ligand. The *anti*-conformer is computed to be more stable by 0.50 kcal/mol (see SI Section 10.3b), in agreement with the *anti*-conformation observed for the molecular structure of **3b** in the solid state (Figure 2). Hydrogen atoms of the methylene bridge show one doublet (between 6 and 7 ppm in DMSO-d_6) in accordance with their diastereotopicity. As the NMR spectra of complexes **3** were recorded in DMSO-d_6, an exchange of the labile CH_3CN ligand by DMSO takes place in the solution and free CH_3CN is observed. The IR spectra of complexes **3** display intense CO bands at low wavenumbers (typically between 1890 and 1720 cm^{-1}) indicative of strong π-backbonding and an electron-rich Mo central atom.

(Pre)catalyst Screening and Optimization of Reaction Conditions. Next, complexes **2** and **3** were tested as

https://doi.org/10.1021/acscatal.4c00019
ACS Catal. 2024, 14, 4082−4092

(pre)catalysts for the hydrogenation of esters (Table 1). As the reduction of fatty acid esters is of high industrial relevance,[30]

Table 1. Testing Various Mo Complexes for the Catalytic Hydrogenation of Ethyl Oleate 4a[a]

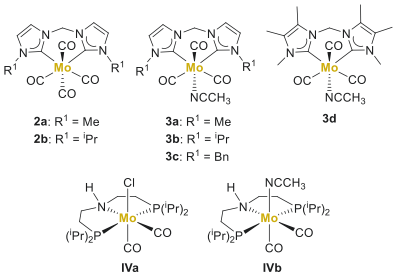

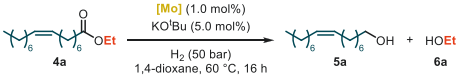

entry	[Mo]	conv. 4a[b] [%]	yield 5a[b] [%]
1	2a	52	17
2	2b	60	23
3	3a	48	14
4	3b	90	73
5	3c	91	76
6	3d	53	18
7[c]	IVa	8	7
8[c]	IVb	9	1

[a]Reaction conditions: 0.5 mmol of ethyl oleate **4a**, 1 mol % [**Mo**], 5 mol % KOtBu, 4 mL of 1,4-dioxane, 50 bar of H_2, 60 °C, 16 h. [b]Determined by GC analysis using hexadecane as internal standard. [c]5 mol % [**Mo**], 5 mol % $NaHBEt_3$, 2 mL toluene, 120 °C, 24 h.

ethyl oleate **4a** was selected as the model substrate. Applying 1 mol % of the corresponding complexes **2** or **3** and 5 mol % of KO^{t}Bu as additive for catalyst activation in 1,4-dioxane at 60 °C under 50 bar H_2 pressure, to our delight, in all cases hydrogenation of the starting material was observed. Catalysts **3b** and **3c** showed similarly high catalytic activities with 90−91% conversion and 73−76% yield of oleyl alcohol **5a** (Table 1, entries 4−5). The difference between conversion and yield is mainly due to oleyl oleate formed by transesterification. Also, at a lower catalyst loading (0.5 mol %) no significant difference in the catalytic performance of **3b** and **3c** was observed (see SI for details). Notably, in no case, hydrogenation of the olefin is observed, which underlines the reactivity differences of these complexes compared to noble metal-based catalysts.

Methyl-substituted complexes (R^1 = Me) **3a** and **3d** were less active (Table 1, entries 3 and 6), which could be caused by their lower solubility in 1,4-dioxane compared to **3b** and **3c**. Tetracarbonyl complexes **2a** and **2b** displayed moderate activities (Table 1, entries 1 and 2). Furthermore, Mo PNP pincer complexes **IVa** and **IVb** were also tested under suitable hydrogenation conditions;[16−19] however, even at 120 °C and with 5 mol % (pre)catalyst loading, only little activity was observed for this model reaction. Due to its lower molecular weight and less steric bulk around the metal center, complex **3b** was selected over complex **3c** for further investigations.

Since additives typically have a strong influence on the catalytic performance in hydrogenation reactions, different bases were tested in the presence of **3b** (Figure 3). With 5 mol

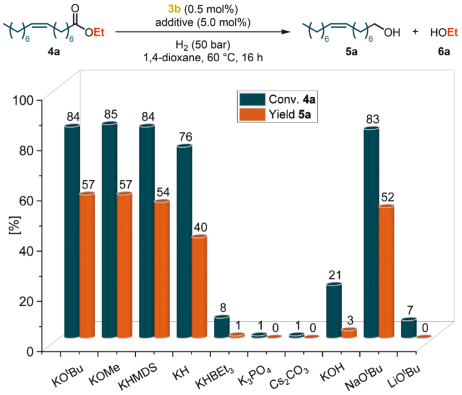

Figure 3. Screening of different additives for the Mo-catalyzed hydrogenation of ethyl oleate **4a**. Conversion of ethyl oleate **4a** and yield of oleyl alcohol **5a** were determined by GC analysis using hexadecane as internal standard. Reaction conditions: 1.0 mmol of ethyl oleate **4a**, 0.5 mol % **3b**, 5.0 mol % additive, 4 mL of 1,4-dioxane, 50 bar H_2, 60 °C, 16 h.

% additive loading, best results were obtained using alkoxide bases KO^{t}Bu and KOMe as well as KHMDS, all showing comparable yields of **5a**. Applying KH also led to high activity, although the conversion and yield were slightly lower. In previous works with Mo- and Mn-based catalysts,[16−19,25] $NaHBEt_3$ and $KHBEt_3$ were the most efficient additives. However, using complex **3b** in combination with $KHBEt_3$ (also with $NaHBEt_3$ or $LiHBEt_3$, see SI), only minor hydrogenation of the model substrate took place. In the case of weaker bases such as K_3PO_4 or Cs_2CO_3, no conversion of the starting material was observed, while KOH showed low activity. Interestingly, the cation strongly influenced the activity of the catalytic system following the trend of K ≥ Na ≫ Li, observed for O^{t}Bu-bases and also other bases (SI Section 3.1.3). To understand this trend, we calculated the Gibbs free energy of the aggregation of a cubic tetramer with respect to its monomer (see SI Section 10.1 for detail) and found that KO^{t}Bu has the lowest aggregation energy, followed by NaO^{t}Bu, and that of LiO^{t}Bu is the highest (−21.30, −26.14, and −29.03 kcal/mol, respectively). This is the same order as their activity, indicating that KO^{t}Bu is most easily converted into its monomer and LiO^{t}Bu most difficult. Additionally, the cation might influence the stabilization of the expected anionic Mo alkoxide and hydride complexes.

Next, the loading of KO^{t}Bu was investigated (Table 2, entries 1−5), showing that generally a higher amount of KO^{t}Bu accelerates the hydrogenation. This phenomenon is commonly observed in homogeneous ester hydrogenation catalysis, and it might be caused by the influence of alkoxide bases on the standard free Gibbs energies of inhibitory equilibria as recently shown by the groups of Pidko et al.[31] Interestingly, higher conversion and yield were observed with 2.5 mol % of KO^{t}Bu than with 5.0 mol % (Table 2, entries 3

https://doi.org/10.1021/acscatal.4c00019
ACS Catal. 2024, 14, 4082−4092

Table 2. Investigation of the Influence of KO^{t}Bu Loading, Temperature, Reaction Time, and Hydrogen Pressure on the Mo-Catalyzed Hydrogenation of Ethyl Oleate 4a[a]

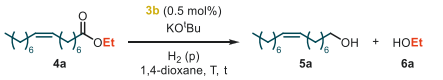

entry	KO^{t}Bu load. [mol %]	p [bar]	T [°C]	t [h]	conv. 4a[b] [%]	yield 5a[b] [%]
1	20	50	60	16	100	82
2	10	50	60	16	96	70
3	5	50	60	16	84(2)[c]	57(4)[c]
4	2.5	50	60	16	89(1)[c]	71(2)[c]
5	1.0	50	60	16	5	4
6	5	30	60	16	76	42
7	5	50	60	24	91	71
8	5	50	80	16	99	90
9	5	50	80	24	98(0)[d]	95(1)[d]

[a]Reaction conditions: 1.0 mmol of ethyl oleate **4a**, 0.5 mol % **3b**, 4 mL of 1,4-dioxane. [b]Determined by GC analysis using hexadecane as internal standard. [c]Average of three independent experiments. Value in parentheses represents the standard deviation. [d]Average of two independent experiments. Value in parentheses represents the standard deviation.

and 4), which could be related to the transesterification with O^{t}Bu. Furthermore, a decreased reaction rate is observed under a lower hydrogen pressure (Table 2, entry 6). By raising the temperature to 80 °C and prolonging the reaction time to 24 h (Table 2, entries 7−9), quantitative conversion of ethyl oleate **4a** and 95% yield of oleyl alcohol **5a** are obtained (Table 2, entry 9). An evaluation of various solvents revealed that polar, aprotic solvents are best suited (SI Section 3.1.2).

Substrate Scope and Limitations. To study the scope and limitations of the novel catalytic system, we tested the hydrogenation of other esters under the optimized conditions (Scheme 2). Aliphatic esters (**4b**, **4c**, and **4d**) with different alkyl chain lengths are smoothly reduced and the corresponding alcohols (**5b**, **5c**, and **5d**) are isolated in high yields (83−92%). Likewise, ester **4g**, bearing a phenyl substituent in the alpha-position to the ester moiety, provided alcohol **5g** with a yield of 79%. The terminal C═C double bond in ester **4e** and the internal C═C double bond in ester **4h** are well tolerated by our catalytic procedure, and as in the case of ethyl oleate, no hydrogenation of the C═C moieties has been observed. Furthermore, ester **4f** containing a hydroxy group is successfully converted to the corresponding alcohol **5f**, although an increased catalyst loading (2 mol %) and higher temperature (120 °C) were required. Interestingly, steric bulk appears to be better tolerated in R^2 than in R^1 as shown by esters **4i** and **4j**. While ester **4i** yielded (−)-borneol **6i** in a

Scheme 2. Mo-Catalyzed Hydrogenation of Aliphatic and (Hetero)aromatic Esters

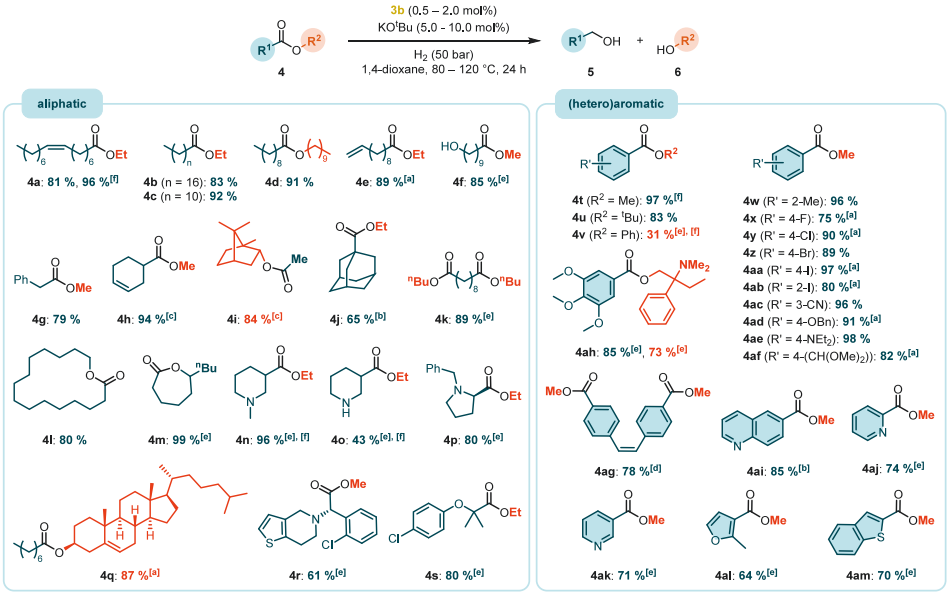

Values below the Lewis structures represent the isolated yield(s) of the corresponding alcohol(s) **5** (blue) and/or **6** (orange). Standard reaction conditions: 1.0 mmol ester **4**, 0.5 mol % **3b**, 5 mol % KO^{t}Bu, 50 bar H_2, 4 mL 1,4-dioxane, 80 °C, 24 h. [a]0.5 mmol ester **4**, 1.0 mol % **3b**, 10 mol % KO^{t}Bu, 2 mL 1,4-dioxane, 80 °C; [b]0.5 mmol ester **4**, 1.0 mol % **3b**, 5 mol % KO^{t}Bu, 2 mL 1,4-dioxane, 100 °C; [c]1.0 mmol ester **4**, 1.0 mol % **3b**, 5 mol % KO^{t}Bu, 4 mL 1,4-dioxane, 100 °C; [d]0.5 mmol ester **4**, 2.0 mol % **3b**, 10 mol % KO^{t}Bu, 2 mL 1,4-dioxane, 100 °C; [e]0.5 mmol ester **4**, 2.0 mol % **3b**, 10 mol % KO^{t}Bu, 2 mL 1,4-dioxane, 120 °C; [f]yield determined by GC analysis using hexadecane as internal standard.

https://doi.org/10.1021/acscatal.4c00019
ACS Catal. 2024, 14, 4082−4092

Scheme 3. ^{1}H NMR Spectroscopic Investigations for Activation of Precatalyst 3b with KO^{t}Bu

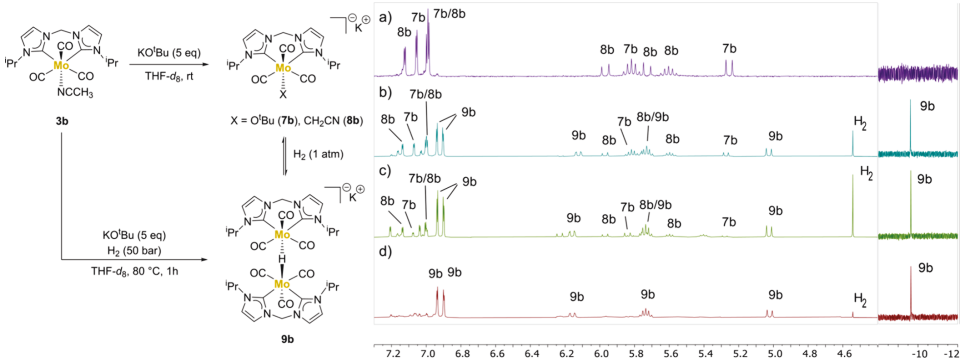

(a) Reaction mixture of **3b** and KO^{t}Bu (5 equiv) at rt after 60 min; reaction mixture 20 min (b) and 24 h (c) after exposure to H_2 (1 atm); (d) reaction mixture of **3b** with KO^{t}Bu (5 equiv) in an autoclave at 80°C under 50 bar H_2 pressure for 1 h, spectrum recorded 30 min after release of H_2 pressure

good yield of 84%, alcohol **5j** was isolated in only 65% yield due to formation of adamantyl adamantate (~20%) by transesterification. Like ester **4f**, diester **4k** also yielded 1,10-decanediol in high yield at 120 °C and with 2 mol % catalyst loading. Lactones are also reduced to the corresponding diols, with the observed activity depending strongly on the respective ring size. While the 16-membered lactone **4l** is completely reduced already at 80 °C with only 0.5 mol % of precatalyst **3b**, for the 7-membered lactone **4m** 120 °C and 2 mol % of **3b** were needed to reach quantitative conversion. Interestingly, for 5-membered lactones, only low conversions around 30% have been detected under these conditions (SI), which might be a result of the increased thermodynamic stability. On the other hand, esters containing tertiary amines (**4n**, **4p**) are well tolerated by the catalytic system, and even ester **4o** with a secondary amine gave the desired amino alcohol in 43% yield. Notably, some late-stage substrates such as the steroid cholesteryl octanoate **4q** and the APIs clopidogrel **4r** and clofibrate **4s** have been successfully exposed to our hydrogenation protocol. Even, in case of clopidogrel **4r** containing several functional groups such as a thiophen moiety, a tertiary amine, and a chloride the corresponding alcohol **5r** could be isolated in a good yield of 61% applying catalyst precursor **3b**. However, under the strongly basic reaction conditions racemization of the chiral center takes place providing alcohol **5r** with 12% *ee* as determined by NMR after derivatization to the corresponding Mosher ester (see SI for detail).

Subsequently, we investigated the hydrogenation of aromatic and heteroaromatic esters (Scheme 2, right). Methyl benzoate **4t** and the bulkier *tert*-butyl benzoate **4u** and methyl 2′-methylbenzoate **4w** are readily hydrogenated to their respective alcohols. In contrast, phenyl benzoate **4v** showed poor conversion even at 120 °C. In a control experiment, no hydrogenation of ethyl oleate was observed in the presence of phenol (see SI Section 3.1.4). Probably, due to the higher acidity of phenol, the formation of the respective stable phenoxy complex under basic conditions is expected. This assumption is further supported by DFT calculations comparing the stability and hydrogenolysis of different molybdenum alkoxide complexes such as $-OCH_3$, $-OCH_2Ph$, $-O^tBu$, and $-OPh$, of which the latter was found to be the most stable (−4.10, −5.63, −8.79, and −19.71 kcal/mol, respectively; see SI Section 10.1b). Halide substituents at sp^2 hybridized carbon atoms are well tolerated by the catalytic system (**4x**, **4y**, **4z**, **4aa**, and **4ab**). For a fluorine substituent in the electron-deficient para-position to the ester group (**4x**), a slightly lower yield of the respective product (75%) was observed, likely due to hydrodehalogenation occurring via nucleophilic aromatic substitution.

In addition, various esters containing a bromide in the aliphatic position showed poor reactivity (see SI), presumably due to catalyst inhibition by halogenation of the Mo center. For substrate **4ac**, exclusive hydrogenation of the ester group occurred, leading to the corresponding alcohol with the intact nitrile group in an excellent isolated yield of 96%. This finding was quite unexpected as many noble and non-noble metal pincer complexes hydrogenate these two functional groups under similar conditions.[32]

Moreover, electron-rich esters such as substrate **4ad** bearing a benzoxy-substituent or substrate **4ae** containing a tertiary amine are smoothly converted to their corresponding alcohols. This has further been demonstrated by the hydrogenation of trimebutine **4ah**. In contrast to tertiary amines, for a substrate featuring a primary amine at the aromatic ring, no reaction was observed (see SI). The acetal in substrate **4af** is tolerated, providing the opportunity for protection of an aldehyde, which otherwise would be reduced under the applied reaction conditions. Similar to the aliphatic esters (*vide supra*), catalyst **3b** selectively hydrogenates diester **4ag** in the presence of C═C double bonds. Remarkably, a very good tolerance of heteroaromatic substrates, which often present a challenge for molecular catalysts, was found. In these cases, higher temperatures (100−120 °C), higher precatalyst loadings (1.0−2.0 mol %), and base loadings (5−10 mol %) were applied. For ester **4ai**, no hydrogenation of the quinoline ring took place, in contrast to related Mn catalysts,[25b] giving an excellent chemo-selectivity for the ester group. Also, pyridine-, furan-, and benzothiophene-containing esters **4aj**, **4ak**, **4al**, and **4am** gave their corresponding alcohols in isolated yields of around 70%.

https://doi.org/10.1021/acscatal.4c00019
ACS Catal. 2024, 14, 4082−4092

Scheme 4. DFT-Supported Mechanistic Rationale for the Mo-Catalyzed Hydrogenation of Esters[a]

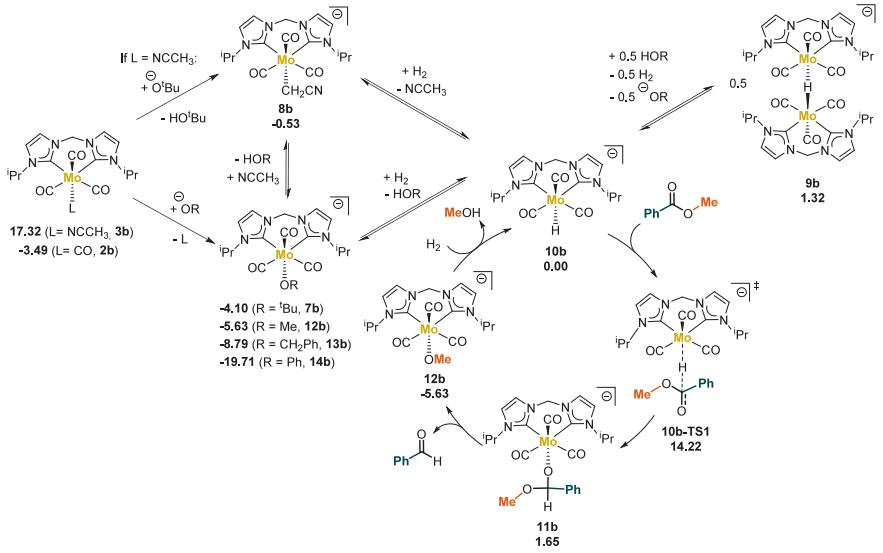

[a]Values below Lewis-structures represent Gibbs Free Energies in kcal/mol calculated on a M06L-SCRF/TZVP level of theory.

Overall, the Mo-based catalytic system operates under comparable conditions to known state-of-the-art Mn- or Fe-based catalysts for ester hydrogenation, for which catalyst loadings of 0.1−2.0 mol % and temperatures between 60−120 °C are common.[25,31,33] In contrast to the related bis(NHC) Mn catalysts[25] no hydrogenation of alkenes, *N*-heteroarenes or nitriles is observed under the applied conditions leading to an improved chemoselectivity and a broader substrate scope. Furthermore, the hydrogenation of heteroaromatic esters is achieved, which proved to be challenging for the Mn-based catalysts.[25]

Mechanistic Investigations. To elucidate the mechanism of this first Mo-catalyzed hydrogenation of carboxylic acid esters, NMR spectroscopic studies, control experiments, and DFT computations were performed. First, the reaction of complex **3b** with an excess of KO^{t}Bu in THF-d_8 was investigated by NMR spectroscopy (Scheme 3 a), see SI Section 9.1 for detail). After 20 min, **3b** has been completely converted into a mixture of two new species. These new compounds were assigned to the anionic complexes **7b** and **8b**, resulting from the replacement of the labile neutral CH_3CN ligand by an anionic O^{t}Bu$^-$ ligand (**7b**) or an anionic CH_2CN^- ligand (**8b**), respectively (Scheme 3). However, no separate NMR resonance for the CH_2CN^- ligand of **8b** is found. Instead, broad peaks for the acidic protons in free **H**O^{t}Bu and C**H**$_3$CN were recorded, which should result from fast dynamic proton exchange, since these compounds exhibit similar pK_a values (in DMSO: HO^{t}Bu: 32.2;[34a] CH_3CN: 31.3[34b]). We assume that fast equilibria between HO^{t}Bu/KO^{t}Bu and CH_3CN/KCH_2CN exist and that additionally exchange of coordinated and non-coordinated CH_2CN^- occurs, leading to the observation of only one resonance for CH_3CN/CH_2CN^-.

To confirm that species **8b** contains a CH_2CN^- ligand, the CH_3CN ligand in **3b** was exchanged for ^{t}BuCN and the resulting complex **3b-^{t}BuCN** was reacted with an excess of KO^{t}Bu (5 equiv). As expected, due to the absence of (acidic) protons in the α-position to the nitrile group, selective formation of alkoxide complex **7b** without formation of complex **8b** was observed (see SI Section 9.2.2 for detail). Upon addition of excess CH_3CN (19 equiv) to this reaction mixture, full conversion of complex **7b** to **8b** took place (see SI Section 9.2.3 for detail). DFT calculations indicate that coordination of the ambidentate CH_2CN^- ligand via C is more favorable than via N by 2.80 kcal/mol (see SI Section 10.3 for detail). Such C-coordinated cyanomethide complexes of several transition metals are known.[35] However, attempts to obtain the molecular structure of **8b** by SC-XRD have been unsuccessful so far. Notably, the deprotonation of a CH_3CN ligand in a Mo PNP pincer complex by $NaHBEt_3$ has been previously reported, resulting in an N-coordinated CH_2CN^- complex with stabilization of the resulting anion by BEt_3 ($MoNCCH_2BEt_3$).[18]

Interestingly, no reaction is observed when complex **2b** is heated with an excess of KO^{t}Bu (5 equiv) to 80 °C (see SI Section 9.7). This is in accordance with the higher barrier for dissociation of the strongly bound CO ligand compared with the relatively labile CH_3CN ligand in **3b**. However, for precatalyst **2b**, catalytic activity is observed at this temperature; therefore, it is assumed that under high H_2 pressure, precatalyst activation still occurs.

Next, we exposed a mixture of complexes **7b** and **8b** to atmospheric pressure of H_2. Selective conversion to a hydrido complex (hydride signal at −9.64 ppm) takes place with its amount increasing over time (Scheme 3 b,c); see SI Section

https://doi.org/10.1021/acscatal.4c00019
ACS Catal. 2024, 14, 4082−4092

9.4 for detail). Since a 1:2 ratio of the hydridic resonance to the resonances of the ligand backbone is found and only one set of signals is observed for the ligand backbone, the formation of binuclear complex **9b** bearing a bridging μ-hydride ligand is proposed. Such binuclear, anionic complexes bearing μ-H ligands are common for group 6 metal carbonyls and several examples (e.g., $[(\mu\text{-H})Mo_2(CO)_{10}]^-$, $[(\mu\text{-H})Mo_2(PPh_3)(CO)_9]^-$, or $[(\mu\text{-H})(\mu\text{-}PPh_2CH_2PPh_2)Mo_2(CO)_8]^-$) have been reported.[36]

When complex **3b** reacts with KOtBu (5 equiv) under 50 bar H_2 pressure at 80 °C for 1 h, compound **9b** is obtained almost exclusively (Scheme 3d, see SI Section 9.3 for detail). Upon release of the hydrogen pressure, complex **9b** decomposes to compounds **7b**, **8b** and some further unidentified species. Therefore, we conclude that species **7b** and **8b** exist in an H_2-dependent equilibrium with **9b** and, consequently, that **9b** is only stable under a H_2 atmosphere. All of these experiments showed that activation of H_2 by the phosphine-free molybdenum complex takes place already at room temperature and atmospheric pressure of H_2. Interestingly, no vacant coordination site appears to be necessary for the hydrogenolysis of complexes **7b** and **8b**. Hydrogenolysis of group 6 alkoxide complexes without a vacant coordination site has been discussed previously.[8d] If D_2 is used instead of H_2, H/D-exchange takes place for the acidic protons in HO^tBu, CH_3CN and, interestingly, also very slowly in one aromatic position of the imidazole moieties in the ligand-backbone. Also, H/D-exchange is observed for the hydridic proton of compound **9b** and the formation of HD and H_2 is detected over time (see SI section 9.5 for detail). These findings indicate heterolytic splitting of H_2 with the protic proton ending up in one of the acidic positions in HO^tBu, CH_3CN or the ligand backbone and the hydridic proton ending up as the hydride-ligand in complex **9b**. This process should be reversible due to the H/D-scrambling. Importantly, no deuteration of the methylene-bridge of the ligand backbone in complexes **7b**, **8b**, or **9b** took place, which excludes the involvement of these protons in the hydrogenation according to the concept of MLC.

To get further insight of the catalytically active species, decyl decanoate (2.5 equiv), precatalyst **3b** (1.0 equiv), and KO^tBu (5.0 equiv) were reacted in THF-d_8 in an autoclave at 80 °C under 50 bar H_2 pressure for 1 h, the pressure was released, and the reaction mixture was consecutively analyzed by NMR spectroscopy (see SI section 9.6 for detail). Full conversion of decyl decanoate and KO^tBu to potassium decanoate and HO^tBu was confirmed. Also, binuclear hydride **9b**, but no other hydride species, were observed. Furthermore, traces of tetracarbonyl complex **2b** and multiple other unidentified species were detected.

Based on these experiments, DFT calculations were conducted to complement the mechanistic picture (Scheme 4, see SI section 10 for detail). Since *syn*- and *anti*-conformers of the Mo complexes regarding the position of the methylene-bridge and the non-CO ligand exhibit different energies, the more stable conformer was used for the calculations, respectively. Furthermore, computations regarding the Me-substituted complexes were performed and can be found in the SI. First, the reaction of complex **2b** (L=CO) or **3b** (L=CH_3CN) with an alkoxide leads to the exergonic formation of alkoxide complexes (**7b**, **12**–**14b**). A high acidity of the corresponding alcohol of the alkoxide results in the formation of very stable alkoxide complexes (e.g., −19.71 kcal/mol for phenoxide **14b**), which are dead ends for catalysis. These alkoxide complexes are assumed to undergo hydrogenolysis, forming the mononuclear hydrido complex **10b**. This reaction was computed to be only slightly endergonic (ΔG = 4.10 kcal/mol from **7b**) and attempts to find the transition state for the formation of complex **10b** failed. In the case of L=CH_3CN, deprotonation of CH_3CN to form CH_2CN^- complex **8b** followed by hydrogenolysis represents an alternative pathway for the formation of complex **10b**, which is also slightly endergonic (ΔG = 0.53 kcal/mol from **8b**). Interestingly, such a mononuclear hydrido complex **10b** was not observed spectroscopically, instead, the binuclear μ-H complex **9b** is the only detected hydride species. Formation of complex **9b** from **10b** is again found to be slightly endergonic (ΔG = 1.32 kcal/mol). From the stoichiometry, it is clear that higher H_2 pressures shift the equilibria from alkoxide complex **7b** and from binuclear hydride complex **9b** to mononuclear hydride **10a**. Therefore, we assume that complex **10b** is formed in sufficient quantities at elevated temperatures and under high H_2 pressures and presents a catalytically competent species. Starting from complex **10b**, direct hydrogen transfer to the ester represents the rate-determining step with an apparent barrier of 14.22 kcal/mol for methyl benzoate (**10b**-TS1). The resulting hemiacetalate complex **11b** eliminates acetaldehyde to form the most stable alkoxide complex **12b** which regenerates the hydrido complex **10b** by hydrogenolysis. Attempts to locate a TS between **11b** and **12b** failed; however, approaching the oxygen atom of the methoxy group to the Mo center resulted in the formation of **12b** and benzaldehyde. Since the transformation of **11b** to **12b** is exergonic by only 7.28 kcal/mol, the barrier, if present, should not be very high. As expected, the barrier for benzaldehyde hydrogenation was calculated to be lower (8.74 kcal/mol). Due to the formation of benzoxide complex **13b** after benzaldehyde hydrogenation, an overall apparent barrier of 23.01 kcal/mol results (see SI Section 10.5 for detail).

In contrast, for related bis(NHC) Mn complexes, an inner-sphere mechanism was proposed for the hydrogenation of esters.[25b] Therefore, creation of a vacant coordination site by the loss of a CO ligand was proposed, although the way of CO dissociation could not be clarified satisfyingly.[25b] Now, in the related Mo complexes **3**, a much stronger coordination of the CO ligands due to increased π-backbonding is expected as confirmed by significantly lower wavenumbers of the CO absorption bands in the IR spectra (e.g., **3b**: 1883, 1741 cm^{-1}, bis(NHC)Mn−H complex: 1962, 1866, 1823 cm^{-1}[25b]). This is further supported by DFT calculations indicating a very high overall energetic barrier for an inner-sphere mechanism (54.5 kcal/mol), mainly resulting from the highly endergonic cleavage of CO from O^tBu-complex **7b** (see SI Section 10.6 for detail). Therefore, the loss of a CO ligand appears energetically unfavorable, rendering hydrogenation via an inner-sphere mechanism in the case of the studied bis(NHC) Mo complexes unlikely.

■ CONCLUSIONS

In summary, we synthesized a family of novel Mo complexes **3** featuring simple and inexpensive bidentate bis(NHC) ligands. Complexes **3** constitute excellent (pre)catalysts for the hydrogenation of various aliphatic and aromatic esters under comparably mild conditions. The scope of the presented optimal precatalyst **3b** is very broad, including electron-rich and -poor aliphatic and aromatic ester substrates. Excellent

https://doi.org/10.1021/acscatal.4c00019
ACS Catal. 2024, 14, 4082−4092

chemoselectivity toward other reducible functional groups like alkenes, nitriles, and *N*-heteroarenes has been demonstrated. Furthermore, various additional functional groups like alcohols, amines and halides are well tolerated by the presented catalyst. Also, substrates containing bulky substituents in proximity of the ester, lactones with larger ring sizes and diesters are readily hydrogenated. Based on NMR spectroscopic investigations and DFT calculations, a non-bifunctional outer-sphere hydrogenation mechanism is proposed. The described phosphine-free system presents the first example of a homogeneous Mo-based catalyst for the hydrogenation of esters and operates at low catalyst loadings in comparison to known molecularly defined Mo-based catalysts. The presented catalyst activities and substrate scope highlight the potential of Mo-based catalysts for the replacement of noble metals in (homogeneous) hydrogenation catalysis.

■ ASSOCIATED CONTENT

Supporting Information

The Supporting Information is available free of charge at https://pubs.acs.org/doi/10.1021/acscatal.4c00019.

Crystallographic data of **3b** (CIF)

Experimental procedures, screening of reaction conditions, unsuccessful ester substrates, NMR and IR spectra for all compounds, crystallographic data, mechanistic experiments and computational details (PDF)

■ AUTHOR INFORMATION

Corresponding Authors

Haijun Jiao − *Leibniz-Institut für Katalyse e.V., Rostock 18059, Germany;* orcid.org/0000-0002-2947-5937; Email: haijun.jiao@catalysis.de

Kathrin Junge − *Leibniz-Institut für Katalyse e.V., Rostock 18059, Germany;* orcid.org/0000-0001-7044-8888; Email: kathrin.junge@catalysis.de

Matthias Beller − *Leibniz-Institut für Katalyse e.V., Rostock 18059, Germany;* orcid.org/0000-0001-5709-0965; Email: matthias.beller@catalysis.de

Authors

Niklas F. Both − *Leibniz-Institut für Katalyse e.V., Rostock 18059, Germany;* orcid.org/0000-0002-0565-4164

Jannik Thaens − *Leibniz-Institut für Katalyse e.V., Rostock 18059, Germany*

Anke Spannenberg − *Leibniz-Institut für Katalyse e.V., Rostock 18059, Germany*

Complete contact information is available at: https://pubs.acs.org/10.1021/acscatal.4c00019

Author Contributions

N.B. conceptualized the work. All authors contributed to further drafting of the project. N.B. and J.T. performed complex syntheses and catalytic experiments for data collection. N.B. performed experiments for investigation of the scope and mechanism. A.S. realized SC-XRD analysis. H.J. performed DFT calculations. M.B. and K.J. supervised the experimental work and provided all resources necessary for the work. N.B. wrote the first draft of the manuscript. All authors contributed to proofreading of the manuscript. All authors have given approval to the final version of the manuscript.

Funding

We acknowledge funding from the state of Mecklenburg-Vorpommern and the Bundesministerium für Bildung und Forschung (BMBF).

Notes

The authors declare no competing financial interest.

■ ACKNOWLEDGMENTS

We thank Katja Andres for her excellent support with the syntheses of bis(imidazolium) salts and bis(NHC)-BEt_3 adducts. The authors acknowledge PD Dr. Wolfgang Baumann and Susann Buchholz for NMR measurements. Furthermore, we are grateful to Johannes Fessler for helpful discussions.

■ ABBREVIATIONS

API, active pharmaceutical ingredient; MLC, metal−ligand cooperativity; NHC, *N*-heterocyclic carbene; PDI,, pyridine-(diimine); dipp, 2,6-di(*iso*-propyl)phenyl; SC-XRD, single crystal X-ray diffraction

■ REFERENCES

(1) Blaser, H. U.; Malan, C.; Pugin, B.; Spindler, F.; Steiner, H.; Studer, M. Selective Hydrogenation for Fine Chemicals: Recent Trends and New Developments. *Adv. Synth. Catal.* **2003**, *345* (1−2), 103−151.

(2) (a) Chelucci, G.; Baldino, S.; Baratta, W. Recent Advances in Osmium-Catalyzed Hydrogenation and Dehydrogenation Reactions. *Acc. Chem. Res.* **2015**, *48* (2), 363−379. (b) Spasyuk, D.; Vicent, C.; Gusev, D. G. Chemoselective Hydrogenation of Carbonyl Compounds and Acceptorless Dehydrogenative Coupling of Alcohols. *J. Am. Chem. Soc.* **2015**, *137* (11), 3743−3746.

(3) (a) Noyori, R. Asymmetric Catalysis: Science and Opportunities (Nobel Lecture). *Angew. Chem., Int. Ed.* **2002**, *41* (12), 2008−2022. (b) Zhang, J.; Leitus, G.; Ben-David, Y.; Milstein, D. Efficient Homogeneous Catalytic Hydrogenation of Esters to Alcohols. *Angew. Chem., Int. Ed.* **2006**, *45* (7), 1113−1115. (c) Saudan, L.; Saudan, C. M.; Debieux, C.; Wyss, P. Dihydrogen Reduction of Carboxylic Esters To Alcohols under Catalysis of Homogeneous Ruthenium Complexes: High Efficiency and Unprecedented Chemoselectivity. *Angew. Chem., Int. Ed.* **2007**, *46* (39), 7473−7476. (d) Balaraman, E.; Gnanaprakasam, B.; Shimon, L. J. W.; Milstein, D. Direct Hydrogenation of Amides to Alcohols and Amines under Mild Conditions. *J. Am. Chem. Soc.* **2010**, *132* (47), 16756−16758. (e) John, J. M.; Bergens, S. H. A Highly Active Catalyst for the Hydrogenation of Amides to Alcohols and Amines. *Angew. Chem., Int. Ed.* **2011**, *50* (44), 10377−10380. (f) Spasyuk, D.; Smith, S.; Gusev, D. G. From Esters to Alcohols and Back with Ruthenium and Osmium Catalysts. *Angew. Chem., Int. Ed.* **2012**, *51* (11), 2772−2775. (g) Kuriyama, W.; Matsumoto, T.; Ogata, O.; Ino, Y.; Aoki, K.; Tanaka, S.; Ishida, K.; Kobayashi, T.; Sayo, N.; Saito, T. Catalytic Hydrogenation of Esters. Development of an Efficient Catalyst and Processes for Synthesising (*R*)-1,2-Propanediol and 2-(*l*-Menthoxy)ethanol. *Org. Process Res. Dev.* **2012**, *16* (1), 166−171. For a review on catalysis by Ru pincer complexes see: (h) Gunanathan, C.; Milstein, D. Bond Activation and Catalysis by Ruthenium Pincer Complexes. *Chem. Rev.* **2014**, *114* (24), 12024−12087.

(4) (a) Bullock, R. M. *Catalysis Without Precious Metals*. Wiley-VCH Verlag GmbH & Co. KGaA: Weinheim, 2010. (b) Teichert, J. F. *Homogeneous Hydrogenation with Non-Precious Catalysts*; Wiley-VCH Verlag GmbH & Co. KGaA: Weinheim, 2020.

(5) (a) Zell, T.; Langer, R. From Ruthenium to Iron and Manganese - A Mechanistic View on Challenges and Design Principles of Base-Metal Hydrogenation Catalysts. *ChemCatChem.* **2018**, *10* (9), 1930−1940. (b) Kallmeier, F.; Kempe, R. Manganese Complexes for (De)Hydrogenation Catalysis: A Comparison to Cobalt and Iron Catalysts. *Angew. Chem., Int. Ed.* **2018**, *57* (1), 46−60. (c) Alig, L.;

Fritz, M.; Schneider, S. First-Row Transition Metal (De)-Hydrogenation Catalysis Based On Functional Pincer Ligands. *Chem. Rev.* **2019**, *119* (4), 2681−2751. (d) Filonenko, G. A.; Van Putten, R.; Hensen, E. J.; Pidko, E. A. Catalytic (de) hydrogenation promoted by non-precious metals − Co, Fe and Mn: recent advances in an emerging field. *Chem. Soc. Rev.* **2018**, *47* (4), 1459−1483. (e) Wang, Y.; Wang, M.; Li, Y.; Liu, Q. Homogeneous manganese-catalyzed hydrogenation and dehydrogenation reactions. *Chem.* **2021**, *7* (5), 1180−1223. (f) Schlichter, P.; Werlé, C. The Rise of Manganese-Catalyzed Reduction Reactions. *Synthesis* **2022**, *54* (3), 517−534.

(6) Schwarz, G.; Mendel, R. R.; Ribbe, M. W. Molybdenum cofactors, enzymes and pathways. *Nature* **2009**, *460* (7257), 839−847.

(7) (a) Mitchell, P. Coordination compounds of molybdenum. *Coord. Chem. Rev.* **1966**, *1* (3), 315−350. (b) Garner, C. Molybdenum. *Coord. Chem. Rev.* **1981**, *37*, 117−156.

(8) (a) Kao, S.; Gaus, P. L.; Youngdahl, K.; Darensbourg, M. Y. Selective Reduction of Acyl Chlorides to Aldehydes by Anionic Group 6B Transition-Metal Hydrides. *Organometallics* **1984**, *3* (10), 1601−1603. (b) Darensbourg, D. J.; Ovalles, C. Anionic Group 6B Metal Carbonyls as Homogeneous Catalysts for Carbon Dioxide/Hydrogen Activation. The Production of Alkyl Formates. *J. Am. Chem. Soc.* **1984**, *106* (13), 3750−3754. (c) Gaus, P. L.; Kao, S.; Youngdahl, K.; Darensbourg, M. Y. Anionic Group 6 Transition-Metal Carbonyl Hydrides as Reducing agents. Ketones, Aldehydes, and Epoxides. *J. Am. Chem. Soc.* **1985**, *107* (8), 2428−2434. (d) Tooley, P. A.; Ovalles, C.; Kao, S.; Darensbourg, D. J.; Darensbourg, M. Y. Anionic Group 6 Hydrides and Carboxylates as Homogeneous Catalysts for Reduction of Aldehydes and Ketones. *J. Am. Chem. Soc.* **1986**, *108* (18), 5465−5470.

(9) (a) Palágyi, J.; Nagy-Magos, Z.; Markó, L. Hydrogenation of Schiff Bases with Group 6 Metal Carbonyls and Sodium Methoxide as Catalyst Precursors. *Transition Met. Chem.* **1985**, *10*, 336−338. (b) Markó, L.; Nagy-Magos, Z. Homogeneous hydrogenation of ketones using chromium hexacarbonyl as catalyst precursor in the presence of bases. *J. Organomet. Chem.* **1985**, *285* (1−3), 193−203.

(10) Fuchikami, T.; Ubukata, Y.; Tanaka, Y. Group 6 anionic μ-hydride complexes $[HM_2(CO)_{10}]^-$ (M= Cr, Mo, W): New catalysts for hydrogenation and hydrosilylation. *Tetrahedron Lett.* **1991**, *32* (9), 1199−1202.

(11) (a) Bullock, R. M.; Voges, M. H. Homogeneous Catalysis with Inexpensive Metals: Ionic Hydrogenation of Ketones with Molybdenum and Tungsten Catalysts. *J. Am. Chem. Soc.* **2000**, *122* (50), 12594−12595. (b) Dioumaev, V. K.; Szalda, D. J.; Hanson, J.; Franz, J. A.; Bullock, R. M. An N-heterocyclic carbene as a bidentate hemilabile ligand: a synchrotron X-ray diffraction and density functional theory study. *Chem. Commun.* **2003**, *9* (14), 1670−1671. (c) Kimmich, B. F.; Fagan, P. J.; Hauptman, E.; Bullock, R. M. Solvent-free ketone hydrogenations catalyzed by molybdenum complexes. *Chem. Commun.* **2004**, *8*, 1014−1015. (d) Kimmich, B. F.; Fagan, P. J.; Hauptman, E.; Marshall, W. J.; Bullock, R. M. Molybdenum Carbonyl Complexes in the Solvent-Free Catalytic Hydrogenation of Ketones. *Organometallics* **2005**, *24* (25), 6220−6229.

(12) Dybov, A.; Blacque, O.; Berke, H. Molybdenum Nitrosyl Complexes and Their Application in Catalytic Imine Hydrogenation Reactions. *Eur. J. Inorg. Chem.* **2011**, *2011*, 652−659.

(13) (a) Chakraborty, S.; Blacque, O.; Fox, T.; Berke, H. Hydrogenation of Imines Catalyzed by Trisphosphine-Substituted Molybdenum and Tungsten Nitrosyl Hydrides and Co-Catalytic Acid. *Chem.—Asian J.* **2014**, *9* (10), 2896−2907. (b) Chakraborty, S.; Blacque, O.; Fox, T.; Berke, H. Trisphosphine-Chelate-Substituted Molybdenum and Tungsten Nitrosyl Hydrides as Highly Active Catalysts for Olefin Hydrogenations. *Chem.—Eur. J.* **2014**, *20* (39), 12641−12654.

(14) (a) Chakraborty, S.; Blacque, O.; Fox, T.; Berke, H. Highly Active, Low-Valence Molybdenum- and Tungsten-Amide Catalysts for Bifunctional Imine-Hydrogenation Reactions. *Chem.—Asian J.* **2014**, *9* (1), 328−337. (b) Chakraborty, S.; Berke, H. Homogeneous Hydrogenation of Nitriles Catalyzed by Molybdenum and Tungsten Amides. *ACS Catal.* **2014**, *4* (7), 2191−2194.

(15) Khusnutdinova, J. R.; Milstein, D. Metal−Ligand Cooperation. *Angew. Chem., Int. Ed.* **2015**, *54* (42), 12236−12273.

(16) Leischner, T.; Spannenberg, A.; Junge, K.; Beller, M. Molecular Defined Molybdenum−Pincer Complexes and Their Application in Catalytic Hydrogenations. *Organometallics* **2018**, *37* (23), 4402−4408.

(17) Leischner, T.; Suarez, L. A.; Spannenberg, A.; Junge, K.; Nova, A.; Beller, M. Highly Selective Hydrogenation of Amides Catalysed by a Molybdenum Pincer Complex: Scope and Mechanism. *Chem. Sci.* **2019**, *10* (45), 10566−10576.

(18) Leischner, T.; Spannenberg, A.; Junge, K.; Beller, M. Synthesis of Molybdenum Pincer Complexes and Their Application in the Catalytic Hydrogenation of Nitriles. *ChemCatChem.* **2020**, *12* (18), 4543−4549.

(19) Both, N. F.; Spannenberg, A.; Junge, K.; Beller, M. Low-Valent Molybdenum PNP Pincer Complexes as Catalysts for the Semi-hydrogenation of Alkynes. *Organometallics* **2022**, *41* (14), 1797−1805.

(20) Joannou, M. V.; Bezdek, M. J.; Chirik, P. J. Pyridine(diimine) Molybdenum-Catalyzed Hydrogenation of Arenes and Hindered Olefins: Insights into Precatalyst Activation and Deactivation Pathways. *ACS Catal.* **2018**, *8* (6), 5276−5285.

(21) Viereck, P.; Hierlmeier, G.; Tosatti, P.; Pabst, T. P.; Puentener, K.; Chirik, P. J. Molybdenum-Catalyzed Asymmetric Hydrogenation of Fused Arenes and Heteroarenes. *J. Am. Chem. Soc.* **2022**, *144* (25), 11203−11214.

(22) (a) Hierlmeier, G.; Tosatti, P.; Puentener, K.; Chirik, P. J. Identification of Cyclohexadienyl Hydrides as Intermediates in Molybdenum-Catalyzed Arene Hydrogenation. *Angew. Chem., Int. Ed.* **2023**, *62* (3), e202216026. (b) Hierlmeier, G.; Tosatti, P.; Puentener, K.; Chirik, P. J. Arene Insertion with Pincer-Supported Molybdenum-Hydrides: Determination of Site Selectivity, Relative Rates, and Arene Complex Formation. *J. Am. Chem. Soc.* **2023**, *145* (38), 21027−21039.

(23) (a) Li, W.; Huang, M.; Liu, J.; Huang, Y.-L.; Lan, X.-B.; Ye, Z.; Zhao, C.; Liu, Y.; Ke, Z. Enhanced Hydride Donation Achieved Molybdenum Catalyzed Direct *N*-Alkylation of Anilines or Nitroarenes with Alcohols: From Computational Design to Experiment. *ACS Catal.* **2021**, *11* (16), 10377−10382. (b) Liu, J.; Li, W.; Li, Y.; Liu, Y.; Ke, Z. Selective C-alkylation Between Alcohols Catalyzed by N-Heterocyclic Carbene Molybdenum. *Chem.—Asian J.* **2021**, *16* (20), 3124−3128.

(24) Su, P.; Chen, Z.; Ni, J.; Yang, Z.; Li, Y.; Ke, Z. Surmounting Alkoxide Trap Strategy: *N*-Heterocyclic Carbene Chromium (0)-Catalyzed C-Alkylation between Alcohols. *ACS Catal.* **2023**, *13*, 12481−12493.

(25) (a) Azouzi, K.; Pedussaut, L.; Pointis, R.; Bonfiglio, A.; Kumari Riddhi, R.; Duhayon, C.; Bastin, S. p.; Sortais, J.-B. Hydrogenation of Carboxylic Esters Catalyzed by Phosphine-Free Bis-N-heterocyclic Carbene Manganese Complexes. *Organometallics* **2023**, *42* (14), 1832−1838. (b) Both, N. F.; Spannenberg, A.; Jiao, H.; Junge, K.; Beller, M. Bis (N-Heterocyclic Carbene) Manganese (I) Complexes: Efficient and Simple Hydrogenation Catalysts. *Angew. Chem., Int. Ed.* **2023**, *62* (35), e202307987.

(26) Vielhaber, T.; Faust, K.; Bögl, T.; Schöfberger, W.; Topf, C. A triphos-modified tungsten piano-stool complex for the homogeneous (conjugate) hydrogenation of ketones and esters. *J. Catal.* **2022**, *416*, 352−363.

(27) (a) Werkmeister, S.; Junge, K.; Wendt, B.; Alberico, E.; Jiao, H.; Baumann, W.; Junge, H.; Gallou, F.; Beller, M. Hydrogenation of Esters to Alcohols with a Well-Defined Iron Complex. *Angew. Chem., Int. Ed.* **2014**, *53* (33), 8722−8726. (b) Elangovan, S.; Garbe, M.; Jiao, H.; Spannenberg, A.; Junge, K.; Beller, M. Hydrogenation of Esters to Alcohols Catalyzed by Defined Manganese Pincer Complexes. *Angew. Chem., Int. Ed.* **2016**, *128* (49), 15590−15594. (c) Junge, K.; Wendt, B.; Cingolani, A.; Spannenberg, A.; Wei, Z.;

https://doi.org/10.1021/acscatal.4c00019
ACS Catal. 2024, 14, 4082−4092

Jiao, H.; Beller, M. Cobalt Pincer Complexes for Catalytic Reduction of Carboxylic Acid Esters. *Chem.—Eur. J.* **2018**, *24* (5), 1046−1052.
(28) Ogata, K.; Yamaguchi, Y.; Kurihara, Y.; Ueda, K.; Nagao, H.; Ito, T. Twisted coordination mode of bis (*N*-heterocyclic carbene) ligands in octahedral geometry of group 6 transition metal complexes: Synthesis, structure, and reactivity. *Inorg. Chim. Acta* **2012**, *390*, 199−209.
(29) For selected examples see: (a) Öfele, K.; Herrmann, W. A.; Mihalios, D.; Elison, M.; Herdtweck, E.; Priermeier, T.; Kiprof, P. Heterocyclische Carbene IV. Metallkomplexe mit heterocyclischen Carben-Liganden: Synthese, Struktur, Strukturdynamik. *J. Organomet. Chem.* **1995**, *498* (1), 1−14. (b) Fehlhammer, W. P.; Bliss, T.; Kernbach, U.; Brüdgam, I. Homoleptic carbene complexes VI. Bis {1,1′-methylene-3,3′-dialkyl-diimidazolin-2,2′-diylidene}palladium chelate complexes by the free carbene route. *J. Organomet. Chem.* **1995**, *490* (1−2), 149−153. (c) Albrecht, M.; Miecznikowski, J. R.; Samuel, A.; Faller, J. W.; Crabtree, R. H. Chelated Iridium (III) Bis-carbene Complexes as Air-Stable Catalysts for Transfer Hydrogenation. *Organometallics* **2002**, *21* (17), 3596−3604. (d) Mata, J. A.; Chianese, A. R.; Miecznikowski, J. R.; Poyatos, M.; Peris, E.; Faller, J. W.; Crabtree, R. H. Reactivity Differences in the Syntheses of Chelating N-Heterocyclic Carbene Complexes of Rhodium Are Ascribed to Ligand Anisotropy. *Organometallics* **2004**, *23* (6), 1253−1263. For reviews on bis(NHC) transition metal complexes see: (e) Mata, J. A.; Poyatos, M.; Peris, E. Structural and catalytic properties of chelating bis- and tris-*N*-heterocyclic carbenes. *Coord. Chem. Rev.* **2007**, *251* (5−6), 841−859. (f) Gardiner, M. G.; Ho, C. C. Recent advances in bidentate bis(*N*-heterocyclic carbene) transition metal complexes and their applications in metal-mediated reactions. *Coord. Chem. Rev.* **2018**, *375* (15), 373−388.
(30) Sánchez, M. A.; Torres, G. C.; Mazzieri, V. A.; Pieck, C. L. Selective hydrogenation of fatty acids and methyl esters of fatty acids to obtain fatty alcohols−a review. *J. Chem. Technol. Biot.* **2017**, *92* (1), 27−42.
(31) Yang, W.; Kalavalapalli, T. Y.; Krieger, A. M.; Khvorost, T. A.; Chernyshov, I. Y.; Weber, M.; Uslamin, E. A.; Pidko, E. A.; Filonenko, G. A. Basic Promotors Impact Thermodynamics and Catalyst Speciation in Homogeneous Carbonyl Hydrogenation. *J. Am. Chem. Soc.* **2022**, *144* (18), 8129−8137.
(32) For Ru compare ref 3g. and (a) Neumann, J.; Bornschein, C.; Jiao, H.; Junge, K.; Beller, M. Hydrogenation of Aliphatic and Aromatic Nitriles Using a Defined Ruthenium PNP Pincer Catalyst. *Eur. J. Org. Chem.* **2015**, *27*, 5944−5948. For Mn compare ref 27b and (b) Elangovan, S.; Topf, C.; Fischer, S.; Jiao, H.; Spannenberg, A.; Baumann, W.; Ludwig, R.; Junge, K.; Beller, M. Selective Catalytic Hydrogenations of Nitriles, Ketones, and Aldehydes by Well-Defined Manganese Pincer Complexes. *J. Am. Chem. Soc.* **2016**, *138* (28), 8809−8814. For Fe compare ref 27a or (c) Chakraborty, S.; Dai, H.; Bhattacharya, P.; Fairweather, N. T.; Gibson, M. S.; Krause, J. A.; Guan, H. Iron-Based Catalysts for the Hydrogenation of Esters to Alcohols. *J. Am. Chem. Soc.* **2014**, *136* (22), 7869−7872. and (d) Bornschein, C.; Werkmeister, S.; Wendt, B.; Jiao, H.; Alberico, E.; Baumann, W.; Junge, H.; Junge, K.; Beller, M. Mild and selective hydrogenation of aromatic and aliphatic (di)nitriles with a well-defined iron pincer complex. *Nat. Commun.* **2014**, *5*, 4111.
(33) (a) Elangovan, S.; Garbe, M.; Jiao, H.; Spannenberg, A.; Junge, K.; Beller, M. Hydrogenation of Esters to Alcohols Catalyzed by Defined Manganese Pincer Complexes. *Angew. Chem., Int. Ed.* **2016**, *55* (49), 15364−15368. (b) Espinosa-Jalapa, N. A.; Nerush, A.; Shimon, L. J. W.; Leitus, G.; Avram, L.; Ben-David, Y.; Milstein, D. Manganese-Catalyzed Hydrogenation of Esters to Alcohols. *Chem.—Eur. J.* **2016**, *23* (25), 5934−5938. (c) van Putten, R.; Uslamin, E. A.; Garbe, M.; Liu, C.; Gonzalez-de-Castro, A.; Lutz, M.; Junge, K.; Hensen, E. J. M.; Beller, M.; Lefort, L.; Pidko, E. A. Non-Pincer-Type Manganese Complexes as Efficient Catalysts for the Hydrogenation of Esters. *Angew. Chem., Int. Ed.* **2017**, *56* (26), 7531−7534. (d) Widegren, M. B.; Harkness, G. J.; Slawin, A. M. Z.; Cordes, D. B.; Clarke, M. L. A Highly Active Manganese Catalyst for Enantioselective Ketone and Ester Hydrogenation. *Angew. Chem., Int. Ed.* **2017**, *56* (21), 5825−5828. (e) Zubar, V.; Lichtenberger, N.; Schelwies, M.; Oeser, T.; Hashmi, A. S. K.; Schaub, T. Manganese-Catalyzed Hydrogenation of Sclareolide to Ambradiol. *ChemCatChem* **2021**, *14* (1), e202101443. (f) Li, X.-G.; Li, F.; Xu, Y.; Xiao, L.-J.; Xie, J.-H.; Zhou, Q.-L. Hydrogenation of Esters by Manganese Catalysts. *Adv. Synth. Catal.* **2022**, *364* (4), 744−749. (g) Wei, Z.; Li, H.; Wang, Y.; Liu, Q. A Tailored Versatile and Efficient NHC-Based NNC-Pincer Manganese Catalyst for Hydrogenation of Polar Unsaturated Compounds. *Angew. Chem., Int. Ed.* **2023**, *62* (23), e202301042. (h) Zell, T.; Ben-David, Y.; Milstein, D. Unprecedented Iron-Catalyzed Ester Hydrogenation. Mild, Selective, and Efficient Hydrogenation of Trifluoroacetic Esters to Alcohols Catalyzed by an Iron Pincer Complex. *Angew. Chem., Int. Ed.* **2014**, *53* (18), 4685−4689. (i) Werkmeister, S.; Junge, K.; Wendt, B.; Alberico, E.; Jiao, H.; Baumann, W.; Junge, H.; Gallou, F.; Beller, M. Hydrogenation of Esters to Alcohols with a Well-Defined Iron Complex. *Angew. Chem., Int. Ed.* **2014**, *53* (33), 8722−8726. (j) Chakraborty, S.; Dai, H.; Bhattacharya, P.; Fairweather, N. T.; Gibson, M. S.; Krause, J. A.; Guan, H. Iron-Based Catalysts for the Hydrogenation of Esters to Alcohols. *J. Am. Chem. Soc.* **2014**, *136* (22), 7869−7872. (k) Elangovan, S.; Wendt, B.; Topf, C.; Bachmann, S.; Scalone, M.; Spannenberg, A.; Jiao, H.; Baumann, W.; Junge, K.; Beller, M. Improved Second Generation Iron Pincer Complexes for Effective Ester Hydrogenation. *Adv. Synth. Catal.* **2016**, *358* (5), 820−825.
(34) (a) Olmstead, W. N.; Margolin, Z.; Bordwell, F. G. Acidities of Water and Simple Alcohols in Dimethyl Sulfoxide Solution. *J. Org. Chem.* **1980**, *45* (16), 3295−3299. (b) Matthews, W. S.; Bares, J. E.; Bartmess, J. E.; Bordwell, F.; Cornforth, F. J.; Drucker, G. E.; Margolin, Z.; McCallum, R. J.; McCollum, G. J.; Vanier, N. R. Equilibrium acidities of carbon acids. VI. Establishment of an Absolute Scale of Acidities in Dimethyl Sulfoxide Solution. *J. Am. Chem. Soc.* **1975**, *97* (24), 7006−7014.
(35) (a) Suzuki, K.; Yamamota, H.; Kanie, S. Cyanoalkyl complexes of transition metals.: II. Preparation and properties of some platinum complexes containing phosphorus as a donor atom. *J. Organomet. Chem.* **1974**, *73* (1), 131−136. (b) Ros, R.; Michelin, R. A.; Bataillard, R.; Roulet, R. Hydridocyanomethyl complexes of platinum(II). *J. Organomet. Chem.* **1977**, *139* (3), 355−359. (c) del Pra, A.; Zanotti, G.; Bombieri, G.; Ros, R. Crystal and molecular structure of *trans*-$PtCl(CH_2CN)(PPh_3)_2$. *Inorg. Chim. Acta* **1979**, *36*, 121−125. (d) English, A. D.; Herskovitz, T. Metalation and Carboxylation of Activated Carbon-Hydrogen Bonds by Complexes of Iridium and Rhodium. *J. Am. Chem. Soc.* **1977**, *99* (5), 1648−1649. (e) McCrindle, R.; Ferguson, G.; McAlees, A. J.; Parvez, M.; Roberts, P. J. Light-induced reactions of *trans*-chloro(cyanomethyl)bis-(triphenylphosphine) palladium(II) and the crystal and molecular structures of its acetone, acetonitrile, and benzene solvates. *J. Chem. Soc., Dalton Trans.* **1982**, *9*, 1699−1708. (f) Henderson, W.; Oliver, A. G. *cis*-Bis(cyanomethyl)bis(triphenylphosphine)platinum(II)-dichloromethane. *Acta Crystallogr., Sect. C* **1999**, *55*, 1406−1408. (g) Crestani, M. G.; Steffen, A.; Kenwright, A. M.; Batsanov, A. S.; Howard, J. A. K.; Marder, T. B. Oxidative Addition of X−H (X = C, N, O) Bonds to $[Ir(PMe_3)_4]Cl$ and Catalytic Hydration of Acetonitrile Using its Peroxo Derivative, $[Ir(O_2)(PMe_3)_4]Cl$, as Catalyst Precursor. *Organometallics* **2009**, *28* (9), 2904−2914. (h) Emeljanenko, D.; Peters, A.; Vitske, V.; Kaifer, E.; Himmel, H.-J. The First Cyanomethyl Complex of Gold, Synthesized by Reaction of a Au^{I} Complex with Acetonitrile in the Presence of a New Guanidine N-Superbase. *Eur. J. Inorg. Chem.* **2010**, *2010*, 4783−4789. (i) Tanabe, T.; Evans, M. E.; Brennessel, W. W.; Jones, W. D. C−H and C−CN Bond Activation of Acetonitrile and Succinonitrile by $[Tp'Rh(PR_3)]$. *Organometallics* **2011**, *30* (4), 834−843. (j) Chambers, M. B.; Groysman, S.; Villagrán, D.; Nocera, D. G. Iron in a Trigonal Tris(alkoxide) Ligand Environment. *Inorg. Chem.* **2013**, *52* (6), 3159−3169. (k) Tehranchi, J.; Donoghue, P. J.; Cramer, C. J.; Tolman, W. B. Reactivity of (Dicarboxamide)M^{II}−OH (M = Cu, Ni) Complexes − Reaction with Acetonitrile to Yield M^{II}−Cyanomethides. *Eur. J. Inorg. Chem.* **2013**, No. 22−23, 4077−4084. (l) Chang, H.-C.; Chang, Y.-F.; Lin, S.-H.; Lin, T.-H.; Lee, W.-Z. Ambient Stable

https://doi.org/10.1021/acscatal.4c00019
ACS Catal. 2024, 14, 4082−4092

Cyanomethylcopper(III) Complex: a Strong Cu−C_{sp^3} Bond Supported by a PS3-Tripodal Chelator. *Inorg. Chem.* **2019**, *58* (1), 22−26. (m) Islam, M. J.; Park, K. C.; Manley, O. M.; Smith, M. D.; Makris, T. M.; Peryshkov, D. V. Room-Temperature Aerobic C−CN Bond Activation in Nickel(II) Cyanomethyl Dicarboranyl Complex. *Organometallics* **2023**, *42* (15), 1997−2004.

(36) (a) Hayter, R. Hydrogen Bridge Bonding in the $[M_2H(CO)_{10}]^-$ Anions (M= Cr, Mo, W). *J. Am. Chem. Soc.* **1966**, *88* (19), 4376−4382. (b) Roziere, J.; Williams, J. M.; Stewart, R. P., Jr; Petersen, J. L.; Dahl, L. F. A Neutron Diffraction Study of $[Et_4N]^+[Cr_2(CO)_{10}(\mu_2\text{-}H)]^-$: a $[M_2(CO)_{10}(\mu_2\text{-}H)]^-$ Monoanion with a Pseudo D_{4h} Nonhydrogen Geometry Together with a Disordered, Bent Symmetric Metal-Hydrogen-Metal Bond. *J. Am. Chem. Soc.* **1977**, *99* (13), 4497−4499. (c) Darensbourg, M. Y.; Atwood, J. L.; Burch, R. R., Jr; Hunter, W. E.; Walker, N. Structural and Chemical Characterization of a Phosphine Bound M-H-M Bridged Carbonylate: $Et_4N^+(\mu\text{-}H)[Mo_2(CO)_9PPh_3]^-$. *J. Am. Chem. Soc.* **1979**, *101* (10), 2631−2637. (d) Petersen, J. L.; Masino, A.; Stewart, R. P., Jr X-ray diffraction studies of the influence of lattice effects on the metal carbonyl framework of the $[Mo_2(CO)_{10}(\mu\text{-}H)]^-$ monoanion. *J. Organomet. Chem.* **1981**, *208* (1), 55−71. (e) Darensbourg, M. Y.; Deaton, J. C. The $HCr(CO)_5^-$ Anion. *Inorg. Chem.* **1981**, *20* (6), 1644−1646. (f) Darensbourg, M. Y.; Bau, R.; Marks, M. W.; Burch, R. R.; Deaton, J. C.; Slater, S. Structural Characterizations of Salts of $HCr(CO)_5^-$ and $(\mu\text{-}H)_2BH_2Cr(CO)_4^-$ and Studies of Their Interconversions. *J. Am. Chem. Soc.* **1982**, *104* (25), 6961−6969. (g) Darensbourg, M. Y.; El Mehdawi, R.; Delord, T. J.; Fronczek, F. R.; Watkins, S. F. Binuclear Molybdenum Carbonyls Bridged Both by Hydride and Bidentate Phosphine Ligands. Crystal and Molecular Structures of Salts of $(\mu\text{-}H)(\mu\text{-}Ph_2P(CH_2)_nPPh_2)Mo_2(CO)_8^-$ (n= 1−4) and Their Reactions with Acids. *J. Am. Chem. Soc.* **1984**, *106* (9), 2583−2591.

https://doi.org/10.1021/acscatal.4c00019
ACS Catal. 2024, 14, 4082−4092